12-2014

The Role of MIR-34a in Inhibition of Prostate Tumor Growth in the bone and Induction of Autophagy

Sanchaika Gaur

THE ROLE OF MIR-34A IN INHIBITION OF PROSTATE TUMOR GROWTH IN THE BONE AND INDUCTION OF AUTOPHAGY

by

Sanchaika Gaur, B.S.

APPROVED:

_____

Gary E. Gallick, Ph.D., Supervisory Professor

_____

Anil K. Sood, M.D.

_____

David J. McConkey, Ph.D.

_____

Mark A. Titus, Ph.D.

_____

Menashe Bar-Eli, Ph.D.

APPROVED:

_____

Dean, The University of Texas
Graduate School of Biomedical Sciences at Houston

THE ROLE OF MIR-34A IN INHIBITION OF PROSTATE TUMOR GROWTH IN THE BONE AND INDUCTION OF AUTOPHAGY

A

DISSERTATION

Presented to the Faculty of

The University of Texas

Health Science Center at Houston

and

The University of Texas

MD Anderson Cancer Center

Graduate School of Biomedical Sciences

in Partial Fulfillment

of the Requirements

for the Degree of

DOCTOR OF PHILOSOPHY

by

Sanchaika Gaur, B.S.

Houston, Texas

December, 2014

Dedication

To my loving husband and pillar of strength, Mukund Ojha and my parents, Som Pratap and Manjula Gaur, Sampurna Nand and Madhu Ojha for their unconditional love and blessings.

Acknowledgements

I express my sincerest gratitude to my mentor Dr. Gary Gallick for his support and tireless efforts in bringing out the best in his students. I admire him for his selfless dedication to the field of Cancer Biology. I am indebted to him for paving the way for me to see the big picture.

Dr. Anil K. Sood has actively participated in my committees and always encouraged thinking outside the box. This work is elevated many folds because of his inputs and I truly appreciate his contributions.

I wish to thank members of committees, Drs. David M. McConkey, Menashe Bar Eli, George A. Calin, Mark A. Titus, Pierre McCrea, E. Scott Kopetz, Nova M. Navone and Faye M. Johnson, for their crucial role throughout my journey in graduate school.

Members of Dr. Gallick's laboratory, Nila U. Parikh, Jian H. Song, Lynnelle W. Thorpe, Andreas Varkaris, Tanushree Chatterji and Jung-Kang Jin have been a family away from home. I am thankful for their help, ideas, and encouragement. A special thank you to Dr. Yunfei Wen for her time and continued help with the autophagy studies.

I consider myself fortunate for the opportunity to collaborate with Dr. Daniel E. Frigo at University of Houston and members of his laboratory. Their inputs helped me immensely in the autophagy gene knockdown studies.

I would like to thank Dr. Bogdan Czerniak and The Center for RNA Interference and Non-coding RNAs for their assistance with miR-34a visualization in clinical samples and Lingegowda S. Mangala for preparing the chitosan nanoparticles.

THE ROLE OF MIR-34A IN INHIBITION OF PROSTATE TUMOR GROWTH IN THE BONE AND INDUCTION OF AUTOPHAGY

Sanchaika Gaur, B.S.

Supervisory Professor: Gary E. Gallick, Ph.D.

Prostate cancer (PCa) is the second leading cause of cancer-related deaths in men in the United States, with most deaths occurring from bone metastasis. Several new therapies have been FDA approved for bone-metastatic PCa, but patient survival has only marginally improved due to therapy resistance, which often arises from constitutive activation of compensatory signaling pathways. This dissertation work focused on a mechanistic understanding of how cross talk between tyrosine kinase receptors contributes to therapy resistance, and how this may be overcome by downregulating expression of these receptors. In PCa cell lines and xenograft models, I demonstrated that activation of IGF-1R receptor tyrosine kinase (RTK) through IGF-1 leads to delayed, ligand-independent activation of another RTK, MET, that requires Src activation and transcription, suggesting that downregulation of expression of these kinases may be required for better inhibition of their functions.

I therefore examined the biologic effects of overexpression of miR-34a, a tumor suppressive microRNA that downregulates multiple proteins involved in PCa progression. I demonstrated

that miR-34a is downregulated in high metastatic PCa cell lines, concomitant with its targets being overexpressed. Overexpression of miR-34a decreased several properties associated with metastasis, including-migration, invasion, and proliferation. I next demonstrated that miR-34a delivery to xenografts grown in the femurs of immunocompromised mice inhibited prostate tumor growth and preserved bone integrity.

To examine the mechanisms by which miR-34a overexpression inhibited cancer growth, autophagy and apoptosis pathways were studied. I determined the expression of autophagy markers and the requirement of key signaling intermediates in the autophagic pathway upon miR-34a overexpression. I demonstrated that miR-34a overexpression induced apoptosis along with a non-canonical form of autophagy that is independent of ATG5, ATG7 and Beclin-1 expression.

In summary, studies in this dissertation provide evidence for IGF-1/1R induced ligand-independent MET activation, suggesting that cross talk among receptors may be responsible for resistance to targeted therapies. To potentially overcome this problem, I demonstrated that delivery of miR-34a that downregulates proteins involved in PCa progression decreases tumor growth in the bone. Overexpression of miR-34a induces apoptosis and a novel form of autophagy that might contribute to its therapeutic effects.

Table of Contents

List of Figures

List of Tables

Abbreviations

PCa	Prostate Cancer
AR	Androgen Receptor
DHT	Dihydrotestosterone
mCRPC	Metastatic Castrate Resistant Prostate Cancer
Rad223	Radium 223
RTK	Receptor Tyrosine Kinase
NSCLC	Non-small Cell Lung Cancer
IGF-1	Insulin-like Growth Factor 1
IGF-1R	Insulin-like Growth Factor 1 Receptor
EGF	Epidermal Growth Factor
CH	Chitosan
N.C.	Negative Control
ISH	In situ hybridization
IHC	Immunohistochemistry
MRI	Magnetic Resonance Imaging
TEM	Transmission Electron Microscopy
Dox	Doxycycline

Chapter 1

Introduction

Overview of Prostate Cancer

Prostate cancer (PCa) is the second most prevalent cancer in men in the United States [1, 2]. It is estimated that in 2014 there will be 233,000 new cases and 29,480 deaths will occur from PCa [1]. Improvements in diagnostic methods that aid in early detection and successful surgical intervention and/or radiation therapy have led to nearly 100% five-year survival rate for patients with localized tumor [1, 2]. However, five-year survival rates drops to 28% with the development of distant metastasis [1], which is most common in the bone, followed by lungs, liver and brain [3]. Bone metastasis contributes to 90% of the deaths from PCa due to lack of effective treatment approaches [4]. Early stage prostate cancer cells are dependent on androgens for their survival and proliferation and androgen-ablation therapies are effective treatment modalities at this stage. However, most patients with advanced stage cancer develop progressive disease even with castrate levels of androgens leading to metastatic castrate-resistant prostate cancer (mCRPC) [5].

Increasing age is the only well-established risk factor for PCa with 60% of the cases being diagnosed in men 65 years of age and older [2]. Other risk factors associated with PCa include, family history, inherited genetic conditions (such as Lynch syndrome and *BRAC2* mutation), obesity, high diary and processed meat diet, and African ancestry [2, 6]. Some of these risk factors might contribute to higher incidence rates for prostate cancer in African American men than in non-Hispanic white men [2]. Thus, it is important to better understand the genetic, epigenetic and molecular alterations in progressive PCa as well as the tumor microenvironment interactions that promote cancer survival and progression for development of successful treatment modalities for advanced disease.

Pathology of Prostate Cancer

The prostate gland is a part of male reproductive system responsible for producing and storing one third of the seminal fluid. Adult prostate is an acorn-shaped gland, located below the bladder comprising of three cell types: luminal, basal and neuroendocrine cells. Luminal cells, the major constituents of the gland, carry out secretory functions, express low-molecular weight cytokeratins (CK8/18), express androgen receptor and are dependent on androgen signaling [6, 7]. Androgens are required for normal prostate function as they bind to androgen receptor (AR) that then translocates to the nucleus and control transcriptional expression of androgen-regulated genes that are required for production of seminal fluids [8]. The basal cells are aligned between luminal cells and the basement membrane and thought to serve as a barrier to protect luminal cells from oncogenic insults. It has been speculated that basal cell layer has stem cell functions and basal cells can differentiate into luminal cells to give rise to prostatic carcinomas [6, 7]. Basal cells express high-molecular weight cytokeratins (CK5/14) and are not dependent on androgen signaling [6, 7]. Neuroendocrine cells express synaptophysin and chromagranin A and constitute a very small fraction of the prostate cells and are involved in secreting serotonin and other neuropeptides [9].

The cell of origin of prostate cancer is controversial with Okada et al. reporting majority of prostate adenocarcinoma with luminal cytokeratin marker staining, suggesting luminal cells as the origin of PCa [10]. However, cancer recurrence after anti-hormonal therapy and progression of metastatic castrate resistant prostate cancer (mCRPC) suggest androgen independent basal cells as the cell of origin [7]. Furthermore, Verhagen et al. identified an intermediate cell population with basal and luminal markers in the primary PCa and hormone-independent PCa [11] and upregulation of prostate stem cell antigen (PSCA), a

marker for intermediate cells in prostate cancer suggests intermediate cells as the cell of origin [7]. The work of Choi, et al. identified that both luminal and basal cell population have self-renewal abilities leading to cancer initiation in a *Pten*-null mouse model further demonstrating that basal cells are capable of differentiating into luminal cells and suggesting the role of basal-luminal differentiation for prostate cancer initiation [12].

McNeal, et al. in their seminal paper defined three distinct morphological regions in the human prostate, which are the peripheral zone, the transition zone and the central zone [13]. The non-malignant Benign Prostatic Hyperplasia (BPH) occurs mostly in the transition zone while prostate carcinoma occurs mainly in the peripheral zone [13, 14].

Prostate cancer is pathologically classified by morphological criteria based on sum of Gleason score and clinically by TNM staging. The Gleason grading system takes into account appearance of the architecture of prostate cancer cells under the microscope and assigns primary and secondary Gleason grades to the most prevalent and second most prevalent pattern of the tumor specimen [15]. The Gleason grades range from 1 to 5, and Gleason score is determined by the sum of primary and secondary grade. The Gleason scores thus, range from 2 to10, with higher score indicative of poorly differentiated cells and more advanced cancer. A Gleason score of 8-10 has higher risk of cancer recurrence, metastasis and death [16]. In addition to the morphology of the cells, the TNM staging system, which evaluates the size and range of the primary tumor (T), the involvement of lymph nodes (N) and the degree of distant metastasis (M) is also widely used by clinicians to predict survival and prognosis with higher staging indicative advanced cancer. The morphological grading and clinical staging system lacks the incorporation of molecular heterogeneity that drives

disease progression and thus, targeted-molecular agents cannot be appropriately provided to individual patients.

Spiral Progression Model

Recognizing the need for a classification system that includes molecular makers for therapy selection in PCa, Logothetis et al. proposed an alternative model of PCa progression which incorporates stage-specific molecular drivers that can be targeted by single or combination therapies [5]. This alternative model **(Fig. 1)** consists of an endocrine-driven phase, a microenvironment-driven phase and a tumor cell autonomous phase [5]. In the endocrine driven phase, tumor growth is dependent on the androgens, testosterone (secreted from the testes) and dehydroepiandrosterone (DHEA) (secreted from the adrenal gland), which are converted by the enzyme 5-α-reductase (SRD5A) to dihydrotestosterone (DHT). DHT binds to androgen receptor (AR) with higher affinity than testosterone and promotes cancer cell proliferation and metabolism. SRD5A inhibitors (e.g., finasteride and dutasteride) are thus effective in the treatment of low-grade endrocrine-driven cancer, while androgen ablation therapy (e.g., Lupron) is effective in the treatment of high-grade cancers that are not DHT-dependent [5]. The responses to these therapies are short-lived and resistance soon develops as PCa transitions to a paracrine-driven phase and enters the progression spiral **(Fig. 1)** where each “turn” of the spiral is driven by molecular marker/s that can be targeted and the “pitch” is indicates the duration of time for which the tumors are responsive to targeted therapy. Chemotherapeutic modalities have limited success in this phase since multiple

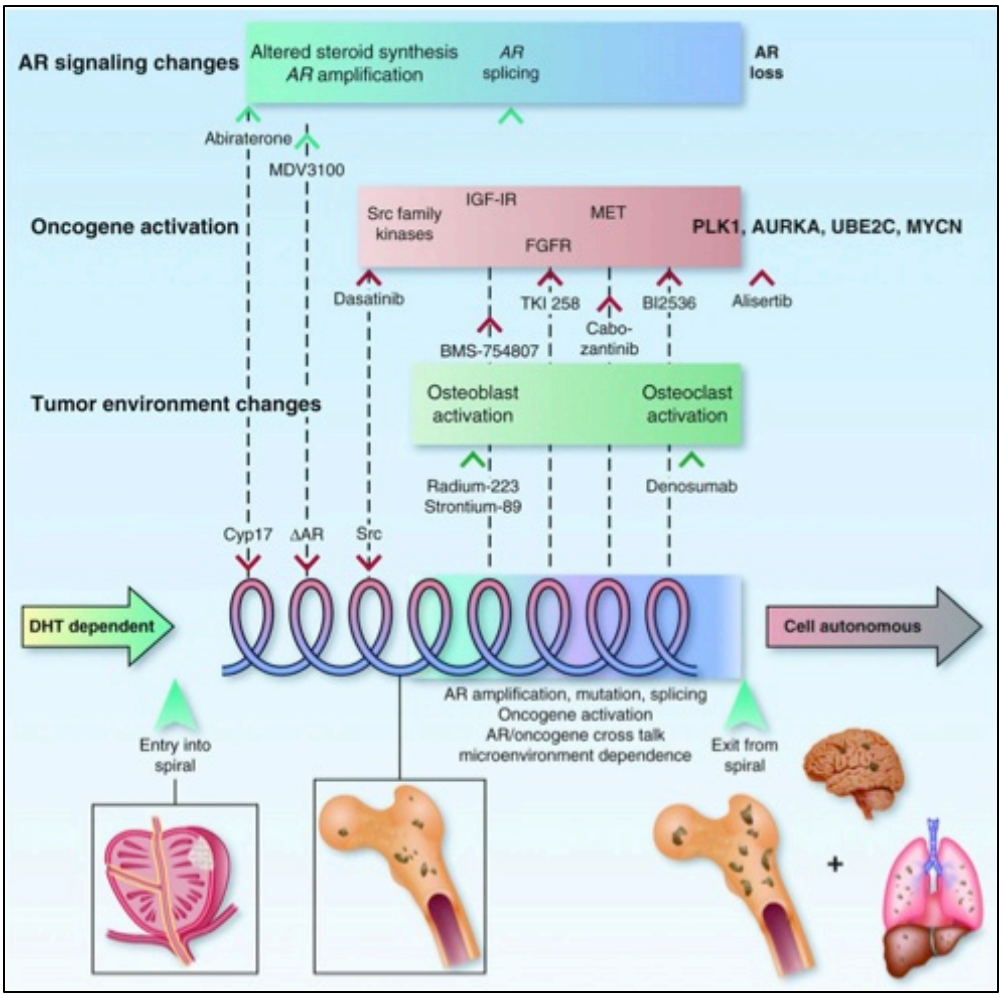

Figure 1 - Spiral Progression model

This alternative model describes different stages of prostate cancer. In the early stage, prostate cancer cells are DHT-dependent. Upon entry into the progression spiral where each turn is driven by a molecular marker/s, the cancer cells are in paracrine-driven phase. Cancer cells can exit from the spiral and enter the cell autonomous stage.

From Logothetis CJ, Gallick GE, Maity SN, Kim J, Aparicio A, Efstathiou E and Lin SH (2013). Molecular Classification of Prostate Cancer Progression: Foundation for Marker-Driven Treatment of Prostate. Cancer Discovery 3; 849. Reproduced with Permission

factors including changes in AR signaling (AR amplification, mutation, splicing), aberrant oncogenic activation (e.g., activation of Src family kinases, Her2, Akt), receptor overexpression (e.g., MET, IGF-1R), downregulation of tumor suppressors (e.g, loss of PTEN, p53) and paracrine mediated effects (activation of osteoblasts and osteoclasts) can drive disease progression and metastatic growth [5]. This progressive disease where patients do not respond to androgen ablation therapies is termed as metastatic castrate-resistant prostate cancer (mCRPC). According to the alternative model described above, prostate cancer cells can exit the spiral and enter a cell autonomous phase where the tumor is androgen independent with neuroendocrine features. This late-stage disease is termed as neuroendocrine prostate cancer or small cell prostate cancer or anaplastic prostate cancer. Surprisingly, whereas earlier stages do not respond well to chemotherapy, this stage responds to chemotherapeutic agents [5]. These distinct features of PCa progression and different responses to therapies, present the need to better understand stages of PCa progression and the underlying genetic, epigenetic and molecular alternations in each stage.

Genetic and Epigenetic Alterations in Prostate Cancer

There are few signature driving oncogenic mutations in PCa; however, tumor cells undergo many genetic and epigenetic alterations that can initiate cancer development and further promote its progression. These include copy number alterations, chromosomal rearrangements and alterations, epigenetic silencing (DNA methylation), histone modifications and chromatin remodeling and miRNA dysregulation. Losses of chromosomes, including 8p, 10q, 13q and 17p have been reported [6, 17] by comparative genomic

hybridization (CGH), which includes regions for the tumor suppressor genes, *NKX3.1, PTEN, Rb and p53* respectively. Less frequent chromosome gains of 8q and 7 [18-20] have also been reported which include regions for candidate oncogene *c-Myc*, *EGFR* and *c-Met*. Most genomic aberrations were identified in the RB, PI3K and RAS/RAF signaling pathway by global copy-number and transcriptome profile analysis [21]. Downregulation of tumor suppressive gene NKX3.1, located on 8p has been implicated in prostate cancer initiation [6, 22]; loss of PTEN located on 10q is involved in PCa development and progression; while loss of Rb and p53 are associated with invasive PCa and progression to castrate-resistant metastatic PCa [6, 23, 24]. The gene loci of *c-Myc*, 8q24.21 is amplified in advanced prostate cancer and in metastases [25], and Myc overexpression in mouse models induces cancer initiation and progression to invasive prostate adenocarcinoma [26]. Chromosomal rearrangements have been identified with fusion of androgen regulated *TMPRSS* with *ETS* family of genes [27, 28], an early event in PCa development and associated with more aggressive cancer [29].

Epigenetic modifications, in addition to genetic alterations are important in cancer initiation and progression. DNA methylation is an epigenetic modification that occurs mostly at the cytosines within the CpG islands, found at the 5'untranslated region (UTR) of promoters of numerous genes. DNA promoter methylation-induced gene silencing has been reported for more than 50 genes in PCa, including Glutathione S-transferase P1 (GSTP1) hypermethylation in more than 90% of PCa [30-32]. Epigenetic modifications of histone include acetylation, methylation, etc. of the histones and in prostate cancer acetylation of H3K18 and methylation of H3K4 has been shown to be predictors of PCa progression [33].

Molecular Mechanisms Driving Prostate Cancer Progression

Several molecular alterations can drive prostate cancer progression that includes overexpression and/or activation of receptor and non-receptor protein tyrosine kinases (PTKs) that promote PCa growth, development, progression, and metastasis and thus driving each spiral of the progression model **(Fig. 1)**. One of the genes implicated in PCa progression and metastasis is receptor tyrosine kinase (RTK), c-Met (MET). MET can be activated by bindings of its ligand, HGF which leads to receptor dimerization and phosphorylation of tyrosines (Tyr), Tyr 1234 and Tyr 1235 in the kinase domain and further phosphorylation of Tyr 1349 and Tyr 1356 in the carboxy-terminal substrate docking site leads to MET activation and recruitment of signaling molecules [34]. MET/HGF signaling can relay activation of downstream signaling cascades important for cell survival, proliferation, differentiation, migration, and invasion [35]. MET expression significantly increases with PCa progression, and increased MET expression is inversely related to poor prognosis [36]. MET is expressed in basal and intermediate cells of normal prostate and is also expressed on PCa cells [37]. Androgen deprivation increases MET expression and also increases HGF expression in prostate cancer and stromal cells [38, 39]. MET expression is higher in PCa tissue compared with normal tissue and in bone metastasis compared with lymph node metastasis of PCa [40]. MET receptor is present on stromal cells including osteoblasts, osteoclasts and endothelial cells and its ligand HGF is also secreted by stromal cells suggesting involvement of the MET/HGF signaling in the bone microenvironment promoting survival and growth of tumor and stromal cells [4]. Thus, targeting of MET in advanced bone metastatic prostate cancer has been thought to be clinically important however, single agent MET inhibitors have not been successful in treating advanced disease [4] and multi-targeted

small molecule inhibitors such as Cabozatinib recently failed in Phase III clinical trial. This could be due to emergence of compensatory pathways and/or MET re-activation in response to inhibitors (Varkaris, unpublished) through different mechanisms that include gene amplifications, mutations and ligand independent receptor cross talk. Integrin binding, G protein coupled receptors, plexins, CD44, EGFR and RET have all been implicated in ligand independent MET activation [41]. In non-small cell lung cancer (NSCLC), MET activation through gene amplification is predicted to be one of the mechanisms of EGFR inhibitor, gefitinib resistance [42]. In NSCLC, MET can be activated by EGF in a ligand independent manner [43] and EGFR can activate MET to promote invasion and brain metastasis [44]. However, in PCa, gene amplifications or mutations of MET are extremely rare and receptor cross talk mechanisms have not been previously reported. It will be thus important to determine whether in PCa, MET can be activated by cross talk with other receptors and interactions with soluble factors in the bone microenvironment that contributes to development of resistance to MET inhibitors.

Axl is another receptor tyrosine kinase that can be activated by its ligand, Gas6 or homophillic interactions [45]. Receptor dimerization leads to autophosphorylation and activation of downstream signaling that can promote cancer cell proliferation, survival, migration, and invasion [46, 47]. Axl expression increases with high-grade prostate cancer and in bone metastasis of PCa [46, 48]. Axl protein and mRNA expression are also higher in more metastatic PCa cell lines and knockdown of Axl decreases expression of mesenchymal markers as well as decreases survival, proliferation, migration and invasion abilities of PCa cell lines [49]. Thus, targeting Axl could be beneficial for treatment of advanced PCa.

c-Myc (Myc) is a proto-oncogene that regulates cell proliferation and transformation. It activates genes involved in cell cycle progression and inhibits genes that are involved in cell cycle arrest [50]. c-Myc mRNA expression is increased in laser capture micro-dissected (LCM) tumor cells compared to benign epithelial cells [51] and Myc is also overexpressed at the protein level in prostate cancer cells [25]. Myc can be upregulated by AR in a ligand independent manner in high-grade metastatic PCa [52] and can be post-transcriptionally controlled by microRNAs [53]. In transgenic mice, Myc overexpression in the prostate can lead to development of prostatic intraepithelial neoplasia (PIN) and followed by progression to invasive carcinoma [26]. Myc being a transcriptional factor is hard to target by conventional small molecule inhibitors [54], however RNAi-mediated silencing of Myc transcription can inhibit tumor initiating capacity and stem-like maintenance of prostate cancer cells [55] and strategies targeting Myc expression can be developed for treatment of prostate cancer.

Since, many genes including MET, Axl, c-Myc can contribute to PCa progression, targeting these multiple genes could be a better approach for treatment of advanced bone metastatic cancer.

Prostate Cancer Metastasis and Tumor Microenvironment

Prostate cancer mostly commonly metastasizes to the bone, followed by lungs, liver and brain. It is not known why prostate cancer cells preferentially metastasize to the bone. There are some suggestions that the tumor microenvironment interactions in PCa can promote tumor growth and metastases in the bone. The bone microenvironment consists of

stromal cells including bone forming osteoblasts, bone dissolving osteoclasts, fibroblasts, endothelial cells and immune cells. Many growth factors including IGF-1, and cytokines like, IL-6, IL-8, chemokines and extracellular matrix (ECM) proteins secreted in the bone microenvironment act on tumor cells enhancing their growth and survival [56]. Tumor cells also secrete factors that act upon the stromal cells and alter their properties favoring tumor growth. Tumor cells secrete osteoblastic and osteoclastic factors including-BMPs, PTHrP, ET-1, PDGF, that act on osteoblasts promoting new bone formation and on osteoclasts promoting bone resorption [57, 58]. Osteoclasts and osteoblasts on the other hand secrete growth factors including- TGF-β, HGF, IGF-1, etc. that promote tumor cell proliferation and survival [57, 58]. Thus, it is important to target both the tumor and the microenvironment compartments to disrupt the tumor-microenvironment interactions and have elevated therapeutic benefit in metastatic prostate cancer.

Treatment Modalities in Prostate Cancer

Prostate cancer in its DHT-dependent stage can be treated by surgical interventions and/or androgen deprivation therapy (ADT). First generation anti-androgens including flutamide, bicalutamide, or first generation androgen synthesis inhibitors including ketoconazole can be given to patients with non-metastatic CRPC [59]. However, the responses to these therapies are heterogeneous and eventually lead to cancer progression. FDA recently approved Abiraterone and Enzalutamide for treatment of metastatic prostate cancer [60]. Abiraterone is a CYP17 inhibitor that inhibits androgen biosynthesis while Enzalutamide is an androgen receptor antagonist that target androgen receptor activation

[60]. These agents have modest improvements in overall survival with development of resistance and/or activation of oncogenic pathways that further drives cancer progression. Radium 223 (Rad 223), an alpha-emitting radiopharmaceutical that targets the bone matrix is used for treatment of bone metastasis in prostate cancer [60]. Rad 223 showed modest improvement in overall survival by 3.7 months compared to placebo arm [60]. Small molecule inhibitors targeting activation of RTKs (e.g., Cabozatinib for MET) or SFKs (e.g. Dasatinib) have severe toxic side effects and are not successful in Phase III clinical trials with mCRPC [4]. Thus, there is a need to develop therapeutic approaches that target multiple oncogenic pathways to combat resistance as well as target both the tumor and the microenvironment for better treatment of metastatic prostate cancer. One such approach is through microRNAs that are deregulated in cancer and their replacement or inhibition could affect multiple targets involved in cancer development and progression.

MicroRNAs in Cancer

Regulation through microRNAs (miRNAs) is an important post-transcriptional mechanism present in a cell. miRNAs are 18- to 22-nucleotide (nt) post-transcriptional modulators that regulate many normal cellular processes, including growth, survival, differentiation, cell cycle arrest, aging; and their dysregulation has been implicated in cancer development and progression. miRNAs are transcribed from the genome as longer primary transcripts (pri-miRNAs) which is cleaved by ribonuclease Drosha (DGCR8) into 70-100 nt long hairpin pre-miRNA structures with 3’overhang. These pre-miRNAs are then exported into the cytoplasm by exportin 5 (XPO5) where the ribonuclease Dicer further cleaves the

hairpin pre-miRNA to ~22 nt long miRNA duplex; and following separation and degradation of the other strand, mature miRNA is loaded in the RNA-induced silencing complex (RISC) [61, 62]. The mature miRNA is led by the RISC and Argonaute (AGO) proteins to interact with the target mRNA at the 3'UTR through partial complementary sequence and inhibits protein translation by either inducing silencing or degradation of the target mRNAs [62-64] **(Fig. 2)**. It has been reported that miRNAs can also bind to the 5'UTR and ORF and can directly bind to DNA to regulate gene expression at the transcriptional level [64]. Thus, miRNA can regulate gene expression through many different mechanisms.

In cancer, miRNAs can act as oncomirs by downregulating tumor suppressor genes or can act as tumor suppressive miRs by downregulating oncogenes. It was first reported that in B-CLL, the loss of chromosome 13q14, which encodes for tumor suppressive miR-15a and miR-16-1, occurs in ~68% of the cases [65]. Amplification of miR-155, an oncogenic miRNA has been found in various B cell lymphomas and it is shown to be overexpressed in many different hematopoietic cancers and solid tumors [66].

Differential expression of miRNA in normal vs. cancer tissue and in indolent vs. metastatic disease can be used for targeted therapy and in biomarker development. Since, a single miRNA can regulate multiple targets that are involved in various tumorigenic processes, miRNA-based therapies can effectively inhibit various oncogenic pathways and provide better treatment options than those that are currently available [63]. For example, a miRNA that targets multiple tumor promoting genes including, MET, Axl, c-Myc in prostate cancer discussed earlier in this introduction could be developed for therapeutic applications.

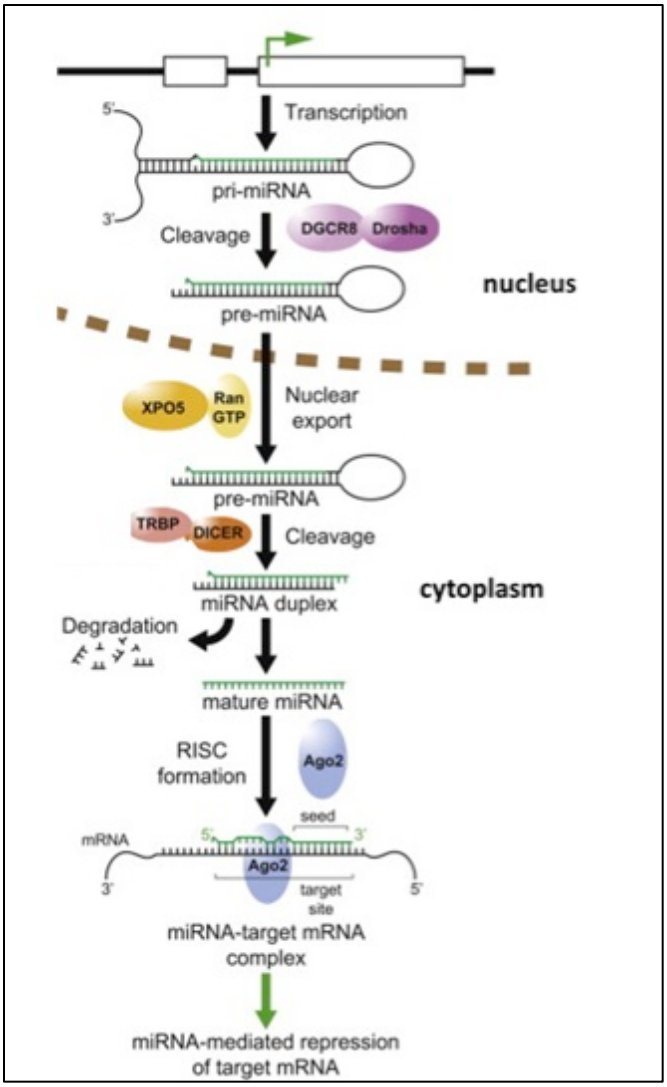

Figure 2 - miRNA biogenesis

miRNA is transcribed from its gene and then processed by the enzyme Drosha and exported from the nucleus by exportin 5. In the cytoplasm, it is further cleaved by the enzyme Dicer to get miRNA duplex and following degradation of the second strand, the mature strand is loaded on the RISC for target mRNA recognition by complementary base pairing to inhibit mRNA translation.

From Jansson MD and Lund AH (2012). MicroRNA and cancer. Mol. Oncol. 6(6): 590-610. Reproduced with permission

There are two emerging strategies for miRNA-based therapies for clinical applications. One strategy involves inhibiting the function of oncogenic miRs by using antagonists like-antagomirs, miRNA sponge or locked-nucleic acids (LNAs) that can bind and inhibit specific miRNAs. Another strategy involves restoring the expression of tumor suppressive miRNA that is downregulated in cancer cells. This can be achieved by delivering mature miRNA mimics through polymer, neutral lipid-based or cationic nanoparticle-based approaches [63]. miRNA replacement therapy is advantageous because the miRNA mimics are very small in size and can be effectively encapsulated and delivered through systemic injections [63]. The mimics have the same sequence as the miRNA that is downregulated in cancer and are expected to behave in a similar manner thus, eliminating nonspecific off-targets effects [63]. A single tumor suppressive miRNA can inhibit multiple oncogenic pathways for example; *let-7* can inhibit Myc, Ras, cyclin D, CDK6 that are involved in promoting oncogenic transformation and cancer cell proliferation [63]. Pre-clinical studies using miRNA delivery have been effective in decreasing tumor growth without toxic side effects in animal models of various cancers. Polyethylenimine (PEI)-mediated systemic delivery of miR-145 and miR-33a reduced tumor growth in a mouse model of colon cancer [67]. Atelocollagen mediated systemic delivery of miR-16 inhibited prostate tumor growth in the bone in an intra-cardiac mouse model [68]. Several approaches including nanoparticle-mediated delivery are currently being tested in pre-clinical miRNA therapeutic studies.

Chitosan Nanoparticles for Therapeutic Applications

Nanoparticles are effective delivery vehicles that can be used for delivering drugs or small RNAs through oral or systemic injections. There are liposomal, solid-lipid, silica, carbon-based and polymeric nanoparticles, each with its unique properties that have the potential for clinical application. Chitosan is a polysaccharide derived from deacetylation of chitin, which is present in the naturally in fungal cell walls and crustaceans shells [69]. Chitosan consists of repeating units of glucosamine and N-acetyl-glucosamine and is insoluble at neutral pH but becomes positively charged and soluble at acidic pH [69]. Chitosan is a naturally occurring biodegradable, biocompatible, non-toxic, low immunogenic polymer and due to its positive charge can effectively bind cell membranes, thus increasing cellular permeability [69, 70]. Chitosan nanoparticles can be formulated by incorporating a polyanion like tripolyphosphate (TPP) into a solution through constant stirring [71]. Further modifications, for e.g., including polyethylene glycol (PEG) can increase its solubility and lead to formulation of cross-linked chitosan nanoparticles for delivering drug combinations for therapeutic applications [72]. Han et al. demonstrated that chitosan nanoparticle can be used for selective delivery in an orthotopic model of ovarian cancer, and silencing of growth-promoting genes by siRNAs delivered through these nanoparticles result in inhibition of tumor growth [70]. Chitosan nanoparticles were used for combination delivery of miR-200 family members that decreased tumor growth and metastasis in different cancer models by inhibiting angiogenesis [73]. Recently, it was shown that systemic delivery of miR-34a through chitosan nanoparticles decreased bone metastasis in a breast cancer and melanoma *in vivo* model [74]. Thus, chitosan nanoparticles have been effectively used for small RNAs delivery in preclinical models and their physiological properties including biocompatibility

and low toxicity makes them an attractive delivery approach for miRNA therapy applications.

Role of miR-34a in cancer

Expression of tumor suppressive miRNA, miR-34 is decreased in several cancers. The miR-34 has three family members: miR-34a, miR-34b and miR-34c that share ~80% homology in their seed sequence leading to targeting similar genes and having redundant functions. However, the expression of miR-34 family members differs in tissue types. miR-34a is more prevalent than other family members in normal human tissues, except, lung, ovary, testes and trachea [75]. The miR-34a gene is located on chromosome 1p3622 while miR-34b and miR-34c are transcribed from polycistronic transcript on chromosome 11q23.1. Both of these gene loci are frequently downregulated in hematopoietic cancers and miR-34a expression is downregulated in many solid tumors including-breast, lung, prostate, liver and pancreatic cancers [66, 75, 76]. Expression of miR-34 family members can be induced in a p53-dependent [77, 78] and p53 independent manner in different cell types and under different conditions [79, 80]. The promoters of miR-34 can be hypermethylated in different cancers leading to their downregulation. For example, miR-34a methylation was detected in ~45% of colon cancer samples and associated with liver metastasis [81]. miR-34a can directly target and repress multiple oncogenic proteins including MET, Axl, c-Myc, Notch-1, JAG-1, Bcl-2, SIRT-1, CDK4 **(Fig. 3)** in different cancers like breast, prostate, hepatocellular carcinoma, NSCLC, among others [45, 53, 75, 82, 83]. These results suggest that there are

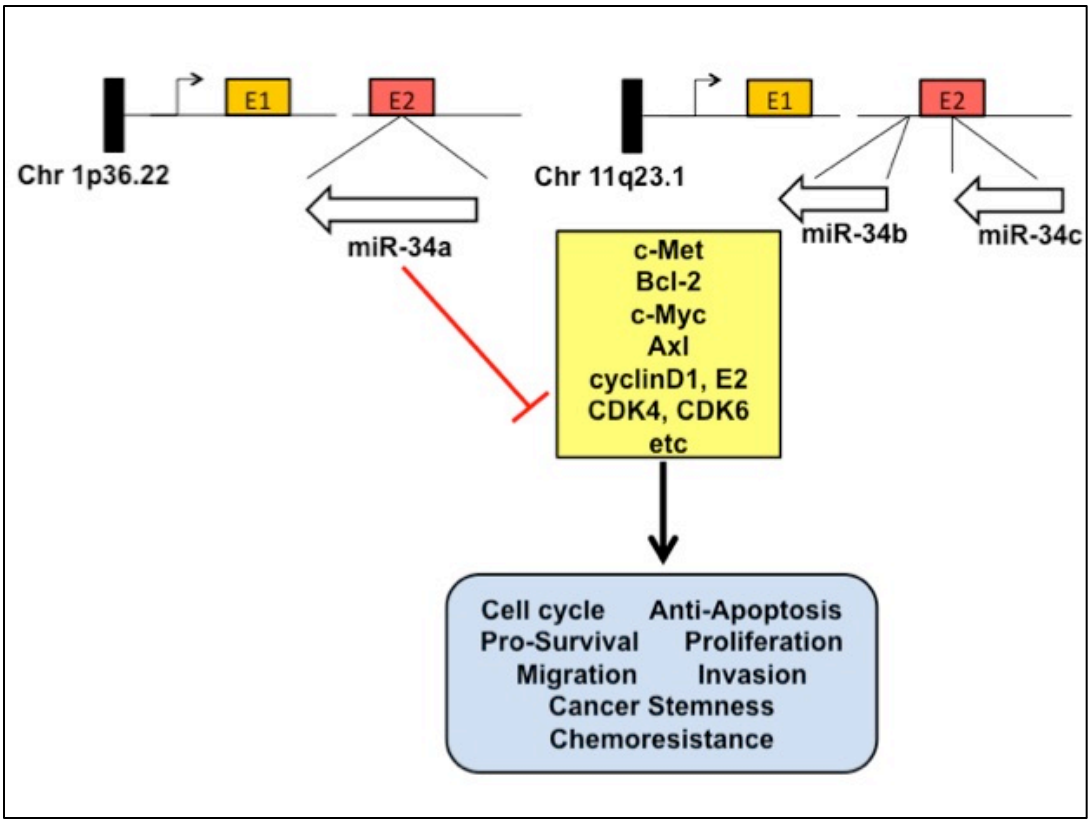

Figure 3 - Role of miR-34a in cancer

miR-34a belong to the miR-34 family and is transcribed from Chr1p36.22 while its other family members are transcribed from gene locus at Chr11q23.1. miR-34a targets and downregulates many genes involved in various pathways promoting cancer development and progression.

multiple mechanisms through which miR-34a expression can be downregulated in cancers which leads to upregulation of its targets that can then promote oncogenic transformation, cell cycle, proliferation, survival, cancer stemness, metastasis and chemoresistance [75] **(Fig. 3)**. Thus, miR-34a replacement therapy could be an attractive strategy to inhibit tumor growth. Liu et al. showed that miR-34a was downregulated in CD44+ prostate cancer cells and it targets CD44 in prostate cancer stem cells (CSCs) [84]. They further show that miR-34a replacement therapy can inhibit tumor growth in an orthotopic model of PC3cells and lung metastasis in LAPC9 model [84]. Systemic delivery of miR-34a in a lipid-based vehicle decreased tumor growth without toxic side effects in a subcutaneous model NSCLC and decreased expression of its targets –MET, CDK4 and Bcl2 [85]. In another study, neutral lipid emulsion based systemic delivery of miR-34a decreased NSCLC growth in an orthotopic and KRAS driven transgenic model [86] and in Kras/p53 double transgenic mouse model by inhibiting known miR-34a targets [87]. In another mouse model of multiple myeloma, miR-34a delivery decreased tumor growth and enhanced survival by decreasing cell proliferation and inducing apoptosis [88]. These works have led to the development of miR-34a formulation in liposomal injection, MRX34 in Phase I clinical trial for the treatment of primary liver cancer.

In prostate cancer, miR-34a has been shown to be downregulated in prostate cancer compared to normal tissue in laser capture microdissected (LCM) specimens [53] and its expression decreases with increasing gleason score in FFPE samples [89]. Overexpression of miR-34a decreases expression of AR, Notch-1 [90], c-Myc [53], MET, CD44 [84] in prostate cancer cells and decreases cancer cell aggressiveness, inhibits proliferation, migration, invasion, and decreases orthotopic tumor growth along with inducing apoptosis [75] **(Fig. 3)**.

The role of miRNAs in regulating autophagy, a process involved in cell death and/or survival is emerging with Liu et al. reporting that miR-34a inhibits autophagy and promotes cell death in retinoblastoma cells [91]. However, autophagic process described below is a complex network of numerous interacting proteins and several forms of autophagy with diverse biological effects in cancer are being discovered.

Autophagy in Cancer

Autophagy is a cellular degradation process, which is induced in response to starvation or stress and leads to clearance of damaged proteins and cellular components [92]. Autophagic process induction begins with the formation of phagophore and following nucleation which involves the class III phosphatidylinositol 3-kinase (PtdIns3k) complex (containing VPS34, Beclin-1, AMBRA-1, ATG14 or UVRAG and BIF1), the vesicle elongates to include cytosolic proteins and organelles **(Fig. 4)**. Vesicle elongation involves conjugation of phosphatidylethanolamine (PE) to LC3 to form LC3II that is attached on the phagophore and helps in phagophore expansion and recognition of cargo. The phagophore then matures into double-layered autophagosomes (AP) that can fuse with the lysosomes to form single layered autolysosomes (AL) **(Fig. 4)**. The lysosomal enzymes lead to vesicle breakdown and degradation of engulfed components. This process requires coordinated network of many essential autophagic genes including –Beclin 1, ATG5 and ATG7 among others. However, Beclin-1, ATG-5 and ATG-7- independent autophagy has also been reported in the literature [93-95]. It is widely accepted that this cellular “self-eating” and evolutionary conserved mechanism promotes survival under cellular stress. However,

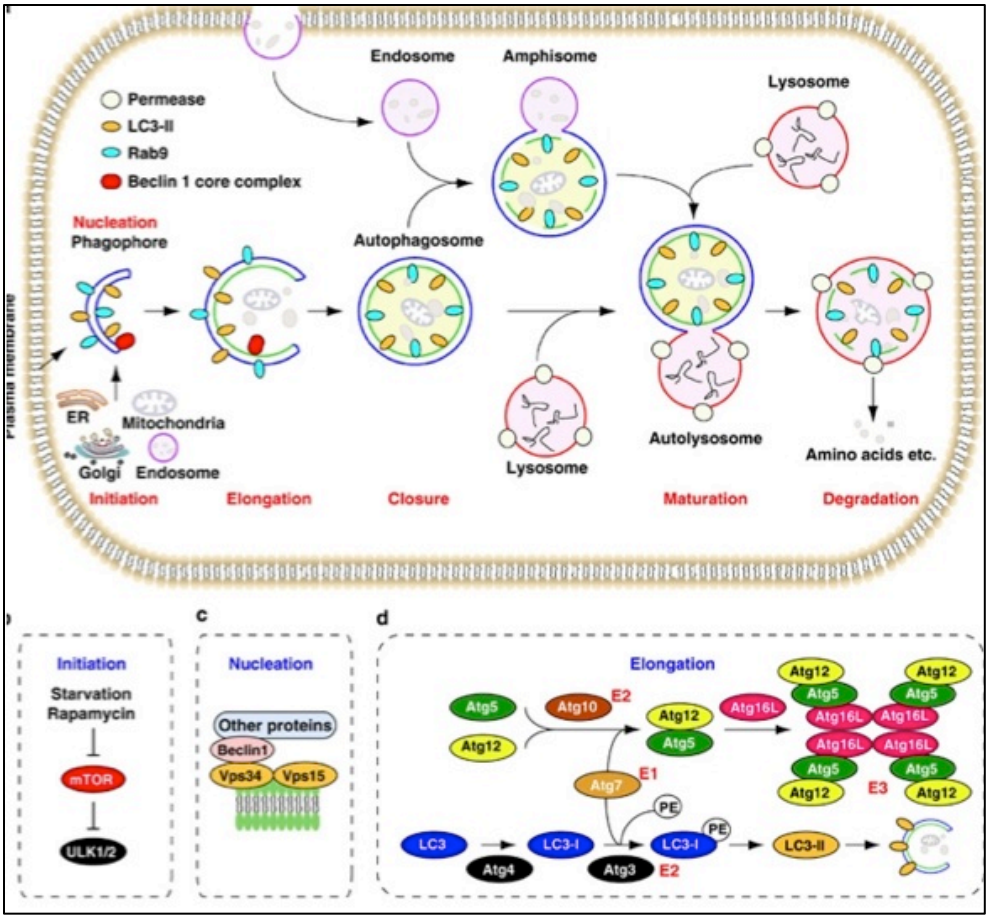

Figure 4 - Autophagic Process

In canonical autophagy, induction of autophagy from stress, nutrient starvation or other conditions leads to nucleation of lipid bilayer to form phagophore, which then elongates to include cytoplasmic components and organelles to form double layered autophagosomes which can then fuse with lysosomes to form single layered autolysosomes where the engulfed components are degraded by lysosome enzymes.

From Kang R, Zeh HJ, Lotze MT and Tang D (2011) The Beclin 1 network regulates autophagy and apoptosis. Cell Death and Differentiation 18, 571–580. Reprinted with permission.

in the context of cancer, autophagy has been implicated to play a tumor promoting as well as a tumor suppressive role.

Autophagy can be induced in cancer cells as a survival mechanism in response to nutrient deprivation, hypoxia, chemotherapeutic and other metabolic stress [92, 96]. Autophagy defects are also found in cancers with loss of essential autophagy gene *beclin1* reported in prostate, breast and ovarian cancer. Loss of *beclin-1* and *atg5* can promote tumorigenesis in different mouse models [96]. Autophagy can induce cell death independent of apoptosis and has been reported as a cell death mechanism in apoptosis deficient cells. It has been shown that prolonged treatment with targeted molecular therapy can induce autophagy leading to cell death. In ovarian cancer, inhibition of prolactin (PRL) and its receptor PRLR leads to non-canonical Beclin-independent destructive autophagy [97]. Inhibition of Akt in sorafenib-resistant HCC can switch protective autophagy to destructive death promoting mechanism [98] while Rottlerin can induce autophagy leading to apoptosis in breast cancer stem cells (CSCs) [99]. In prostate cancer, CCL2 protects PC3 cells from autophagic cell death prolonging their survival in serum-starved conditions through PI3K/Akt/survivin pathway and inhibition of this pathway decreases cell survival [100]. Thus, autophagy can lead to cell death along with or without apoptosis in different cancer cell lines.

Autophagy Regulation by MicroRNAs

miRNAs have been implicated in the regulation of autophagy either directly by targeting mRNAs of autophagic genes or indirectly by modulating autophagy inducers and

repressors [101, 102]. miR-101 can inhibit autophagy by targeting ATG4D and RAB5A involved in nucleation and elongation of vesicles while miR-30a can target BECN1 and reduce rapamycin and cisplatin induced autophagy [101, 103]. While most of the studies have focused on negative regulation of miRNAs on autophagy induction, Tazawa, et al. reported that miR-7 induces autophagy leading to cell death by downregulating EGFR [104]. Under starvation and chemotherapy conditions, miR-34a has been reported to inhibit autophagy by downregulating HMGB1 and promoting cell death [91]. However, downregulation of miR-34a targets including MET and Axl can induce autophagy along with apoptosis in certain cell lines [105, 106] though the mechanism of autophagy induction is not known. It is thus, important to further understand the mechanism and the biological effects of miR-34a-induced autophagy with the introduction of miR-34a therapy in clinical trials.

Summary of Problem and Hypotheses

Prostate cancer is the second most lethal cancer with most deaths resulting from bone metastasis. Several factors including genetic and epigenetic changes leading to multiple molecular alterations contribute to prostate cancer initiation and progression. While organ confined early-stage disease can be treated with androgen ablation or surgical interventions; metastatic disease has dismal survival rates. It is thus essential to develop more effective therapeutic approaches for treatment of advanced disease.

Numerous receptor tyrosine kinases (RTKs) are overexpressed in prostate cancer including, MET, IGF1R, Axl and Her2 that play a role in PCa progression. However, it is not known whether these RTKs cross talk and activate downstream signaling pathways in prostate cancer. One of the goals of this Ph.D. dissertation work was to understand the involvement and interactions of RTKs implicated in prostate cancer. I focused on RTK, MET that is overexpressed in PCa by studying its activation through another RTK overexpressed in PCa, IGF-1R that promotes cancer survival and proliferation. I hypothesized that activation IGF-1/1R pathway leads to ligand independent MET activation in prostate cancer cell lines. I tested this hypothesis in Chapter 3 by determining MET activation and its effects on downstream signaling components after IGF-1/1R pathway activation.

Activation of multiple oncogenic pathways that drive cancer progression asserts the need for therapeutic approaches that target different pathways involved in cancer development and growth. Tumor suppressive miRNA, miR-34a is downregulated in many cancers and targets some of the genes implicated in prostate cancer including RTKs, MET and Axl. The second goal of this Ph.D. dissertation was to determine whether miR-34a delivery decreases tumor growth. I hypothesized that decreased miR-34a expression leads to

upregulation of targets that promote PCa progression, and thus *in vivo* miR-34a replacement therapy could be a novel strategy for treating advanced PCa. I tested this hypothesis by determining miR-34a expression in PCa cell lines and by delivering miR-34a through chitosan nanoparticles in *in vivo* models (Chapter 4 and 5).

Several studies report that autophagy, involved in clearance of damaged organelles and proteins, plays a critical, albeit complex role in cancer. There is evidence for tumor promoting as well as tumor suppressive role of autophagy in cancer. Autophagy and apoptosis can occur simultaneously or exclusively and promote cancer cell death as demonstrated by downregulation of miR-34a targets-Axl and MET that induce autophagy and apoptosis in cell line models. The third goal of this Ph.D. dissertation work was to determine whether miR-34a induces autophagy. To address this question, I performed miR-34a overexpression in multiple cell lines and further knocked down essential genes involved in the autophagic pathway to determine the mechanism of miR-34a-induced autophagy (Chapter 6 and 7).

The work in this dissertation has led to the understanding that MET may be activated by multiple receptor tyrosine kinase receptors, and multi-targeting of these receptors may be important therapeutically. The work in this dissertation further presents miR-34a delivery as an alternative strategy for treatment of bone metastatic prostate cancer for which current therapies are not very effective. Finally, this work identified a novel role of miR-34a in inducing a non-canonical form of autophagy that occurs along with apoptosis and is involved in promoting cell death.

Chapter 2

Materials and Methods

This Chapter is partly based upon "Varkaris A*, **Gaur S*,** Parikh NU, Song JH, Dayyani F, Jin JK, Logothetis CJ, and Gallick GE (2013) Ligand-independent Activation of MET Through IGF-1/IGF-1R Signaling. Int J Cancer. 2013 Oct 1;133(7):1536-46", with permission from International Journal of Cancer and Wiley.

* Equal contribution, shared first authorship.

Materials and Methods:

Cell lines and media:

PC3 and PC3MM2 cells were a gift from Dr. Isiah Fidler's laboratory at MD Anderson. LNCaP and MDA MB 231 cells were purchased from American Type Culture Collection, and C42B4 and PC3MM2-LG (luciferase-GFP labeled) cells were a gift from Dr. Sue Hwa Lin's laboratory at MD Anderson. A549 were a gift from Dr. John Heymach, HepG2 were a gift from Dr. Mein Chie Hung and SKOV3 cells were provided by Dr. Anil Sood's laboratory at MD Anderson. PC3 cells with doxycycline inducible shRNA knockdown of ATG7 (PC3 shATG7 no Dox/+Dox) were provided by Dr. Daniel Frigo's laboratory at University of Houston. PC3, PC3MM2, A549, HepG2 and MDA MB 231 cells were maintained in Dulbecco's modified Eagle medium nutrient mixture F-12 (DMEM/F12, Sigma, St. Louis, MO) with 10% fetal bovine serum (Sigma, St. Louis, MO) and 1% penicillin/streptomycin (Hyclone, Logan, UT). LNCaP cells were cultured in RPMI-1640 media (Sigma, St. Louis, MO) with 10% fetal bovine serum (FBS), supplements (sodium pyruvate, non-essential amino acids, and modified Eagle medium vitamin solution; Invitrogen), and 1% penicillin/streptomycin. C42B4, DU145 and PC3 shATG7 no Dox/+Dox

cells were cultured in RPMI-1640 media (Sigma, St. Louis, MO) with 10% fetal bovine serum (FBS) and 1% penicillin/streptomycin. SKOV3 cells were maintained in RPMI-1640 media with 15% FBS and 0.1% gentamicin (Gemini Bioproducts, Calabasas, CA). 800 ng/ml of Doxycycline was used for inducing knockdown of ATG7 as described previously [107]. Cells were checked every six months and found to be mycoplasma free. The M.D. Anderson Cancer Center Department of Systems Biology performed fingerprinting analysis to confirm the correct identity of the cell lines. All cell lines were validated by STR DNA fingerprinting using the AmpF_STR Identifiler kit according to manufacturer's instructions (Applied Biosystems cat 4322288). The STR profiles were compared to known ATCC fingerprints (ATCC.org), and to the Cell Line Integrated Molecular Authentication database (CLIMA) version 0.1.200808 (http://bioinformatics.istge.it/clima/) (Nucleic Acids Research 37:D925-D932 PMCID: PMC2686526). The STR profiles matched known DNA fingerprints.

Reagents and chemicals

IGF-1 (Catalog # 291-G1) and HGF (Catalog # 294-HGN-005) were purchased from R&D Systems (Minneapolis, MN). Actinomycin D (Catalog # A1410) was purchased from Sigma. Dasatinib (SPRYCEL®) was a gift from Bristol-Myers Squibb (Princeton, NJ).

miRNA Transfection:

Transient transfections were performed using Lipofectamine 2000 transfection reagent (Invitrogen, Carlsbad, CA) for 24 hours, or 48, 72 or 96 hours for time course experiments. Briefly, 100,000 or 200,000 cells were placed in a 6-well plate in growth media without

antibiotics 24 hours prior to transfection. Cells were then transfected with either negative control (N.C.) miRNA or miR-34a mimics/precursors (Ambion, Austin, TX) at a final concentration of 30 nM, according to the manufacturer's instructions.

RNA isolation and quantitative polymerase chain reaction (qPCR):

Total RNA was isolated from the cells by using RNeasy mini kit (Qiagen, Valencia, CA) or using the mirVana kit (Ambion, Austin, TX) according to the manufacturer's instructions. For IGF-1/1R and MET activation studies, cells were serum starved 24 hours prior to IGF-1 stimulation and then 100 ng/ml of IGF-1 was added in serum free media for 0, 18 and 24 hours. To determine miR-34a and U6 (endogenous control) expression, 10 ng of total RNA was reverse transcribed using the TaqMan miRNA reverse transcription kit (Applied Biosystems, Foster City, CA). qPCR was performed on the Agilent 3000P system using the human miR-34a and U6 miRNA TaqMan expression assays and the TaqMan Universal PCR master mix (Applied Biosystems, Foster City, CA). Relative miR-34a expression was determined using the gene comparative C_T method. For gene expression analysis, 200 ng of total RNA was reverse transcribed using ThermoScript^{TM} RT-PCR system for First strand cDNA synthesis (Invitrogen, Carlsbad, CA) according to the manufacturer's instructions. Gene expression was then determined by qPCR using the KiCq Start SYBR Green kit (Sigma, St. Louis, MO) on the Agilent 3000P system. The primers sequences used for gene expression SYBR Green qPCR are listed in **Table 1**.

Table 1 - List of Primers and siRNA Sequences

mRNA/siRNA	Sequence ID	Primer sequence
Axl	Axl-F	5’-CGCAGGAGAAAGAGGATGTC-3’
	Axl-R	5’-ACCTACTCTGGCTCCAGGATG-3’
c-Met	Met-F	5’-CAGATGTGTGGTCCTTTG-3’
	Met-R	5’-ATTCGGGTTGTAGGAGTCT-3’
c-Myc	Myc-F	5’-TCAAGAGGTGCCACGTCTCC-3’
	Myc-R	5’-TCTTGGCAGCAGGATAGTCCTT-3’
ATG5	ATG5-F	5’-GAGTAGGTTTGGCTTTGGTTGA-3’
	ATG5-R	5’-CGTCCAAACCACACATCTCG-3’
ATG7	ATG7-F	5’-GCATCCAGAAGGGGGCTATG-3’
	ATG7-R	5’-AGGCTGACGGGAAGGACAT-3’
BECN1	BECN1-F	5’-GCGATGGTAGTTCTGGAGGC-3’
	BECN1-R	5’-AGACCCTTCCATCCCTCAGC-3’
18s rRNA	18S-F	5’-GTAACCCGTTGAACCCCATT-3’
	18S-R	5’-CCATCCAATCGGTAGTAGCG-3’
siATG5 #4	siATG5 #4-F	5’-GGUUUGGACGAAUUCCAACUUGUUU-3’
	siATG5 #4-R	5’-GAUCACAAGCAACUCUGGAUGGGAU-3’
siATG5 #5	siATG5 #5-F	5’-UCUUCGAAGUGAAGCUUCCAGAAAU-3’
	siATG5 #5-R	5’-CCAAUCCUGUGAGGCAGCCUCUCUA-3’

Enzyme-linked Immunosorbent Assay

To examine the endogenous secretion of HGF, PC3 cells were serum starved for 24 hours and then stimulated with IGF-1 (100 ng/ml) for 0, 18 and 24 hours. Cell culture media was harvested and analyzed in triplicate by human HGF Quantikine ELISA kit (R&D Systems), according to the manufacturer's instructions.

Immunoblotting:

For *in vitro* studies of IGF-1/1R and MET activation, cells were serum starved for 24 hours prior to stimulation with growth factors. For the IGF-1 time-course study, 100 ng/ml of IGF-1 was used in serum free media for different time points. For the IGF-1 dose-dependent study, 0, 10, 25, 50, 100 and 200 ng/ml of IGF-1 were used to stimulate the cells. For Dasatinib studies, cells were pretreated with 100 ng/ml Dasatinib before stimulation with 100 ng/ml IGF-1 or 15 ng/ml HGF for 24 hours and 10 minutes respectively. Protein lysates were prepared using RIPA B lysis buffer (150mM NaCl, 5mM ethylenediaminetetraacetic acid, 20mM sodium phosphate buffer, and 1% Triton X-100, pH 7.4, along with 1 tablet of protease and phosphatase inhibitor cocktail (Roche, Indianapolis, IN). For *in vivo* samples, tumor sections were cut and homogenized by magnetic beads in RIPA A lysis buffer (1% Triton X-100, 0.% SDS, 0.5% sodium deoxycholate, 150mM NaCl, 5mM EDTA, 5mM sodium pyrophosphate, 20mM sodium phosphate buffer, pH 7.4 along with 1 tablet of protease and phosphatase inhibitor cocktail). Total protein lysates (15 or 30 µg) were loaded onto an 8% or 12% polyacrylamide gel, which were then transferred to a polyvinylidene

difluoride (PVDF) membrane and blocked with 5% milk in tris-buffered saline with Tween-20. Membranes were probed with specific primary antibodies: c-Met (C12; Santa Cruz Biotechnology, Santa Cruz, CA), Axl, cleaved caspase 3, LC3B, Beclin-1, ATG5 and ATG7, phospho-Met Y1234/35, phospho-Met Y1349, phospho-Src Y416, Akt, phospho-Akt (S473), MAPK, phospho-MAPK, IGF-1R, phospho-IGF-1R beta Y1135/36, ERK1/2 (Cell Signaling, Danvers, MA), Src (EMD Millipore, Temacula, CA), c-Myc (Santa Cruz Biotechnology), GAPDH (EMD Millipore), Vinculin (Sigma) and horseradish peroxidase-conjugated goat anti-mouse or goat anti-rabbit secondary antibody (Bio-Rad, Hercules, CA).

Migration and invasion assay:

Migration and invasion assays were performed using migration and invasion assay inserts (BD Biosciences, Bedford, MA). For IGF-1/1R and MET activation studies, PC3 cells expressing the non-targeting and shMET targeting vector were serum starved for 24 hours and then incubated with IGF-1 (100 ng/ml) for 24 hours in a culture dish. Cells were trypsinized and for each cell type, a total of 50,000 cells were seeded on top of the inserts in serum-free media. Media containing IGF-1 (100 ng/ml) or HGF (15 ng/ml) was used as chemoattractant and cells were allowed to migrate for 24 hours. A total of 100, 000 cells were seeded on top of the inserts in serum-free media 24 hours after transfection with negative control or miR-34a mimic. Serum-free media was used as a chemoattractant and cells were allowed to migrate or invade for 24 hours. The bottom of the inserts was then stained with Hema-Stain (Millipore, Temacula, CA). The number of migrated or invaded

cells for five fields was counted under a bright-field microscope and plotted as the number of cells migrated or invaded per field. Each experiment was performed in triplicate.

Cell Proliferation assay:

For measuring cell viability, The CellTiter 96® AQueous Non-Radioactive Cell Proliferation Assay kit (Promega, Madison, WI) was used according to the manufacturer's instructions. Briefly, 1000 N.C. or miR-34a transfected cells were plated in a 96-well plate for 48, 72 and 96 hours post-transfection time points of cell viability in growth media. A solution of MTS and PMS was added to each well, incubated at 37°C 5% CO_2 for 2 hours and absorbance measured at 490 nm by EnVision® multilabel reader (Perkin Elmer, Shelton, CT). Cell proliferation using Hoechst 33342 dye (Life Technologies) was performed according to manufacturer's instructions. Briefly, 2000 N.C. or miR-34a transfected cells with or without siATG5 and siATG7, and with or without shATG7 or shBeclin-1 were seeded in a 96-well plate and fluorescence from Hoechst dye was measured for different time points by a plate reader and plotted as fold change relative to control (N.C. at 48h).

Flow cytometry

Propidium iodide (PI) and RNAse A (Sigma) solution was prepared according to the manufacturer's instructions. For cell cycle analysis, cells transfected with N.C. or miR-34a for different time points were fixed in 70% Ethanol overnight. Fixed cells were then resuspended in 50 µg/ml PI solution in PBS for 1 hour in the dark and then 0.2 mg/ml DNAase-free RNase A was added and the samples incubated at 37°C 5% CO2 for 30 minutes and read on Beckman Coulter Gallios flow cytometer and analyzed on Kaluza®

Software (Beckman Coulter). Singlet cell population was gated to exclude cell aggregates and percentage of cells in sub-G1, G1, S and G2M phase were recorded. GFP-Certified® Apoptosis/Necrosis detection kit (Enzo Life Sciences, Farmingdale, NY) was used for detection of early and late-stage apoptotic as well as necrotic cells. An Annexin V-EnzoGold (enhanced Cyanine-3) (Ex/Em: 550/570nm) conjugate was used for detection of early stage apoptotic cells in the FL2 channel and Necrosis Detection Reagent (Red) similar to the red-emitting dye 7-AAD (Ex/Em: 546/647nm), was used for late apoptosis and necrosis detection in FL3 channel by FACS Gallios. Acridine Orange (AO) (Life Technologies) was used to measure acidic vesicular organelles (AVOs). Cells transfected with N.C. or miR-34a for different time points were incubated with 1ug/ml acridine orange for 30 min in the dark. In AO-stained cells, the cytoplasm or nucleolus fluoresce bright green and dim red, whereas acidic compartments fluoresce bright red. Green (510–530 nm) and red (>650 nm) fluorescence emissions from 10,000 cells illuminated with blue (488 nm) excitation light were measured with a FACS Gallios.

Transmission Electron Microscopy (TEM)

Samples fixed with a solution containing 3% glutaraldehyde plus 2% paraformaldehyde in 0.1 M cacodylate buffer, pH 7.3 were washed in 0.1 M cacodylate buffer and treated with 0.1% Millipore-filtered buffered tannic acid, postfixed with 1% buffered osmium tetroxide for 30 min, and stained en bloc with 1% Millipore-filtered uranyl acetate. The samples were washed several times in water, then dehydrated in increasing concentrations of ethanol, infiltrated, and embedded in LX-112 medium. The samples were polymerized in a 60°C oven for 2 days. Ultrathin sections were cut in a Leica Ultracut microtome (Leica, Deerfield, IL),

stained with uranyl acetate and lead citrate in a Leica EM Stainer, and examined in a JEM 1010 transmission electron microscope (JEOL, USA, Inc., Peabody, MA) at an accelerating voltage of 80 kV. Digital images were obtained using AMT Imaging System (Advanced Microscopy Techniques Corp, Danvers, MA). Mr. Kenneth Dunner, Jr., performed TEM at the TEM core (Institutional Core Grant #CA16672 High Resolution Electron Microscopy, UTMDACC).

siRNA and shRNA transfection

Ready-to-transfect short hairpin (sh) RNA–GFP–puromycin constructs against human IGF1-R (#SR302344) and Src (#SR304574) were purchased from OriGene Technologies (Rockville, MD). An universal non-targeting negative control shRNA (#SR30004) was provided by the manufacturer. An activated Src (Y527F) expression vector was used as described previously (Allgayer, et al. JBC 1999). Cells were transfected using Fugene 6 reagent (Roche) or JetPRIME (Polyplus transfection, Radnor, PA) according to the manufacturer's instructions. Lentiviral shc-*met* constructs were a gift from Dr. Menashe Bar Eli at The University of Texas MD Anderson Cancer Center. Stable clones were selected with puromycin or sorted with GFP. Target knockdown was verified 3–4 weeks after transfection by western blots. Two siRNA sequences each for ATG5 and ATG7 were provided by Dr. Daniel Frigo's laboratory. PC3 cells were transfected with 100nM of siATG5 or siATG7 sequences using DharmaFECT1 (GE Healthcare, Lafayette, CO) transfection reagent and 24 hours later, siATG5 or siATG7 cells were transfected with N.C. or miR-34a using lipofectamine 2000. Lentiviral shRNA constructs for Beclin-1 were provided by MD Anderson shRNA and ORFeome core facility. GIPZ lentiviral shBeclin-1

(GE Healthcare) constructs were packaged in lentivirus and PC3 cells were transduced with the concentrated vial titer with 8 μg/ml polybrene and following infection GFP positive cells were sorted by Becton Dickinson FACS Aria II to get shBeclin-1 cells.

Immunohistochemistry (IHC) and Immunofluorescence (IF)

Paraffin embedded tumor sections were deparaffinzed and hydrated. Citrate buffer (0.1M , pH 6.0) was used for antigen retrieval, 3% H_2O_2 (Fisher Scientific, fair Lawn, NJ) in PBS was used for endogenous peroxidase blocking and 4% fish gelatin (Electon Microscopy Sciences, Hatfield, PA) was used for protein blocking. Met (Santa Cruz) or Axl (Thermo Scientific) primary antibody diluted in 4% fish gelation were added to the slides overnight in a humidity chamber at 4°C. Slides were then washed with PBS and incubated with MACH4 polymer (Bio Care Medical, Concord, CA) for 1 hour at RT. DAB (Dako, Carpinteria, CA) chromogen was used for visualization of the signal and the nuclei were counterstained with Hematoxylin (Sigma). Slides were then dried and mounted with Universal mount and examined under bright field microscope. For TUNEL staining, DeadEnd colorimetric TUNEL system (Promega) was used according to manufacturer's instructions. Briefly, FFPE slides were deparaffinized and antigen retrieval performed with 1X Dako Antigen Retrieval buffer. Slides were then washed with PBS, blocked with 3% H_2O_2 in methanol for peroxidase blocking and in 4% fish gelatin for protein blocking. The slides were incubated with 4% paraformaldehyde in PBS for 10 minutes at RT, washed with PBS, incubated in 0.2% TritonX-100 in PBS for 15 min at RT, washed with PBS and incubated with Equilibration buffer (Promega) for 10 min at RT. TUNEL incubation buffer (Promega) was added to each slide for 1 hour at 37°C in the dark. Slides were washed in 2X SSC (Pomega) and

counterstained with Hoechst mounting media (Life Technologies) and visualized under fluorescence microscope. IHC and IF images were quantified by ImageJ software as previously described [108].

In situ hybridization(ISH):

Clinical sample slides were obtained from MDACC GU Medical Oncology department. H&E slides for each sample were provided along with unstained freshly cut slides containing normal and prostate tumor samples. DIG-labeled probed for miR-34a and U6 endogenous control were purchased from Exiqon (Woburn, MA) and *in situ* hybridization (ISH) was performed according to manufacturer's instructions by the Center for RNA Interference and non-coding RNA at MD Anderson.

Animal studies:

One million PC3MM2 cells were injected sub-cutaneously in nude mice. One week after cell injection, mice were randomized and divided into Control (N.C.) or miR-34a group. Chitosan nanoparticles complexed with N.C. or miR-34a were prepared by the Center for RNA Interference and non-coding RNA at MD Anderson. Nanoparticles containing N.C. or miR-34a were delivered through tail vein injection, every three days for two weeks. Tumor volume was measured by caliper instrument every three days. After two weeks of treatment, the animals were sacrificed and tumors harvested for protein, IHC, ISH and IF. For intra-femur experiment, $1x\ 10^6$ PC3MM2-LG cells labeled with luciferase and GFP were injected in the femur of the mice. Ten days after cell injection, mice were randomized into two groups- control and miR-34a. The chitosan nanoparticles containing N.C. or miR-34a were

delivered via tail-vein injection every three days for three weeks. Tumor growth was monitored through bioluminescence imaging (IVIS 200) and tumor volume was measured before the start of treatment and at the end of treatment by magnetic resonance imaging (MRI) (Bruker 4.7T). Micro CT imaging was performed on the Explore Locus RS pre-clinical in vivo scanner (GE Medical Systems, London Ontario) to visualize bone integrity at the end of the experiment in control and miR-34a treated mice.

Statistics:

Student's *t* tests and one-way ANOVA analysis of variance were used for all statistical comparisons and a p value of <0.05 was considered statistically significant. Statistical analyses were performed using the GraphPad Prism software.

Chapter 3

Ligand-independent MET Activation by the IGF-1/1R Pathway

This Chapter is based upon "Varkaris A*, **Gaur S*,** Parikh NU, Song JH, Dayyani F, Jin JK, Logothetis CJ, and Gallick GE (2013) Ligand-independent Activation of MET Through IGF-1/IGF-1R Signaling. Int J Cancer. 2013 Oct 1;133(7):1536-46", with permission from International Journal of Cancer and Wiley.

* Equal contribution, shared first authorship.

Multiple receptor and non-receptor tyrosine kinases promote metastatic growth of prostate cancer resulting in numerous clinical trials with small molecule inhibitors focusing on targeting these kinases. Unfortunately, most of the clinical trials have not demonstrated significant improvements in survival. There are multiple reasons for lack of success of these inhibitors including involvement of multiple drivers of PCa progression as discussed in the spiral model (see Introduction). Activation of alternative compensatory pathways or activation of targeted kinase through non-canonical mechanism/s could also result in failure of the inhibitors. An example of a tyrosine kinase receiving considerable attention in prostate cancer is MET. MET is a receptor tyrosine kinase involved in embryonic development and in adults MET facilitates tissue regeneration [34, 109]. In cancer, aberrant expression and activation of MET can promote tumor progression by activating MAPK signaling, PI3K-Akt axis and STAT pathway involved in cell invasion, migration, survival and proliferation [34, 41]. In the past few years, several inhibitors have targeted MET oncogene, frequently associated with progression of solid tumors, including antibodies targeting its ligand HGF; antibodies targeting the receptor, and small molecule inhibitors targeting the kinase activity. While trials are ongoing, many have not been promising as exemplified in the recent failure

of cabozatinib, a multi-kinase inhibitor with MET and VEGFR2 as the principle targets. These failures demonstrate the necessity to understand more about the regulation of the targeted kinase. More evidence is accruing for receptor cross talks, and ligand independent pathways of MET activation have been reported in other cancers [41]. However, in prostate cancer (PCa), ligand independent MET activation through other growth factor receptors has not been investigated. In this chapter, I analyzed the ability of the IGF-1/1R pathway, aberrantly activated in PCa [110] and in PCa bone metastasis [111], to affect MET signaling. I hypothesized that activation of IGF-1/1R pathway leads to activation of MET and downstream signaling components that promote tumorigenic and metastatic properties of PCa cells. To test this hypothesis, I used PCa cell line, PC3 with high levels of MET and IGF-1R receptor that are representative of the majority of metastatic PCa tumors [40, 112] and examined the effects of IGF-1 stimulation on MET phosphorylation. I identified one of the essential components required to mediate IGF-1/1R induced MET activation and further determined the effects of MET inhibition on IGF-1-mediated migration in PC3 cells.

IGF-1 induces delayed activation of MET in PCa cell lines and xenograft tumors

Insulin-like Growth Factor (IGF) is aberrantly expressed in the microenvironment of prostate cancer bone metastases and known to be a poor prognostic marker for PCa survival [113]. To determine if IGF-1 affected MET phosphorylation, a time course assay was performed in which IGF-1 was added to serum-starved cells and activation of signaling enzymes was examined as described in Materials and Methods.

As shown in **Fig. 5**, robust activation of IGF-1R was observed within 10 min, with no activation of MET at this time. Activation of Src, Akt, and MAPK were observed with similar kinetics to IGF-1R activation **(Fig. 6)**, as expected. No change in protein expression was observed for any of these signaling enzymes. In contrast to the acute activation of signaling enzymes after IGF-1 addition, MET phosphorylation was observed beginning at 12h, reaching maximal levels at 18h, with sustained phosphorylation for at least 24h after stimulation of PC3 cells with IGF-1 **(Fig. 5)**. Both Y1234-1235 (tyrosine kinase domain) and Y1349 (multi-substrate docking) sites were phosphorylated **(Fig. 5)**, suggesting full activation of MET occurs at these later time points. No differences in MET protein and mRNA expression were evident by immunoblotting **(Fig. 5)** and qPCR **(Fig. 7)** respectively.

To determine if IGF-1 induction of MET phosphorylation were dose-dependent, PC3 cells were stimulated with different doses of IGF-1 ranging from 10-200 ng/ml. Under these conditions, IGF-1R phosphorylation increased at each concentration of IGF-1 **(Fig. 8)**. In contrast, 25 ng/ml IGF-1 was sufficient to induce delayed phosphorylation of MET, and no further increases in phosphorylation were observed with higher concentrations of IGF-1. These results suggest a threshold of IGF-1R activation is sufficient to fully induce MET phosphorylation. MET and IGF-1R protein levels remain unchanged under these conditions **(Fig. 8).**

To examine the magnitude of MET phosphorylation due to IGF-1 (100ng/ml) relative to HGF (15ng/ml), PC3 cells were stimulated with these growth factors for 10 min and 24h and activation of IGF-1R and MET were examined. IGF-1 induced a strong delayed

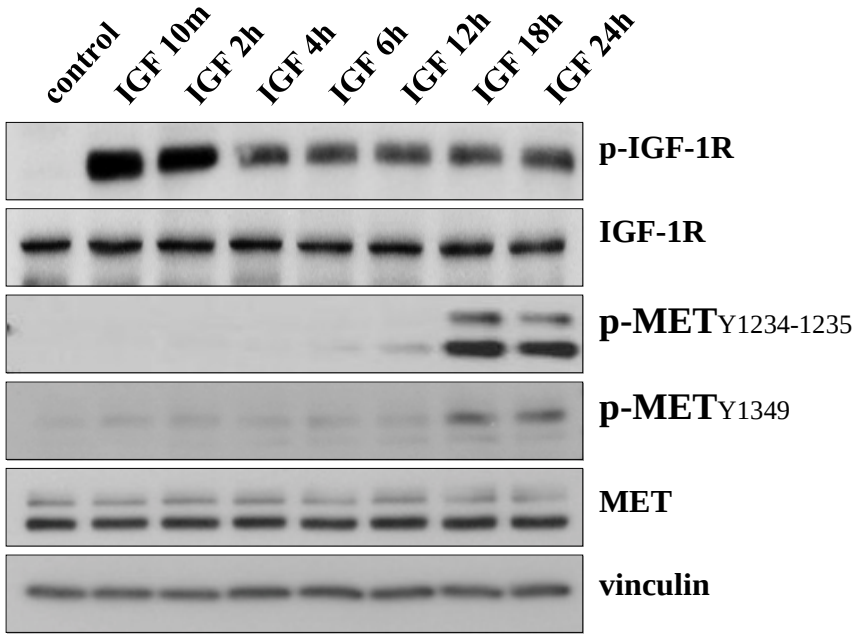

Figure 5 - IGF-1 induces delayed MET activation

IGF-1 was added (100 ng/ml) to PC3 cells and expression and phosphorylation of IGF-1R and MET was examined at indicated times by immunoblotting.

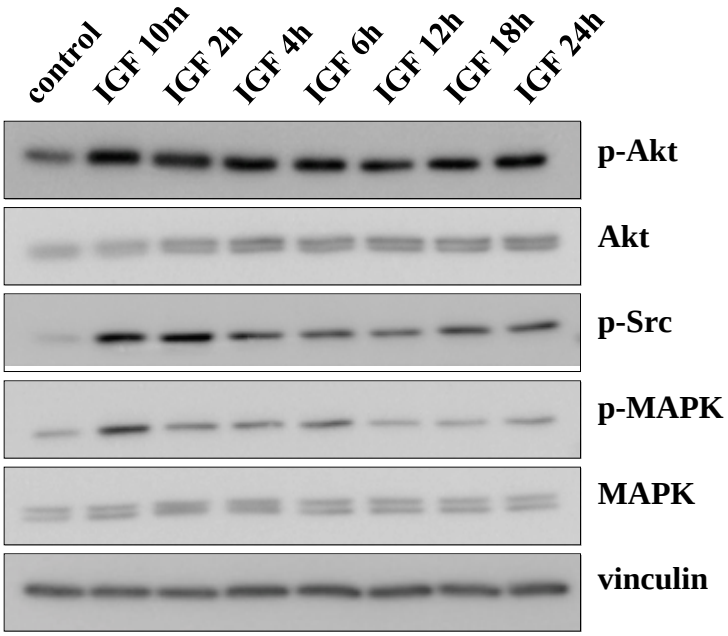

Figure 6 - IGF-1 phosphorylates downstream signaling components

IGF-1 was added (100 ng/ml) to PC3 cells and expression and phosphorylation of Akt, Src and MAPK was examined at indicated times by immunoblotting.

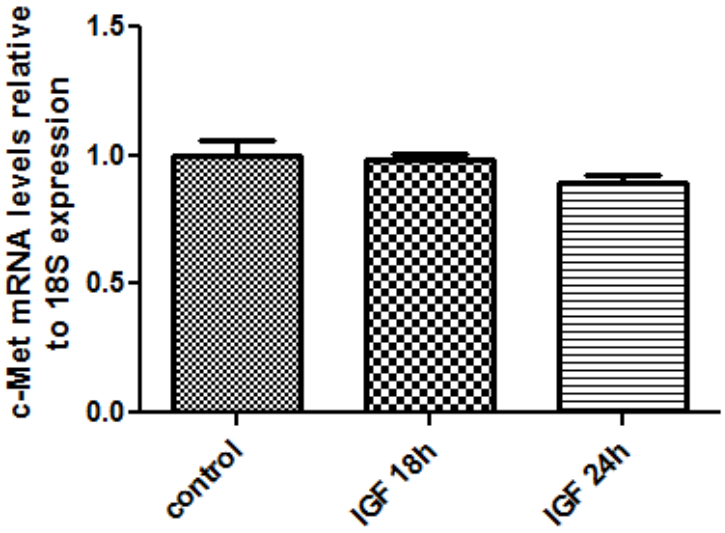

Figure 7 - Expression of MET following IGF stimulation of PC3 cells

To determine if IGF-1 increased the expression of *c-met* RNA, cells were treated with IGF-1 and *c-met* RNA was measured by qPCR 18 and 24h after IGF-1 addition. Expression was normalized to 18s RNA expression. Data represents Mean and SEM from three independent experiments

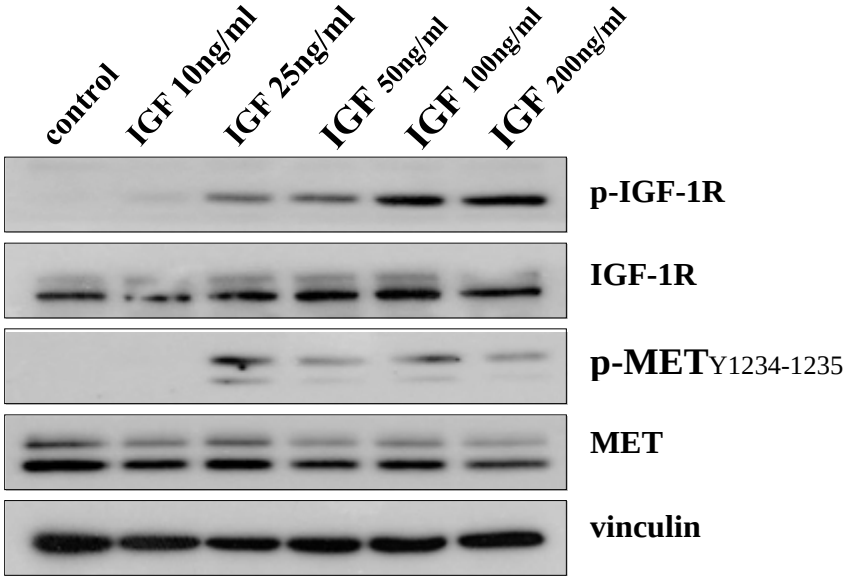

Figure 8 - Dose-dependent effects of IGF-1 on receptor activation

Different concentrations of IGF-1 were added to PC3 cells at indicated times and the magnitude of MET and IGF-1R activation was examined.

activation of MET at 24h that was only slightly less than the rapid (10 min) MET phosphorylation by HGF **(Fig. 9)**, demonstrating that activation of MET by IGF-1 is likely to activate MET functions.

Next, the effects of IGF-1 stimulation on MET activation in PC3 xenograft tumors were examined. Briefly, 20µl of IGF-1 (100 ng/ml) were injected directly into established PC3 xenografts and tumors were harvested 24h after injection. Immunoblotting analysis showed that treated tumors had significantly higher levels of MET and IGF-1R phosphorylation compared to control tumors, whereas no changes in MET and IGF-1R expression were observed **(Fig. 10)**. These experiments demonstrate that, IGF-1 is capable of inducing MET phosphorylation *in vitro* and *in vivo*.

IGF-1-induced delayed MET activation is HGF-independent

HGF is the sole known ligand of MET [34, 41]. To examine if endogenous expression/secretion of HGF could play a role in IGF-1-mediated MET activation, HGF mRNA was examined by qPCR in PC3 cells treated with IGF-1 for time points that correspond to minimal and maximal MET activation by IGF-1. The results show no statistically significant differences between control and treated groups **(Fig. 11A)**. To further examine potential HGF expression, cell culture media from each group was harvested and levels of HGF were determined by enzyme-linked immunoabsorbent assay (ELISA). Secreted HGF levels were beneath the level of detection in all groups **(Fig. 11B)**, suggesting that PC3 cells do not secrete HGF before or after IGF-1 addition.

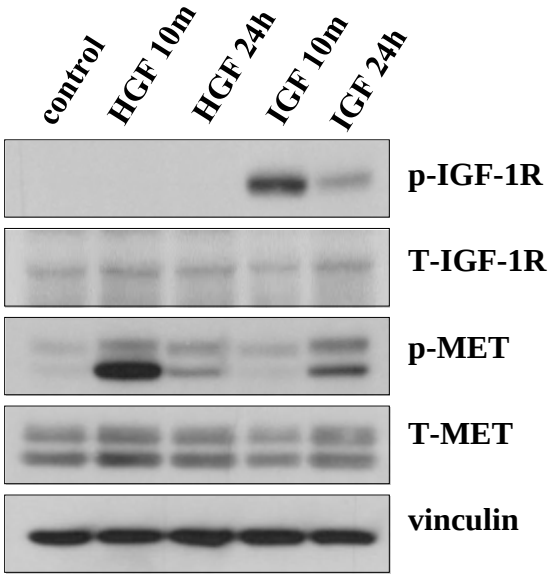

Figure 9 - Comparison of HGF and IGF induced MET activation

IGF-1 (100 ng/ml) and HGF (15 ng/ml) were added to PC3 cells at indicated times and activation of MET and IGF-1R was examined.

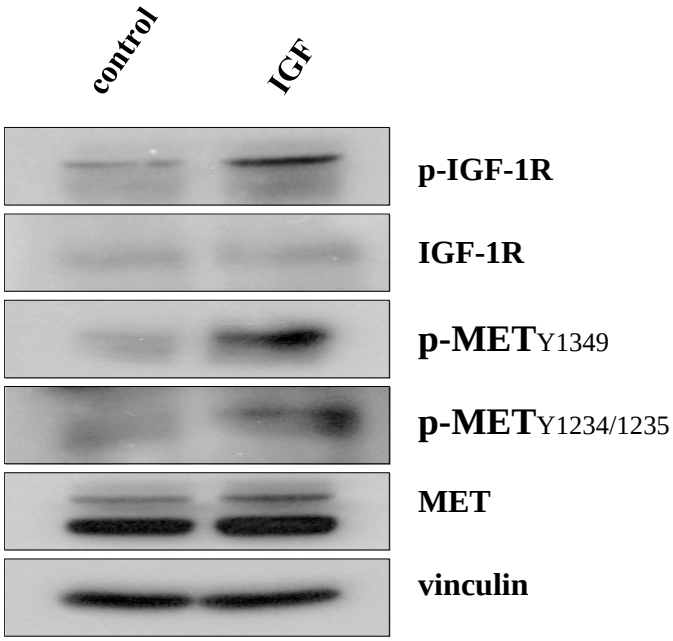

Figure 10 - IGF-1 induces MET activation in PC3 tumor xenografts

PC3 tumors were grown subcutaneously until they reached a volume of 500 mm^3. IGF-1 (100 ng/ml, 20µl total volume) was injected into the tumor. Tumors were harvested 24h later, and expression and phosphorylation of IGF-1R and MET was examined.

A

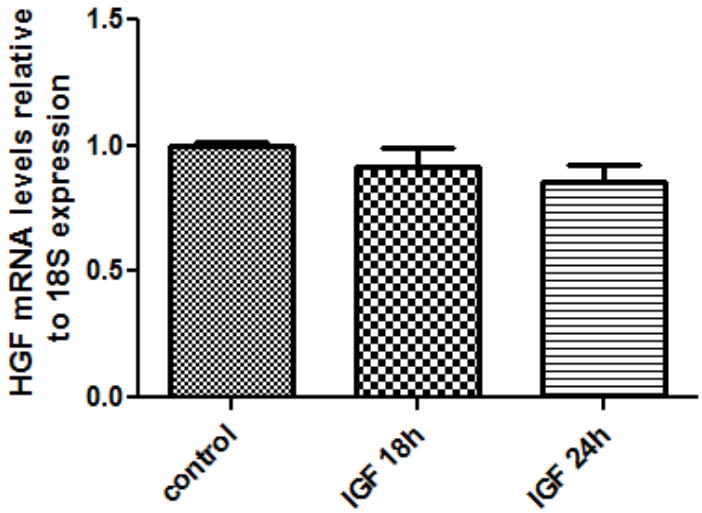

B

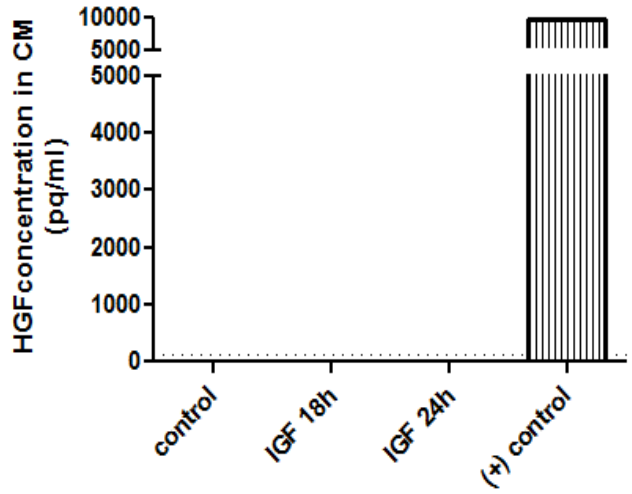

Figure 11 - Expression of HGF after IGF-1 addition

Total RNA was isolated from PC3 cells 24h after IGF-1 addition (100ng/ml), and HGF expression was examined by qPCR (A) and ELISA (B). Data represent Mean and SEM from three independent experiments.

IGF-1-mediated MET phosphorylation requires IGF-1R activation

To examine whether IGF-1R activation were required for "lateral" MET phosphorylation, we generated a PC3 cell line in which IGF-1R was stably knocked down by expression of an shIGF-1R construct as described in Materials and Methods. Expression of IGF-1R was reduced >90% **(Fig. 12**, lane 5 and 6**)**. When the shIGF-1R cells were stimulated with IGF-1, delayed MET phosphorylation was abolished; demonstrating activation of IGF-1R is required for inducing MET phosphorylation **(Fig. 12**, lane 5 and 6**)**.

Src activation is essential for IGF-1-induced delayed MET activation

In a study of Dulak et al. tyrosine kinase, Src, was shown to be an essential mediator of lateral activation of MET by EGFR [43]. To examine potential roles of Src family kinases in delayed MET activation by IGF-1R, I first used the multi-targeted SFK inhibitor, dasatinib. PC3 cells were pretreated with 100 nM of dasatinib for 2h before stimulating with IGF-1 and HGF for 24h and 10 min respectively. Under these conditions, IGF-1-induced delayed MET activation was abolished, suggesting that activation of a Src family kinase may be required for delayed MET phosphorylation **(Fig 13)**. In contrast, dasatinib had little effect on HGF-induced direct MET activation **(Fig 13)**. Decreases in MET activation were observed in dasatinib only treated cells **(Fig 13**, lane 2**)** suggest that dasatinib might have a small effect on MET phosphorylation (dasatinib is a multi-kinase inhibitor). To determine if activation of Src (as opposed to other Src family kinases) were essential to delayed MET phosphorylation by IGF-1, I stably expressed a shRNA for Src in PC3 cells. As shown in **Fig. 12**, greater than 90% knockdown of Src was observed **(Fig 12**, lane 3 and 4).

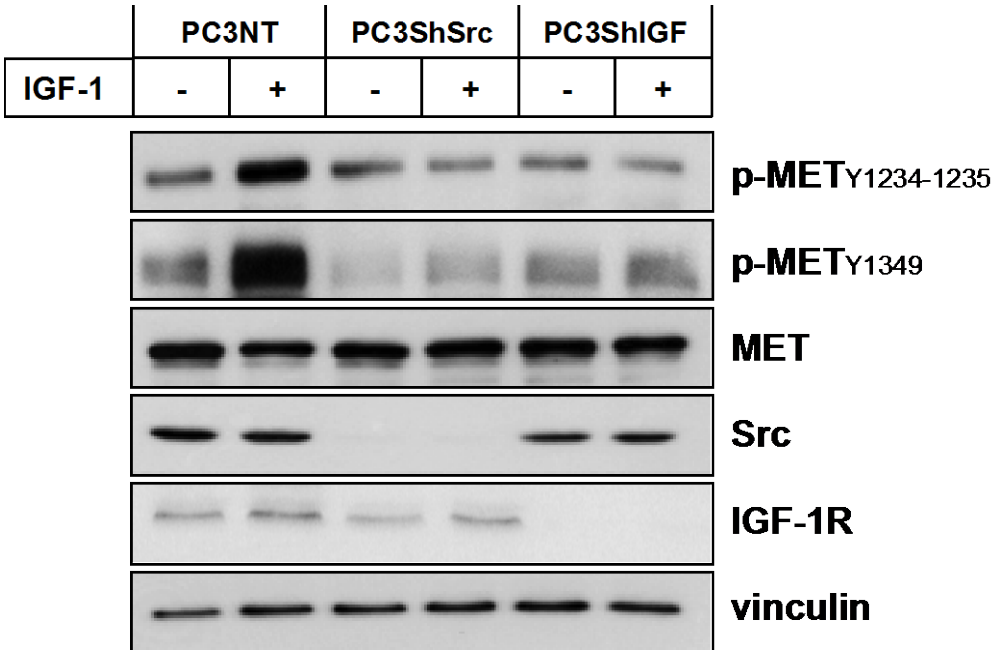

Figure 12 - Effects of IGF-1 and Src knockdown on IGF-1-mediated MET activation

IGF-1 (100ng/ml) was added to non-targeting cells or cells with stable knockdown of IGF-1R (shIGF-1R) or Src (shSrc), following which MET phosphorylation was examined. Vinculin was used as a loading control.

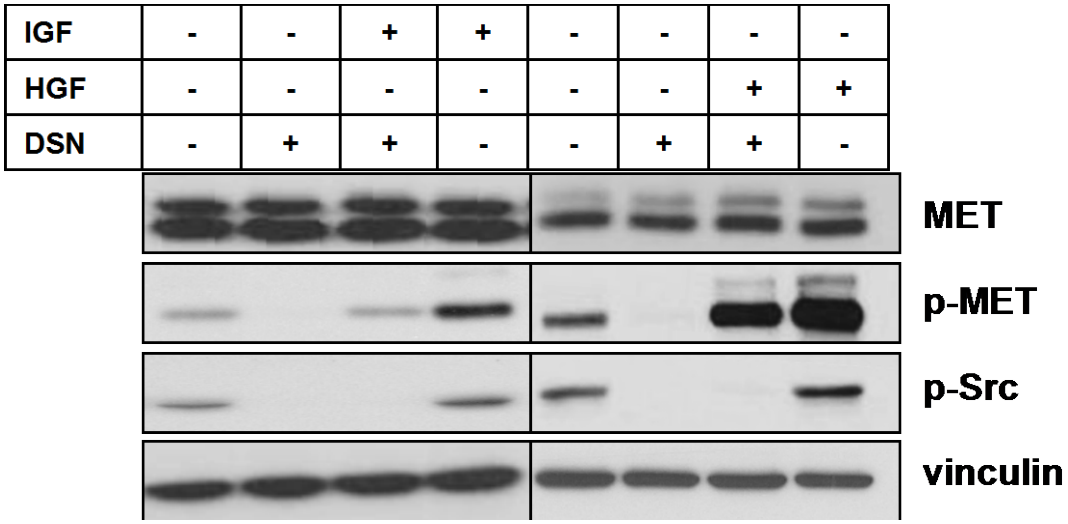

Figure 13 - Effects of Dasatinib on IGF-1-mediated MET activation

PC3 cells were pre-treated with100nM of Dasatinib for 2h after which they were stimulated with IGF-1 (100 ng/ml) for 24h or HGF (15 ng/ml) for 10min. MET and Src phosphorylation were then examined.

As with non-targeting clones, IGF-1 was added and MET phosphorylation was examined 18h later. In PC3 cells expressing a non-targeting shRNA, MET was phosphorylated under these conditions **(Fig. 12**, lane 1 and 2**)**. In contrast, the shSrc cells were unable to induce delayed MET activation, with expression of MET unchanged, suggesting Src is required for IGF-1 induced MET activation **(Fig. 12**, lane 3 and 4**)**. To further determine whether Src activation was required for IGF-1-induced MET phosphorylation, I transfected PC3 ShSrc cells with a plasmid harboring a Src mutant (Y527F) that leads to constitutive Src activation and then stimulated the cells with IGF-1 for 24h. Expression of an activated Src led to MET phosphorylation in the presence or absence of IGF-1 **(Fig. 14)**, suggesting Src activation alone is necessary and sufficient to trigger the cascade leading to MET activation.

Inhibition of transcription abolishes IGF-1R-mediated MET phosphorylation

Since, MET phosphorylation occurs much later than activation of other signaling intermediates (Src, Akt, MAPK), I determined if transcription were required for IGF-1R to MET cross talk. For these experiments, PC3 cells were treated with the pan-transcription inhibitor, actinomycin D, alone or in combination with IGF-1 for time points corresponding to the maximal IGF-1-induced MET activation. Lack of synthesis of the precursor of MET **(**upper band, **Fig. 15)** indicates actinomycin D blocked *de novo* c-*met* mRNA synthesis. Processed MET (lower band) was still present, as expected. These results suggest no further transcription of MET occurred under these conditions. Successful inhibition of transcription abolished IGF-1-induced MET activation **(Fig. 15)**, whereas IGF-1-induced IGF-1R

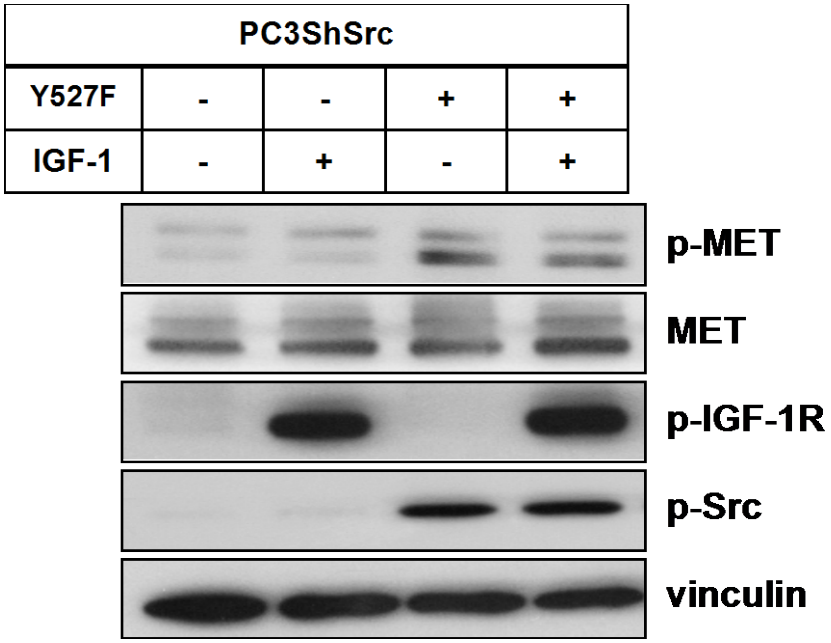

Figure 14 - Src activation is required for IGF-1-mediated MET activation

PC3 cells with stable knockdown on Src (PC3shSrc) were transfected with a constitutively active SRC (Src Y527F) mutant for 48h followed by stimulation with IGF-1 (100 ng/ml) for 24h. Phosphorylation of MET (pY1349), IGF-1R and Src were then examined after 24h of IGF-1 stimulation.

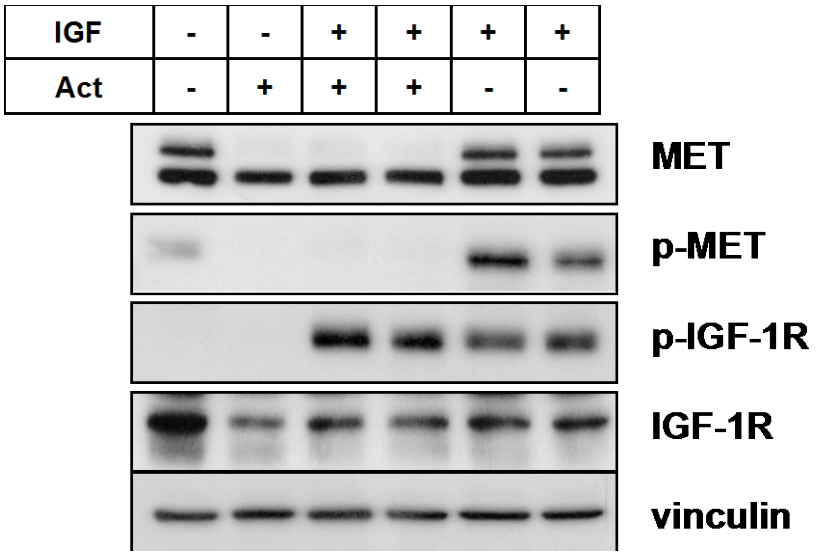

Figure 15 - Inhibition of transcription abolishes IGF-1R-mediated MET phosphorylation

Actinomycin D (0.01 mg/ml) was added to cells to inhibit transcription. IGF-1 was then added (100 ng/ml) and IGF-1R and MET phosphorylation was examined 18h (lanes 3 and 5) and 24h (lanes 4 and 6) later.

activation (which occurs within 10 min and does not require transcription) was unaffected. These findings indicate that transcription is essential for IGF-1-induced MET activation.

MET inhibition abrogates IGF-1-induced migration

Upon activation, MET signaling plays a critical role in prostate cancer cell invasive growth (scattering, migration, invasion and metastasis) [34, 35]. I therefore determined if IGF-1-induced MET activation affected cellular migration. These experiments were performed with a PC3 cell line stably expressing shRNA to c-*met*, constructed as described in Materials and Methods. Expression of the c-*met*-specific shRNA resulted in >95% reduction of MET protein expression compared to PC3 cells expressing a non-targeting shRNA **(Fig.16A)**. A migration assay was then performed with cells expressing MET or in cells in which MET had been knocked down and migrated cells were counted. Under these conditions, IGF-1 induced a 2.5 fold increase in migration in cells expressing a non-targeting vector relative to non-stimulated cells ($p<0.0001$), **(Fig. 16B)**, in agreement with data previously published from other groups [114]. In contrast, in cells in which MET was decreased by expression of shRNA, no induction of migration by IGF-1 was observed **(Fig. 16B)**. In cells not stimulated with IGF-1 but in which HGF was used as a chemoattractant, a 3 fold increase in migration was observed ($p<0.0001$), consistent with the role of activated MET in promoting migration **(Fig. 16C)**. These results suggest that IGF-1-mediated increased migration is mediated by MET activation. Overall, the experiments confirm that delayed phosphorylation of MET leads to a functional MET capable of inducing one of its principal roles, migration.

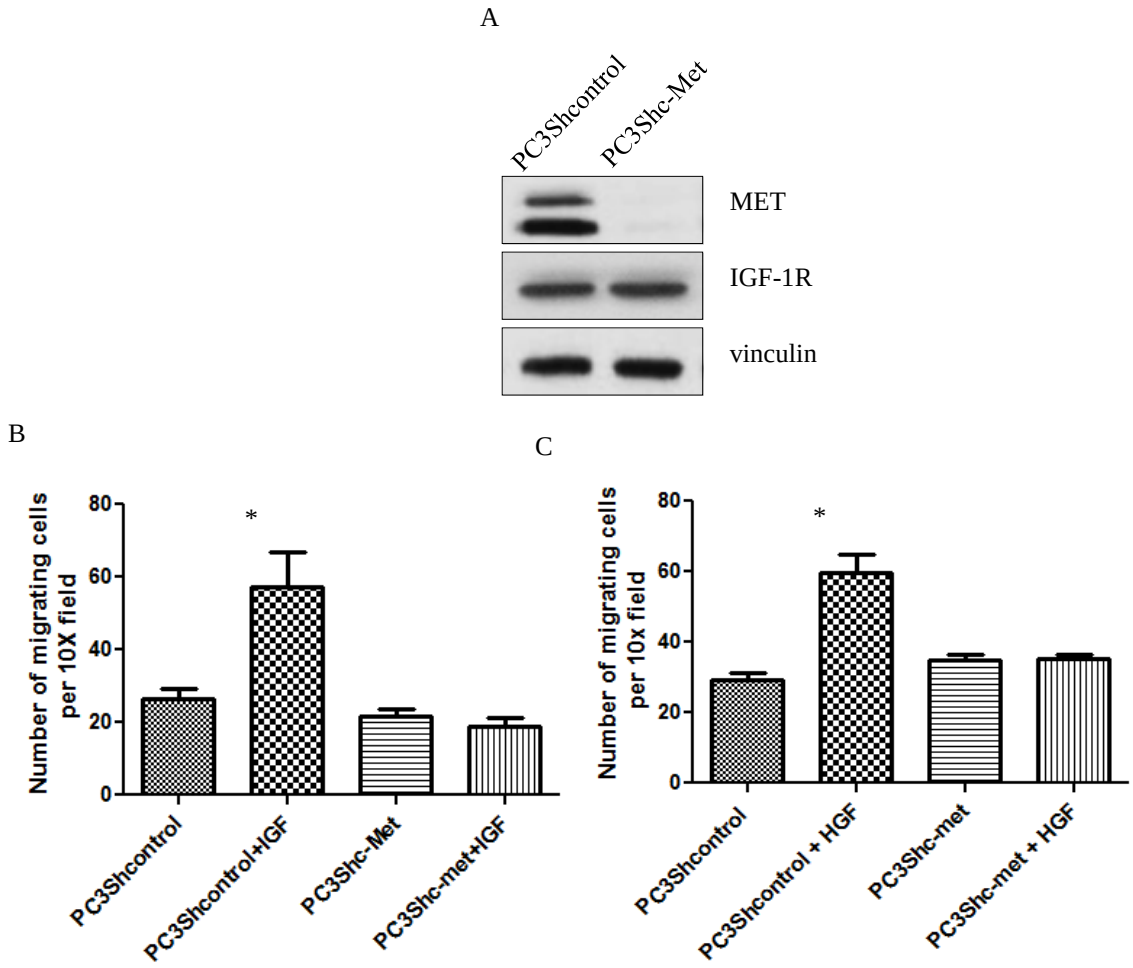

Figure 16 - Role of MET in IGF-1-mediated migration of PC3 cells

Stable knockdown of MET expression by achieved by using an shRNA construct (A). Effects of IGF-1 (B) and HGF (C) on migration of PC3 cells were determined. $5x10^4$ Cells were plated on top of a Boyden Chamber as described in Materials and Methods. IGF-1 (100ng/ml) (B) or HGF (15ng/ml) (C) were used as a chemoattractant. Migration was compared in *shc-Met* knockdown cells and respective controls. Data represent Mean and SEM from three independent experiments; *$p<0.0001$ (one-way ANOVA analysis of variance).

MET is Activated in Multiple Cell Lines Expressing IGF-1R

I next examined whether IGF-1-induced MET activation occurred in another commonly used metastatic prostate cancer cell line, DU145, which expresses both IGF-1R and MET. As before, analysis of MET expression and phosphorylation was performed after 0h, 18h and 24h of IGF-1 treatment. Kinetics of MET phosphorylation in these DU145 cells were similar to that of PC3 **(Fig. 17)**. Finally, as IGF-1 is abundantly expressed in the serum of patients with other types of cancer, I examined the effect of IGF-1 on HT29 colon cancer cells and A549 lung cancer cells, both of which express IGF-1R and MET to differing levels. Delayed phosphorylation of MET was observed in both of these cell lines **(Fig 18A, B)**, though not to the extent of the prostate cancer cells that express higher basal levels of MET. These results suggest that delayed activation of MET is likely a common cross talk pathway in cells expressing both IGF-1R and MET, and this process may contribute to phenotypes associated with MET activation in multiple types of cancer.

Integrins do not mediate cross talk between IGF-1R and MET

While several mechanisms might contribute to non-ligand mediated MET phosphorylation, integrins are an attractive possibility as increased integrin clustering and activation not only leads to MET activation, but also to that of Src and downstream pathways [115, 116]. To examine this possibility, PC3 cells with stable expression of an Shβ1integrin were stimulated with IGF-1. MET was phosphorylated in both non-targeting and shβ1 integrin knock down cells, suggesting that β1 integrin is not required for delayed MET activation **(Fig 19)**.

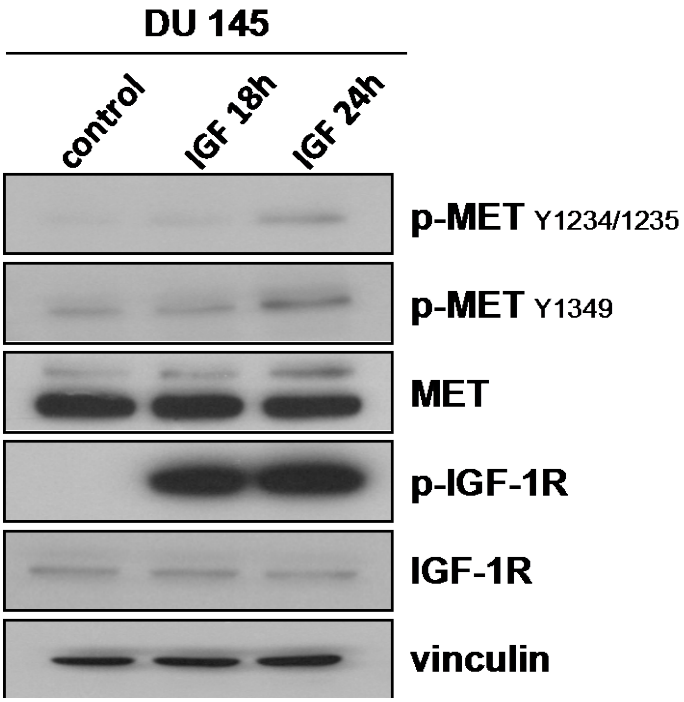

Figure 17 - Effects of IGF-1 on MET phosphorylation in DU145 cells

DU145 (Prostate Cancer cells) expressing both IGF-1R and MET were stimulated with IGF-1 (100 ng/ml) as described in Materials and Methods. Expression and phosphorylation of MET and IGF-1R examined 18 and 24h later.

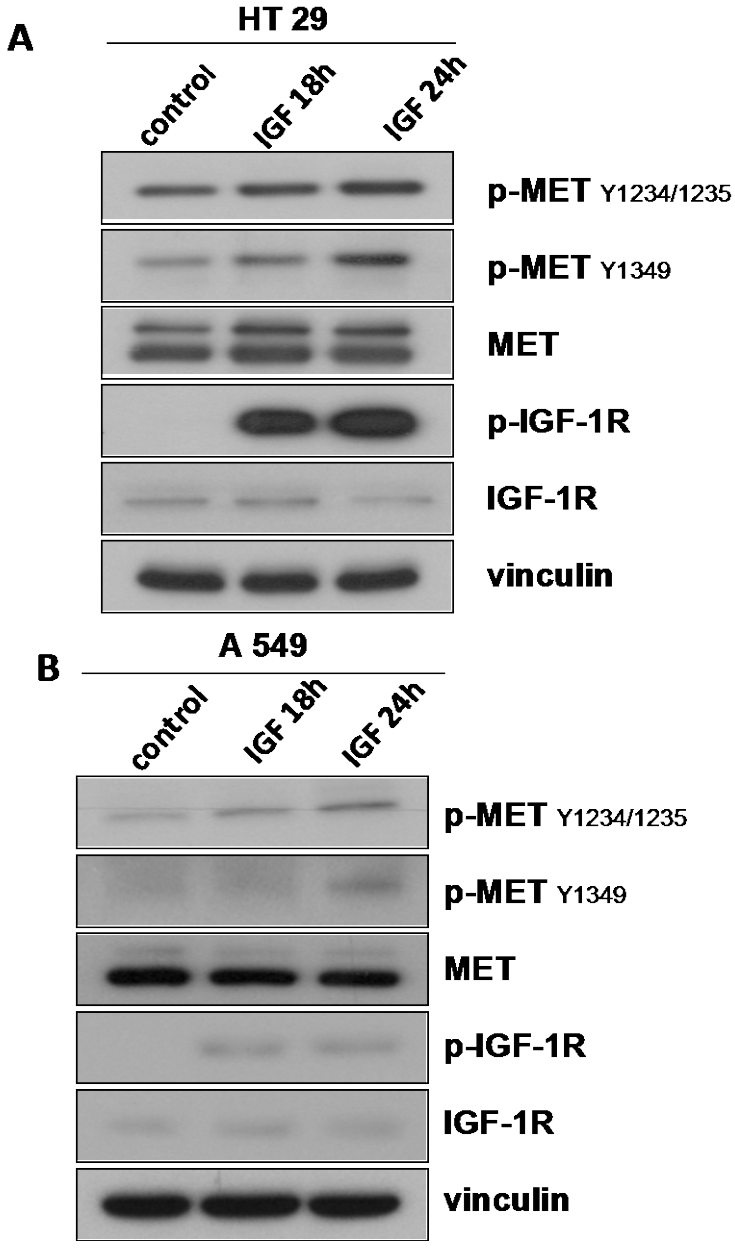

Figure 18 - Effects of IGF-1 on MET phosphorylation in different cancer cell lines

HT29 (Colon Cancer) (A) and A549 (Lung Cancer) (B) cell lines, expressing both IGF-1R and MET were stimulated with IGF-1 and expression and phosphorylation of MET and IGF-1R was examined 18h and 24h later.

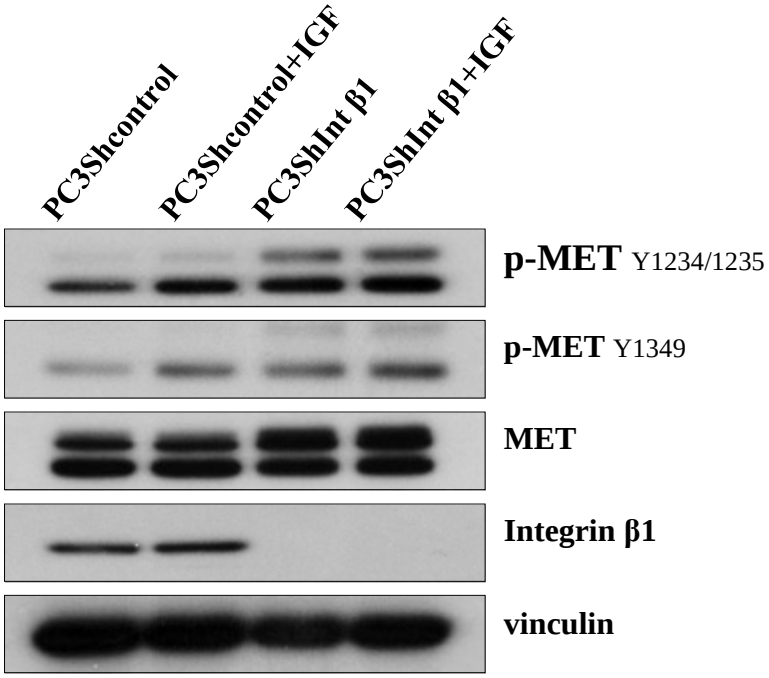

Figure 19 - Effect of integrin β1 knockdown on MET phosphorylation

IGF-1 (100 ng/ml) was added to non-targeting cells (PC3Shcontrol) or cells that had stable knock down of integrin β1 (PC3ShIntβ1) and MET phosphorylation (and expression) was determined 24hr later.

Discussion

In this chapter, I demonstrate for the first time that in tumor cell lines in which both IGF-1R and MET are expressed, IGF-1R activation is sufficient to lead to a delayed phosphorylation of MET in a process that is independent of MET ligand, HGF and without increasing MET expression. Phosphorylation of MET occurs at each tyrosine examined, suggesting that MET becomes fully activated, in accord with the results demonstrating requirement of MET for IGF-1-mediated migration. IGF-1R and Src are required to induce delayed MET phosphorylation in a mechanism dependent on transcription since inhibiting transcription abolished IGF-1-induced MET activation. The transcriptional mediator/s involved in this pathway remains to be identified. It is possible that Src activation facilitates the transcription of an unknown factor by enhancing activity of a transcriptional factor and the transcription of this unknown factor then leads to MET activation. The results from this chapter demonstrate an alternate mechanism of MET activation suggesting that MET re-activation through receptor cross talk might be one of the reasons for failure of MET inhibitors in clinical trials. These findings suggest utilization of another strategy to inhibit aberrantly expressed tyrosine kinases in cancer by inhibiting the protein expression of these kinases. One such strategy is through miRNA-mediated gene regulation and inhibition of multiple targets implicated in cancer progression, which I further examined in the next chapters.

Chapter 4

Effects of miR-34a Overexpression on Expression of Targets and Properties Associated with Metastasis *in vitro*

MicroRNA-mediated gene regulation and development of miRNA-based therapies for therapeutics is one approach to inhibit expression of multiple oncogenic proteins and thereby inhibit several cancer-promoting pathways. In prostate cancer, increased expression of receptor tyrosine kinases MET and Axl is reported with disease progression, further enhancing tumor growth at the metastatic site, principally the bone [40, 48]. Both of these receptor tyrosine kinases promote cancer cell survival, proliferation, migration and invasion [4, 35, 46, 47, 117]. Aberrant expression of transcription factor c-Myc is reported in prostate cancer and evidence from transgenic models implicates c-Myc in driving development of invasive prostatic carcinomas [25, 26, 51]. Myc is a proto-oncogene that regulates transcription of genes involved in promoting cancer cell growth and proliferation [50]. As discussed in Introduction (Chapter 1), targeting multiple gene products is important to inhibit activation of disparate signaling pathways that promote cancer progression. MicroRNA-34a is a tumor suppressive miRNA that targets and inhibits many of the genes involved in cancer development and metastasis. Importantly, miR-34a inhibits protein expression of MET, Axl and c-Myc in several cancers [45, 53, 75, 83, 84]. I therefore hypothesized that decreased miR-34a expression leads to upregulation of targets that promote PCa progression, and *in vitro* overexpression of miR-34a will inhibit tumor-promoting properties. To test this hypothesis, I determined miR-34a expression in prostate cancer cell lines and studied the effects of modulating miR-34a expression on biological properties associated with increased metastatic potential.

Expression of miR-34 family members in PCa cell lines

To examine the role of miR-34 family in prostate cancer, I used qPCR to quantify relative expression of miR-34 family members: miR-34a, miR-34b and miR-34c in PCa cell lines. I compared the expression of these miRs in LNCaP cells (which do not metastasize in immunocompromised mice) and C42B4 (with low metastatic potential) cells to more aggressive PC3 (high metastatic potential) and PC3MM2 (selected for increased metastatic potential relative to parental PC3). Expression of miR-34b **(Fig. 20A)** and miR-34c **(Fig. 20B)** was very low in all the tested PCa cell lines. In contrast, expression of miR-34a was high in cells of low metastatic potential and decreased substantially in cells of high metastatic potential **(Fig. 20C)**. Specifically, expression of miR-34a was decreased by 8-fold in PC3 and by 12-fold in PC3MM2 compared to C42B4 and LNCaP cells (Fig. 20). This result demonstrates that miR-34a expression is inversely proportional to aggressiveness and metastatic potential of PCa cell lines, in agreement with a potential role as a tumor suppressor in PCa. Among the miR-34 family, I thus chose miR-34a to determine if it regulated targets critical to PCa progression, and biological properties associated with increased metastasis potential *in vitro*.

miR-34a targets are overexpressed in aggressive PCa cells

To examine whether miR-34a overexpression could regulate targets associated with increased metastatic potential of PCa cell lines, I determined the expression of MET, Axl and c-Myc in LNCap, C42B4, PC3 and PC3MM2 cells. These targets are increased in mRNA **(Fig. 21A-C)** and protein expression **(Fig. 21D)** in PC3MM2 and PC3 cells relative to LNCaP and C42B4 cells, in accord with the different metastatic potentials described above.

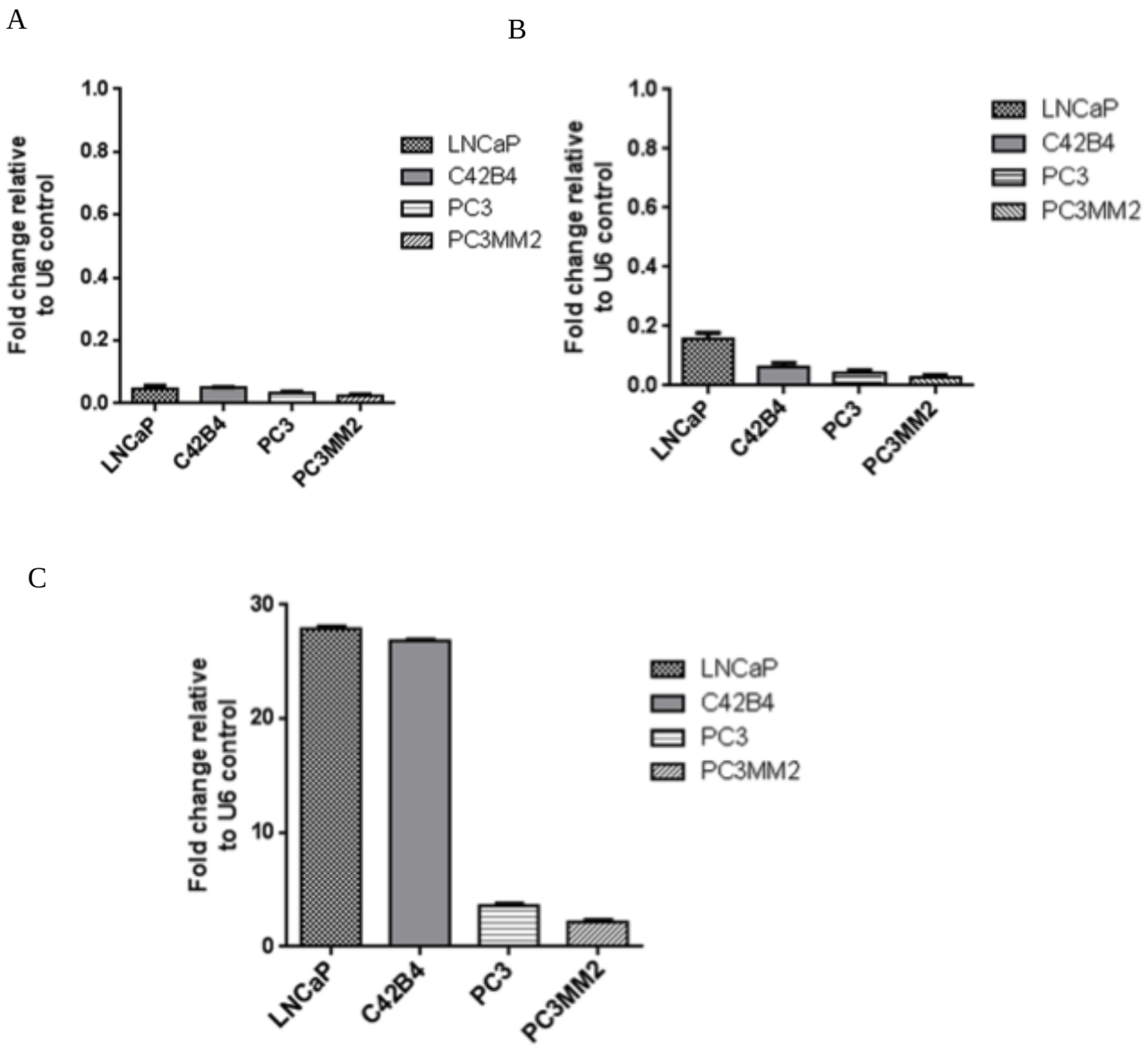

Figure 20 – Expression of miR-34 family members in PCa cell lines

Total RNA was isolated from cell lines and qPCR performed for miR-34b (A), miR-34c (B) and miR-34a (C) using TaqMan assays as described in Materials and Methods. U6 was used as endogenous control and ΔCt method was used for quantification. Data represents Mean and SD from three independent experiments.

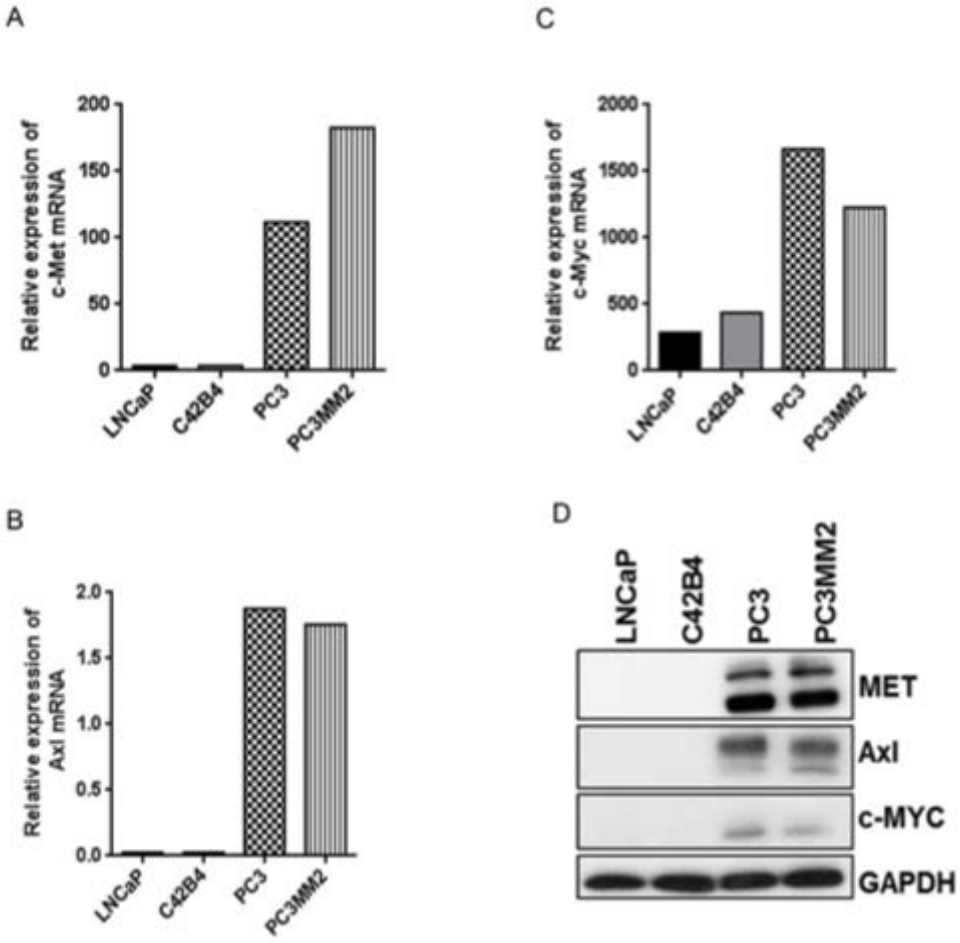

Figure 21 - miR-34a targets are overexpressed in aggressive PCa cell lines

Total RNA and protein was isolated from cell lines and mRNA expression of c-Met (A), c-Myc (B) and Axl (C) was measured using SYBR Green qPCR using 18S RNA expression as endogenous control. Data represents Mean and SD from three independent experiments. Protein expression was measured by immunoblotting (D). GAPDH was used as loading control.

To determine if miR-34a regulated expression of these targets, I overexpressed miR-34a by transiently transfecting low miR-34a expressing PC3 and PC3MM2 cells with negative control miRNA (N.C.) or miRNA-34a (miR-34a) mimics as described in Materials and Methods. Overexpression of miR-34a **(Fig. 22A)** led to decreased expression of protein **(Fig. 22B)** as well as mRNA **(Fig. 23)** of MET, Axl, and c-Myc in PC3 and PC3MM2 cells. These data thus demonstrate that miR-34a overexpression simultaneously inhibits the expression of these targets in PCa cell models commonly used to study tumor progression and metastasis.

Effects of miR-34a overexpression on properties associated with aggressiveness and metastatic potential of PC3 cell line

I next determined the biological effects of miR-34a overexpression in PC3 cells. Cells transfected with N.C. or miR-34a for 24h were seeded on Boyden chamber inserts as described in Materials and Methods. Overexpression of miR-34a significantly decreased the ability of PC3 cells to migrate by 50% **(Fig. 24A)** and the ability to invade by 75% **(Fig. 24B)**. I then determined the effects of miR-34a on cell proliferation by using a MTS assay. Cells after 24h of N.C. or miR-34a were counted and seeded in 96-well plates. Absorbance at 490nm was measured for different time points by EnVision® multilabel plate reader. Overexpression of miR-34a decreased cell proliferation by 1.6-fold at 72 hours and by 2-fold at 96 hours compared to N.C. **(Fig. 25A)**. I next performed cell cycle analysis using propidium iodide (PI) at various times after N.C. or miR-34a transfection in PC3 cells. A 4-fold decrease in S-phase was observed beginning at 48 hour, which is maintained through 96 hours post-transfection **(Fig. 25B)**. After 72 hours, the sub- G1 phase increased by 1.5 fold in miR-34a overexpressing cells, reaching a maximum of 2-fold at 96 hours relative to N.C.

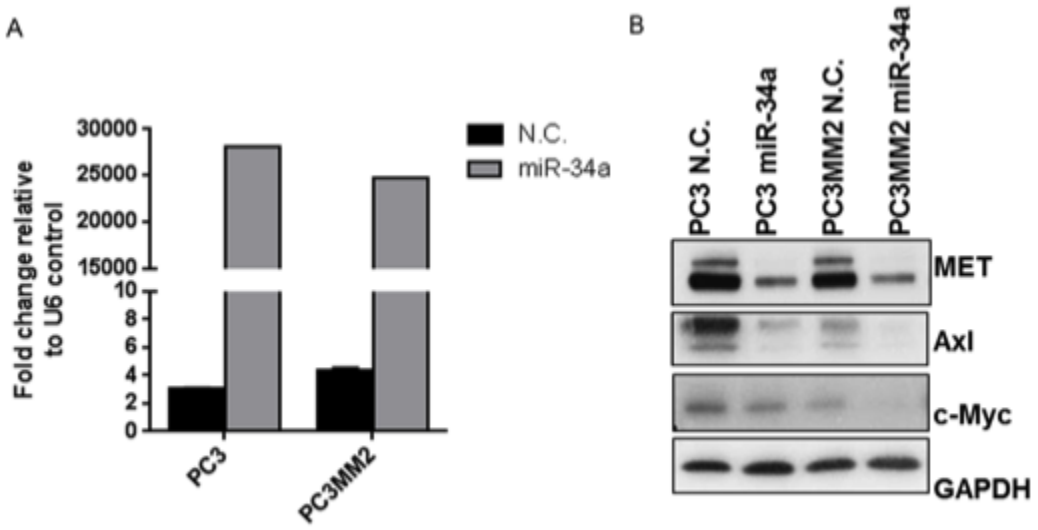

Figure 22 - Overexpression of miR-34a decreases protein expression of its targets

miR-34a expression after transient transfection was measured and plotted by using the TaqMan assay for miR-34a and U6 as a control (A). Protein expression of miR-34a targets (MET, Axl and c-MYC) after N.C. or miR-34a transfection is shown by immunoblotting (B). GAPDH was used as loading control.

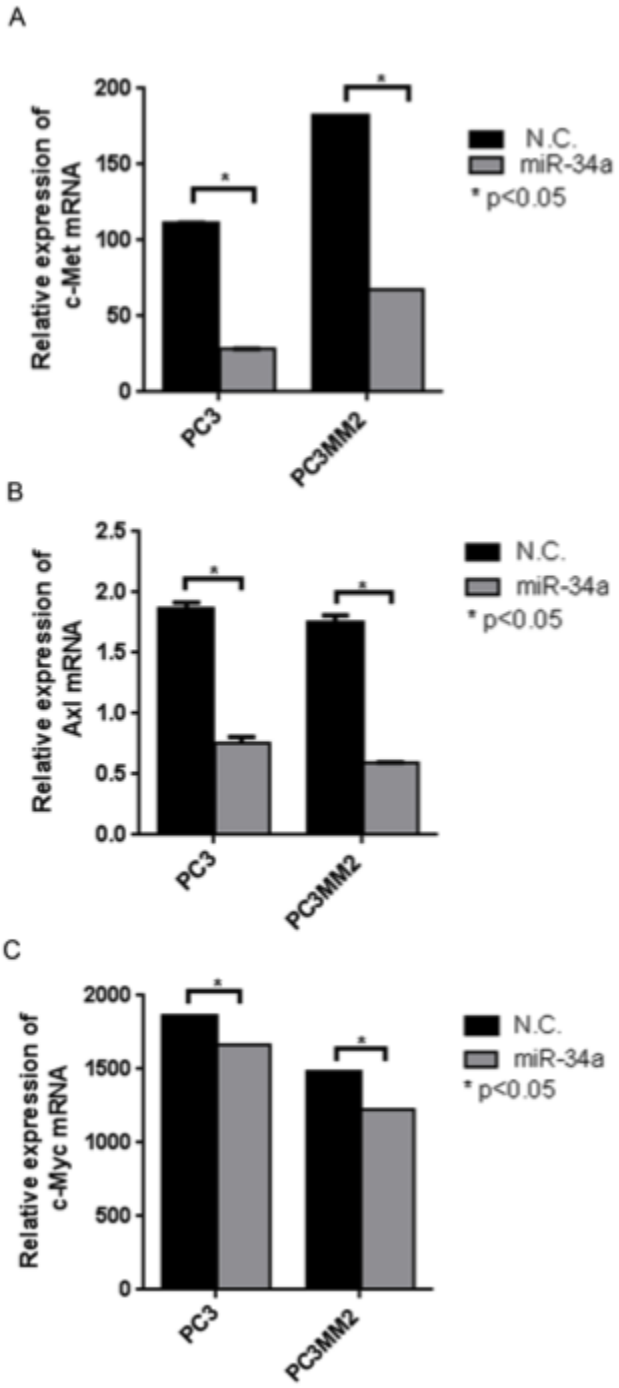

Figure 23 - Overexpression of miR-34a decreases mRNA expression of its targets

mRNA expression of c-Met (A), Axl (B) and c-Myc (C) after miR-34a overexpression are quantified using SYBR Green qPCR in PC3 and PC3MM2 cell lines. * denotes p value <0.05 as measured by student's t test.

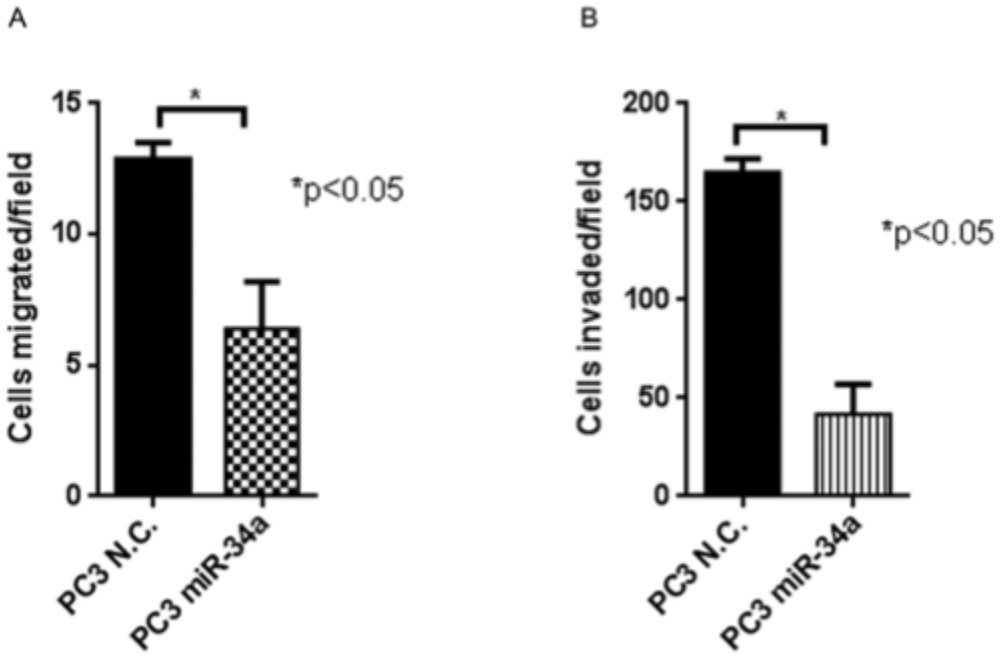

Figure 24 - Effects of miR-34a overexpression on migration and invasion abilities of PC3 cells

Migratory (A) and invasive (B) ability of PC3 was measured after N.C. or miR-34a transfection by using Boyden chamber inserts in serum free media. Cells that migrated or invaded the matrigel layer were stained, quantified and plotted. * denotes p value <0.05 as measured by student's t test.

A

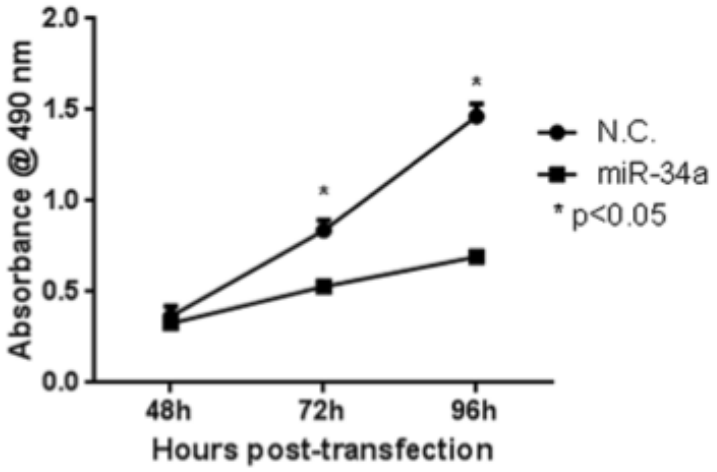

B

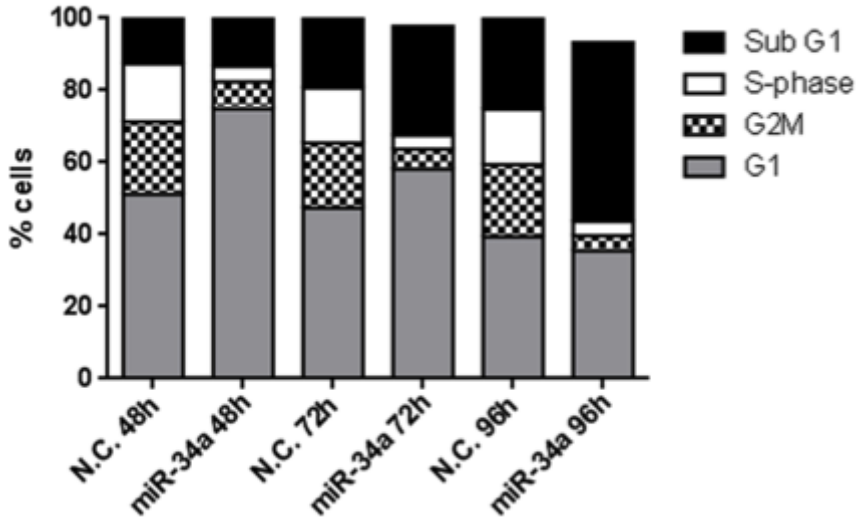

Figure 25 - Effects of miR-34a overexpression on cell proliferation and cell cycle

MTS assay was performed on N.C. or miR-34a transfected for different time points and mean absorbance at 490 nm from triplicate wells was plotted (A). Propidium iodide staining was used for cell cycle analysis and the different cell cycle phases from N.C. or miR-34a transfected cells for 48h, 72h and 96h were analyzed and quantified (B). * denotes p value <0.05 as measured by student's t test.

transfected cells **(Fig. 25B)**. These results demonstrate that overexpression of miR-34a both decreased cell proliferation and increased cell death. To determine what type(s) of cell death were occurring, I used a GFP-Certified® Apoptosis/Necrosis detection kit as described in the Materials and Methods. An increase in early (AnnVEnzoGold^{+}/7AAD^{-}) and late apoptotic (AnnVEnzoGold^{+}/7AAD^{+}) cell populations were observed at 72 and 96 hours post miR-34a transfection compared to N.C. transfected cells **(Fig. 26A)**. In addition, an increase in cleaved caspase 3 were observed with miR-34a overexpression at 72 and 96 hours **(Fig. 26B)** demonstrating that apoptosis occurred at these time points.

These results thus demonstrate that overexpression of miR-34a decreases properties associated with metastasis by inducing apoptosis, decreasing cell proliferation, cell migration and invasion, in accord with miR-34a being a tumor suppressive miRNA. Overexpression of miR-34a decreases both mRNA and protein expression of MET, Axl and c-Myc, targets implicated in prostate cancer progression further corroborating the application of miR-34a delivery as a treatment strategy for metastatic prostate cancer which I tested in next the chapter.

A

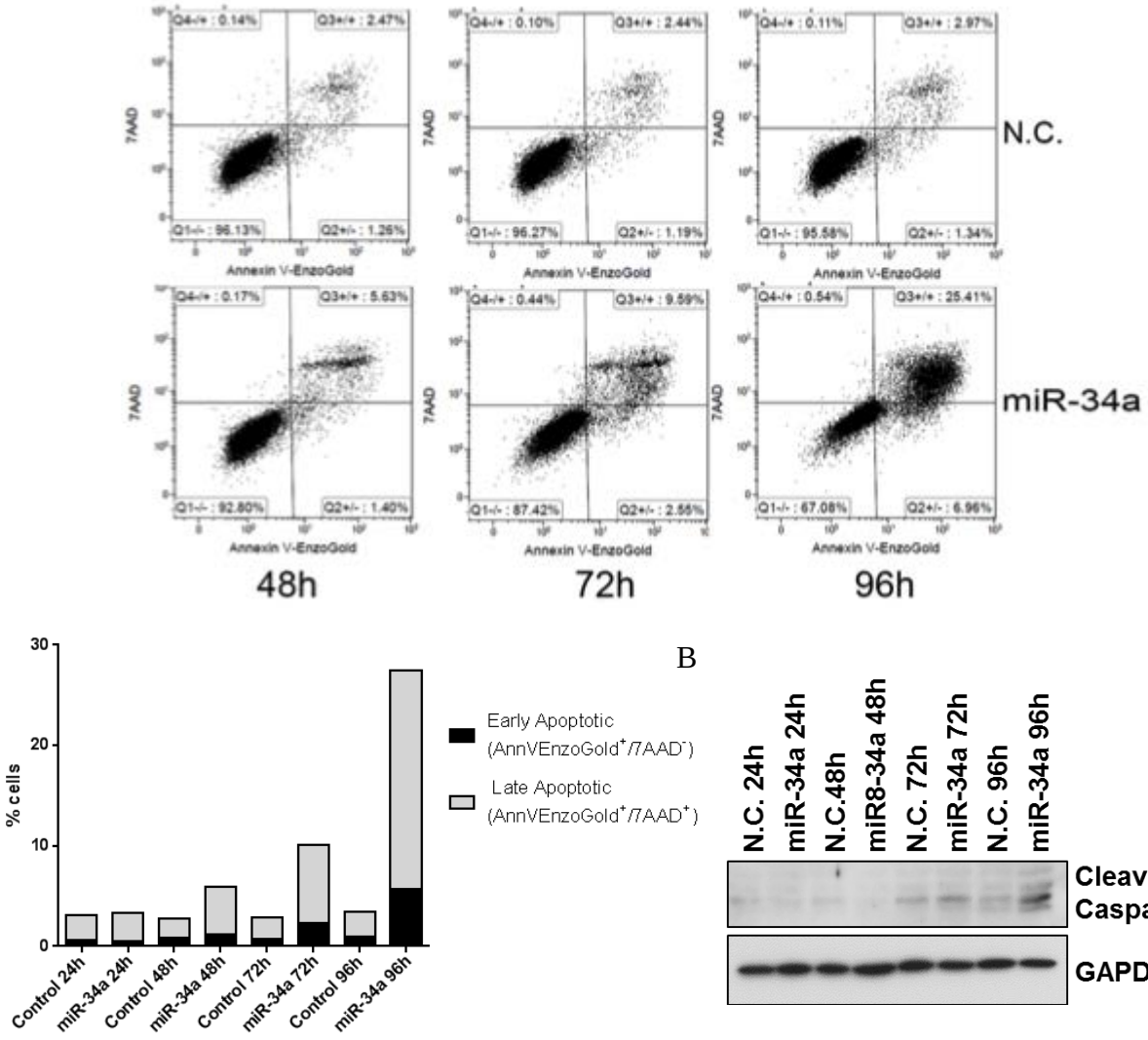

Figure 26 - miR-34a overexpression increases apoptosis in PC3 cells

Apoptotic cells and necrotic cells in N.C. or miR-34a transfected cells for different time points were analyzed and quantified by Gallios FACS using a GFP-Certified® Apoptosis/Necrosis detection kit as described in Materials and Methods (A). Protein expression of Cleaved Caspase 3 is visualized by immunoblotting after time course transfection with N.C. or miR-34a (B).

Chapter 5

Chitosan Nanoparticle Mediated Delivery of miR-34a Decreases Prostate Tumor Growth in *in vivo* Models

Most deaths of prostate cancer patients are due to development of bone metastasis. Currently available therapies have severe toxicities and limited success in treatment of bone metastasis. It is thus essential to develop alternate treatment strategies such as miRNA replacement therapy to deliver tumor suppressive miRNA/s that will inhibit multiple genes that contribute to growth to cancer progression and growth at metastatic site. Previous studies have demonstrated that delivery of tumor suppressive miRNAs in different *in vivo* cancer models is effective in inhibiting primary tumor growth and experimental metastasis [118]. Delivery of miR-34a has been shown to be effective in inhibiting growth of orthotopic prostate tumor and lung metastasis [84]. However, it is not known whether miR-34a delivery will decrease prostate tumor growth in the bone, the principal site of PCa metastasis. In this chapter, I determined whether miR-34a could be delivered in *in vivo* model systems, inhibit its known targets and decrease tumor growth. I used PC3MM2-LG cells as they have been shown previously to grow in the bone. I used chitosan nanoparticles, currently in development for clinical applications due to their favorable biocompatible properties making them an attractive delivery vehicle [70, 119]. Previous studies demonstrated effective siRNA and miRNA delivery using chitosan nanoparticles in *in viv*o models without severe toxicities [70, 73] further corroborating their clinical application.

miR-34a delivery by chitosan nanoparticles inhibits prostate tumor growth in sub-cutaneous model

I first tested whether delivery of miR-34a in chitosan nanoparticles would lead to downregulation of the targets I examined, MET, Axl and c-Myc in *in vivo* model system. For these studies, tumors were grown subcutaneously as described in Materials and Methods and

miR-34a was delivered to these tumors systemically encapsulated in chitosan, a cationic, biodegradable, naturally occurring polymer [70, 119]. I first determined whether miR-34a in chitosan nanoparticles could be delivered systemically and whether its delivery inhibited known targets and decreased tumor growth in a sub-cutaneous model. PC3MM2 cells were injected in nude mice and one week after tumor injection, intra-venous (i.v.) treatment was started to deliver miRNAs encapsulated in chitosan (CH) nanoparticles for control miR or miR-34a and continued for two weeks. Robust expression of miR-34a expression was observed in tumors that received miR-34a-CH nanoparticles as visualized by ISH **(Fig. 27A)**. Next, I examined the expression of MET, Axl and c-Myc. Expression of these proteins was decreased as determined by IHC **(Fig. 27A, B)** and immunoblotting **(Fig. 27C)** in miR-34a treated tumors. Tumor volume measurements demonstrated that miR-34a delivery decreased tumor growth compared to control tumors **(Fig. 28)**. The delivery of miR-34a also induced apoptosis as measured by an increase in TUNEL positive cells in miR-34a treated tumors **(Fig. 29)** compared to control tumors. This result suggests that miR-34a delivery decreases tumor growth by inducing apoptosis.

Effects of miR34a delivery on growth of PCa cells in the bone

The main question I wished to address was whether systemic miR-34a delivery affected tumor growth in an intra-femur model to represent PCa bone metastasis, as no effective therapies for bone metastases currently exist. First, to determine whether chitosan could deliver small RNAs to the bone, I used Cy5.5-labeled siRNA to detect Cy5.5 fluorescent signal from the femurs by *ex vivo* imaging. PC3MM2-LG cells were

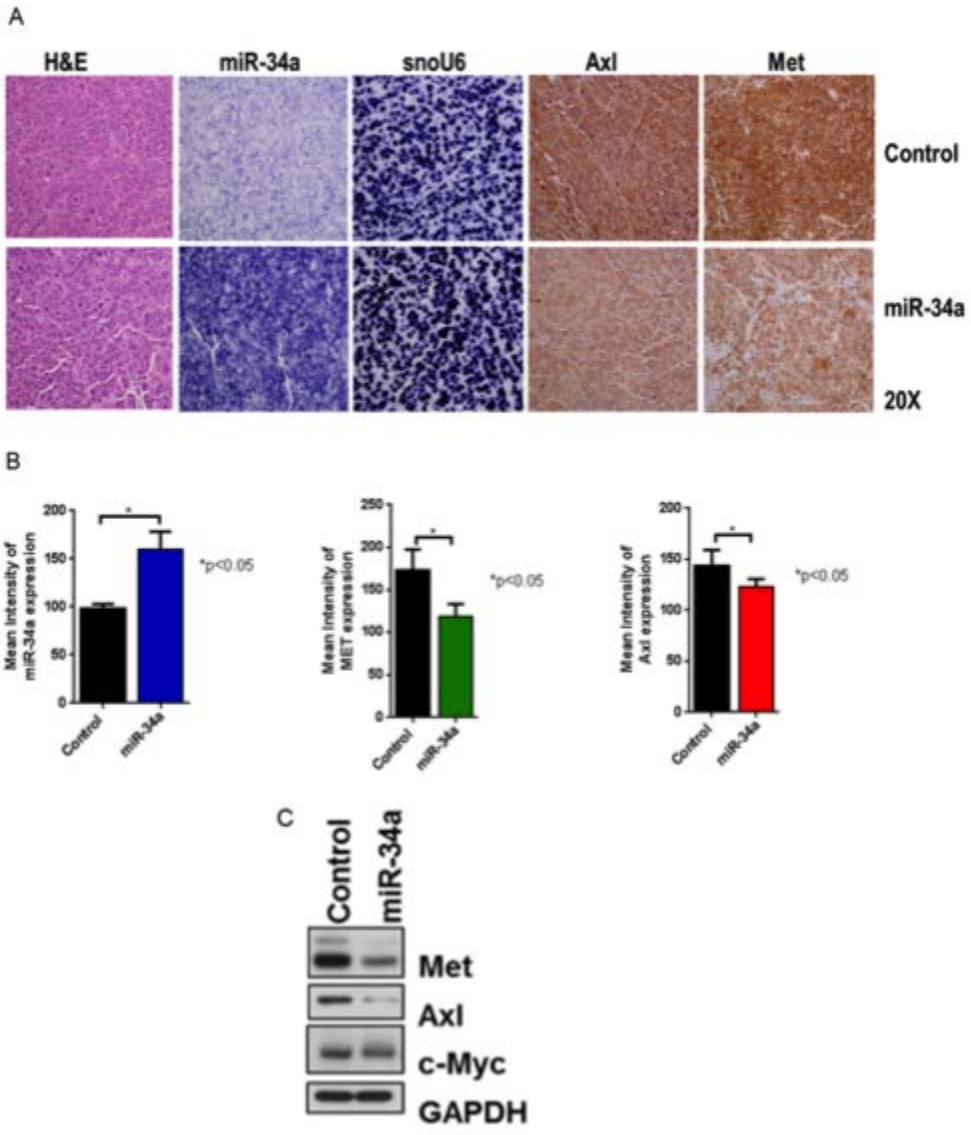

Figure 27 - Chitosan mediated delivery of miR-34a decreases target expression

FFPE slides were stained with H&E and *in situ* hybridization was performed for miR-34a and endogenous control U6 along with IHC for MET and Axl (A). The mean intensities for 10 areas from each slide at 10x magnification was quantified using color deconvulation H DAB macros in ImageJ software or mean intensities were measured with NIS Elements software (B). Protein expression of MET, Axl and c-Myc from control and miR-34a treated tumors were analyzed by immunoblotting (C) * denotes p value <0.05 as measured by student's t test.

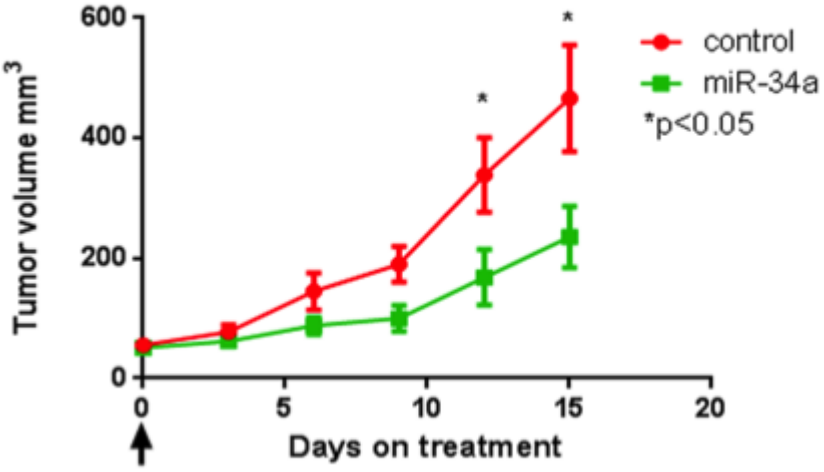

Figure 28 - Systemic miR-34a delivery by chitosan nanoparticles decreases sub-cutaneous prostate tumor growth

Tumor volume of sub-cutaneous PC3MM2 tumors was measured by caliper and plotted for control and miR-34a treated group. * denotes p value <0.05 as measured by student's t test.

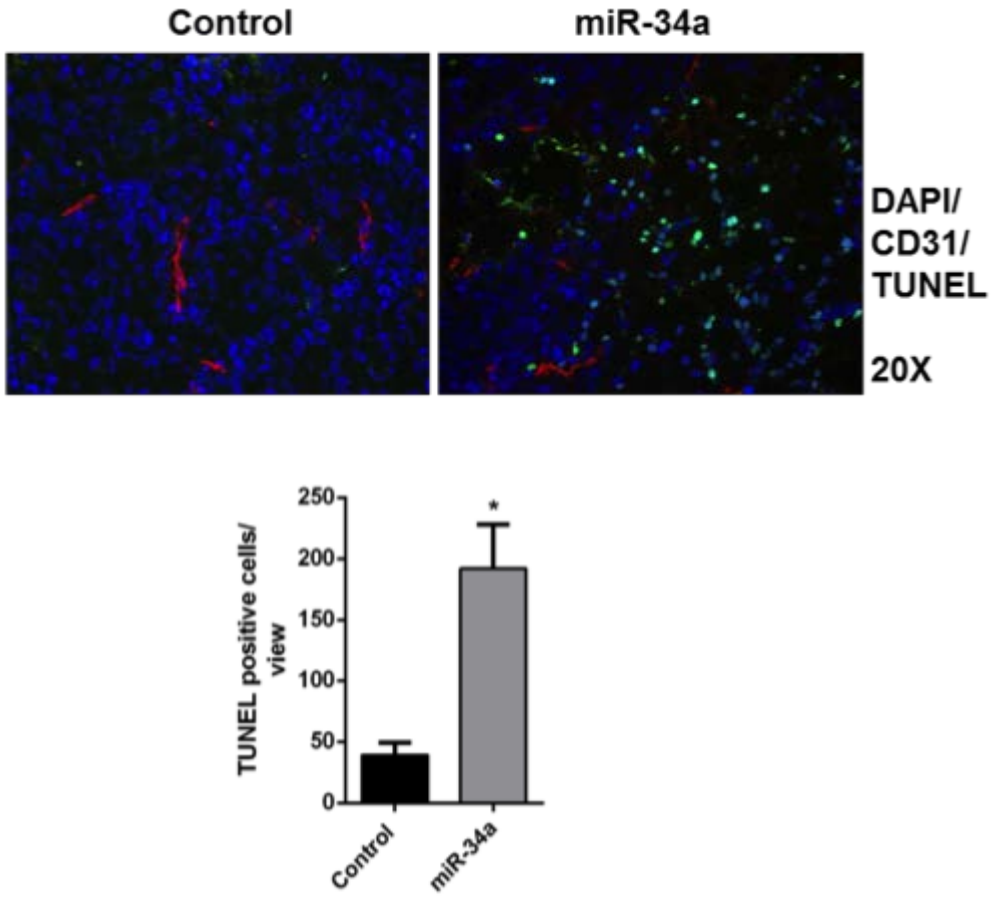

Figure 29 - miR-34a delivery induces apoptosis in sub-cutaneous model

TUNEL staining was performed on tumors as described in Materials and Methods. TUNEL positive (Green) cells were quantified using ImageJ software from 10 fields per tumor and the mean and standard deviation is plotted and a representative image is shown for control and miR-34a treated tumor for nuclear DAPI (blue) and CD31 (red) staining. * denotes p value <0.05 as measured by student's t test.

injected in the femur of nude mice and ten days after tumor injection, unlabeled control or Cy5.5-siRNA in chitosan nanoparticles were delivered by tail-vein administration. Animals were sacrificed three days after delivery and IVIS 200 visualized fluorescent intensities from harvested legs. Fluorescence imaging demonstrates an increase in Cy5.5-siRNA signal intensity in the femur with tumor than in the femur without tumor **(Fig. 30)** suggesting that tumor retains the siRNA delivered by chitosan nanoparticle.

I next determined the effect of miR-34a delivery on established tumors in the femur to best mimic treatment of men presenting with bone metastasis. For this experiment, PC3MM2-LG cells were injected in the femur of nude mice and bioluminescent activity and MRI was used to measure tumor growth and volume. After ten days, when tumors were evident in the femurs (as measured by MRI), mice were randomized and treated with either control-miR-CH or miR-34a-CH nanoparticles every three days for three weeks through i.v. administration. The delivery of miR-34a decreased growth of established prostate tumors in the bone compared to control **(Fig. 31)** as measured by bioluminescent activity of PC3MM2-LG cells. This finding is supported by decreased tumor volume in miR-34a treated group compared to control group as measured by MRI **(Fig. 32)**. PC3MM2 cells cause lytic reaction in the bone and miR-34a delivery preserved bone integrity as visualized by micro CT analysis **(Fig. 33)**. This study thus demonstrates that miR-34a can be delivered to the bone and its delivery decreases tumor growth as well as preserves bone integrity in an intra-femur mouse model representative of PCa bone metastasis.

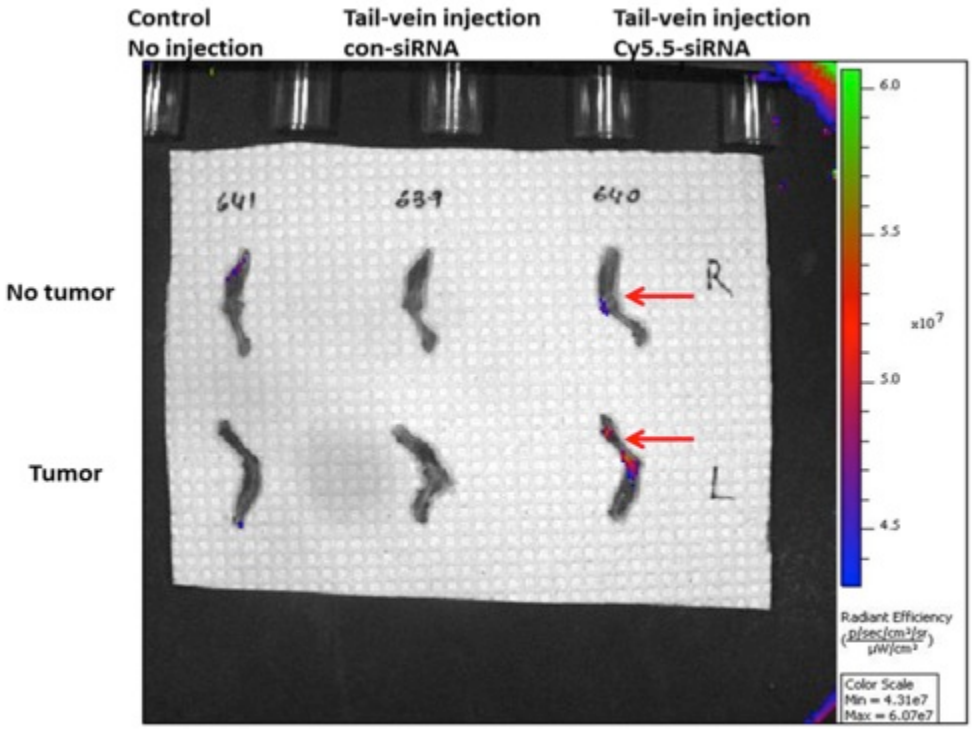

Figure 30 - Chitosan delivers Cy5.5-siRNA to the femur

Control or Cy5.5-labeled siRNAs were encapsulated in chitosan nanoparticles and injected i.v. and fluorescent imaging performed as describe in Materials and Methods. Both Femurs (with and without tumor growing) were harvested and subjected to *ex vivo* imaging. Red arrow indicates fluorescent signal from Cy5.5-siRNA.

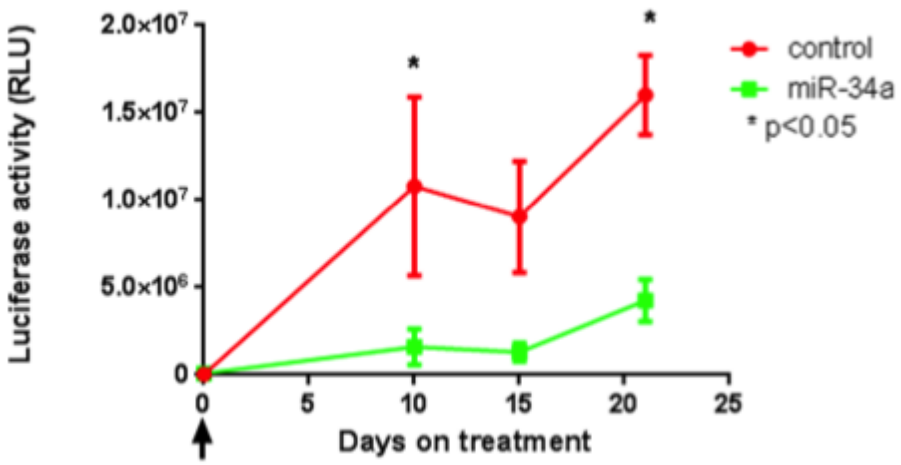

Figure 31 - Systemic miR-34a delivery by chitosan nanoparticles decreases prostate tumor growth in the bone

Bioluminescent activity from the femur was measured using IVIS 200 and plotted for control and miR-34a treatment groups (n=5) and *denotes $p<0.05$ as measured by student's t test.

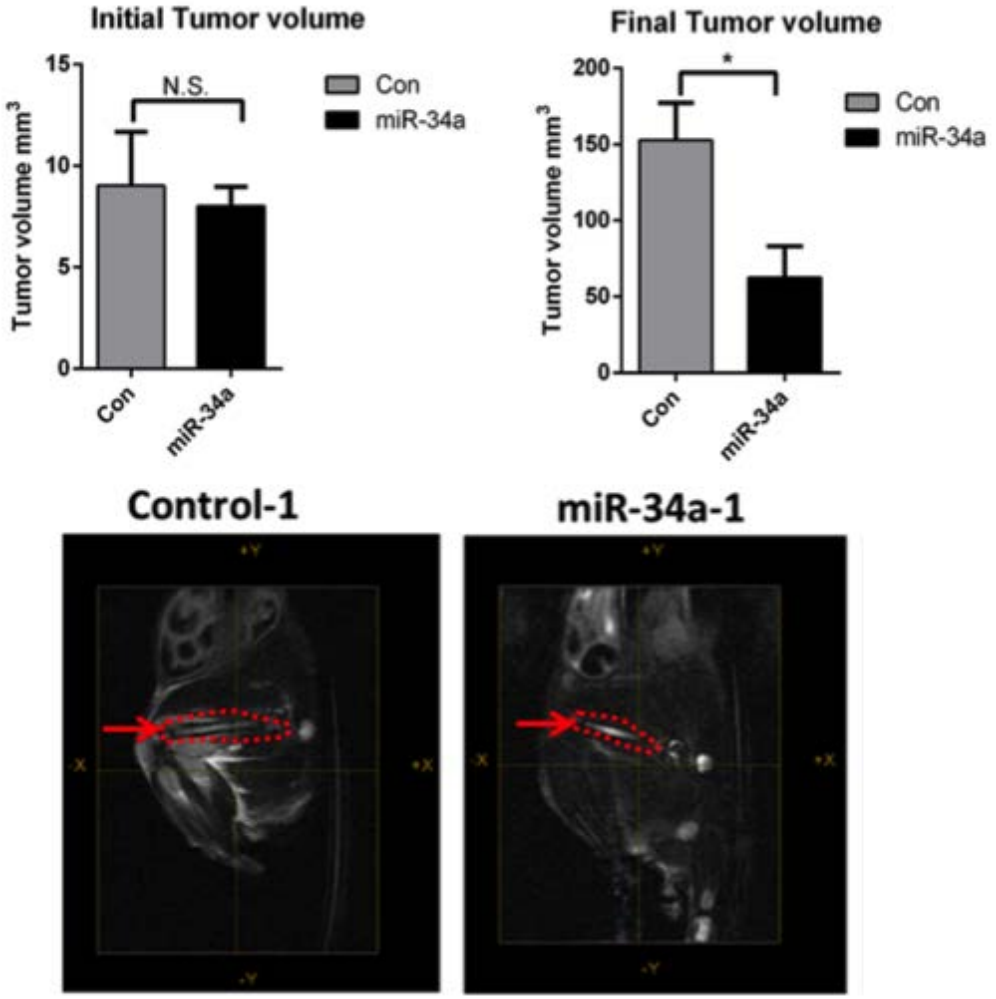

Figure 32 - miR-34a delivery decreases prostate tumor volume in the bone

Tumor volume was measured before and after miR-34a delivery by MRI and plotted (*top*). Representative images from the MRIs of the femurs (red dotted line) for control-CH and miR-34a-CH treated mice are shown (*bottom*). *denotes $p<0.05$ as measured by student's t test.

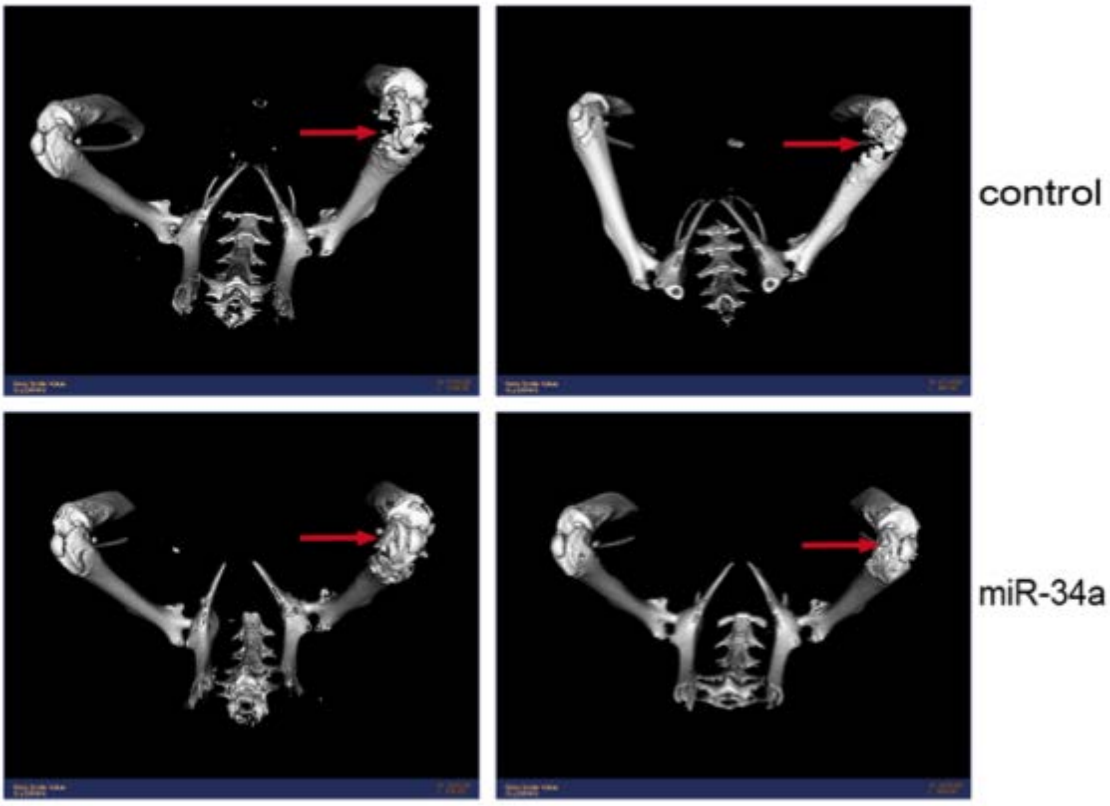

Figure 33 - miR-34a delivery preserves bone integrity

micro CT images for control and miR-34a treated mice are shown and red arrow indicates bone lesions.

Discussion

Results presented in this chapter providence evidence for miR-34a delivery as a strategy to decrease growth of established tumors in the bone with preservation of bone integrity. The delivery of miR-34a in an intra-femoral model demonstrates stronger tumor inhibition than the sub-cutaneous model. Krzeszinski et al. recently demonstrated that miR-34a delivery decreased tumor growth primarily by inhibiting osteoclast activity in breast cancer and melanoma mouse model [74]. Liu et al. demonstrated that miR-34a delivery decreases prostate tumor growth in an orthotopic model [84]. These findings combined with my previous results demonstrating anti-tumor effects of miR-34a suggest that miR-34a could be affecting both tumor as well as the microenvironment and further corroborates miR-34a delivery strategy for treatment of primary and metastatic prostate cancer. The effects of miR-34a on inducing apoptosis *in vivo* are much more profound than inducing apoptosis *in vitro*, implicating that additional cell death mechanism/s might be mediated by miR-34a.

Autophagy, a cellular stress induced survival mechanism has complex role in cancer with several studies reporting autophagy-mediated tumor suppression and demonstrating involvement of autophagy in promoting cancer cell death [96, 97, 99, 120, 121]. Thus, with the goal to address whether autophagy mediates cell death *in vitro*, in the next chapter I determined the effects of miR-34a overexpression on inducing autophagy in cell line models.

Chapter 6

Overexpression of miR-34a Induces Autophagy

Autophagy is a process important in maintaining cellular homeostasis by removing damaged organelles and proteins from the cell [92]. In cancer, autophagy is induced in response to stress conditions for example, nutrient and growth factor starvation, hypoxia and chemotherapy [92, 96]. Autophagy can be tumor promoting by enhancing cancer cell survival; however, many reports suggest tumor suppressive role of autophagy by regulating various cell death pathways including apoptosis [121]. There is evidence of cross talk between the apoptosis and autophagy pathways and both processes have been reported to occur simultaneously in cancer cells [121]. Downregulation of MET or Axl, two of miR-34a targets studied in this dissertation have both been shown to induce both apoptosis and autophagy in several cell lines [105, 106]. My observations of cell morphology with bright field microscopy indicated changes in cell size and structure occurred over time following miR-34a overexpression in PC3 cells **(Fig. 34)**. Specifically, cells overexpressing miR-34a appeared are more flattened and larger than N.C. transfected cells starting at 48 hours. By 96 hours, miR-34a overexpressing cells had a morphology characteristic of cells undergoing autophagy. Since, miR-34a downregulates both MET and Axl, in this chapter, I examined whether miR-34a overexpression induces autophagy in addition to apoptosis first in PCa cell lines, and then determined whether miR-34a overexpression caused similar effects in cell lines derived from other tumor types.

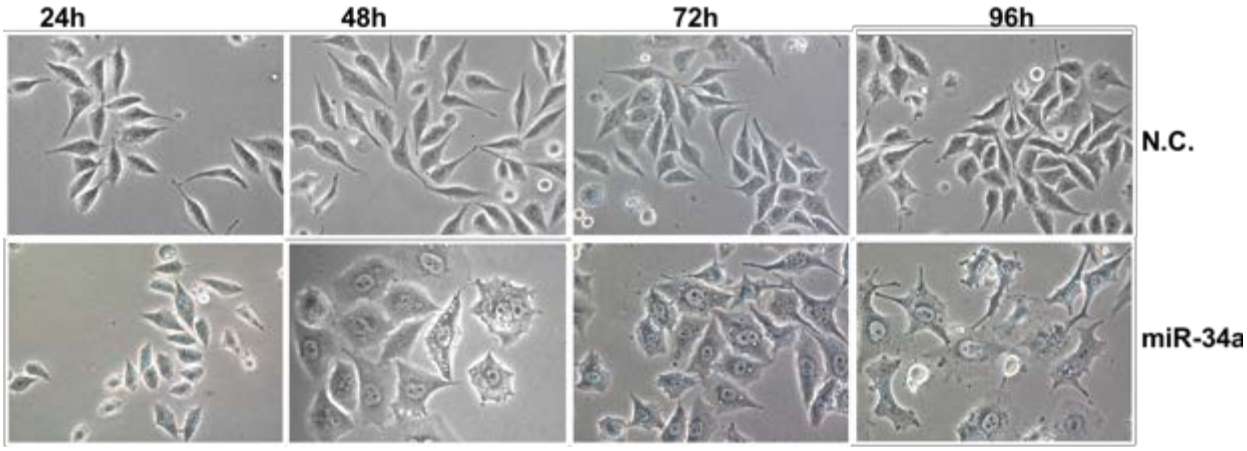

Figure 34 - miR-34a overexpression alters PC3 cell morphology

PC3 cells transfected with N.C. or miR-34a at different time points were imaged by bright field microscopy at 10X magnification using Nikon camera and representative images are shown.

Overexpression of miR-34a induces autophagy in cancer cell lines

Several markers indicative of autophagic process were examined in this chapter. I first analyzed Beclin-1 expression in cells transfected with N.C. or miR-34a, as it is involved in vesicle nucleation and autophagosome formation [122]. An increase in Beclin-1 protein but not mRNA expression (not shown) was observed at 48 hours in miR-34a cells, and continues throughout the time course examined **(Fig. 35A)**.

Next, as a classic marker of autophagy, conversion of LC3I to LC3II, involved in autophagosome maturation [123, 124], was examined. LC3II expression was increased in miR-34a-overexpressing cells 48 hours after transfection and is maintained at 72, and 96 hours **(Fig. 35A)**. Next, to quantitatively measure the presence of acidic vesicular organelles (AVOs), cells transfected with N.C. or miR-34a for increasing times were stained with acridine orange and analyzed by flow cytometry as described in Materials and Methods. An increase in acridine orange-positive cells (AO+) was observed in miR-34a overexpressing cells at 48 hours with further increases noted at 72 and 96 hours **(Fig. 35B)**, a time frame similar to that observed for LC3II increase. To determine whether autophagic structures were present in miR-34a overexpressing cells, transmission electron microscopy (TEM) was performed. As shown in **Fig. 36**, miR-34a led to an abundant accumulation of autophagosome (AP)-like structures (black arrows) as well as autolysosome (AL)-like structures (red arrows) that are not observed in N.C. cells. This result confirms the presence and accumulation of autophagic structures in miR-34a-induced autophagy in PC3 cells. These data demonstrate that miR-34a overexpression increases molecular markers associated with initiation, maturation and progression of autophagy.

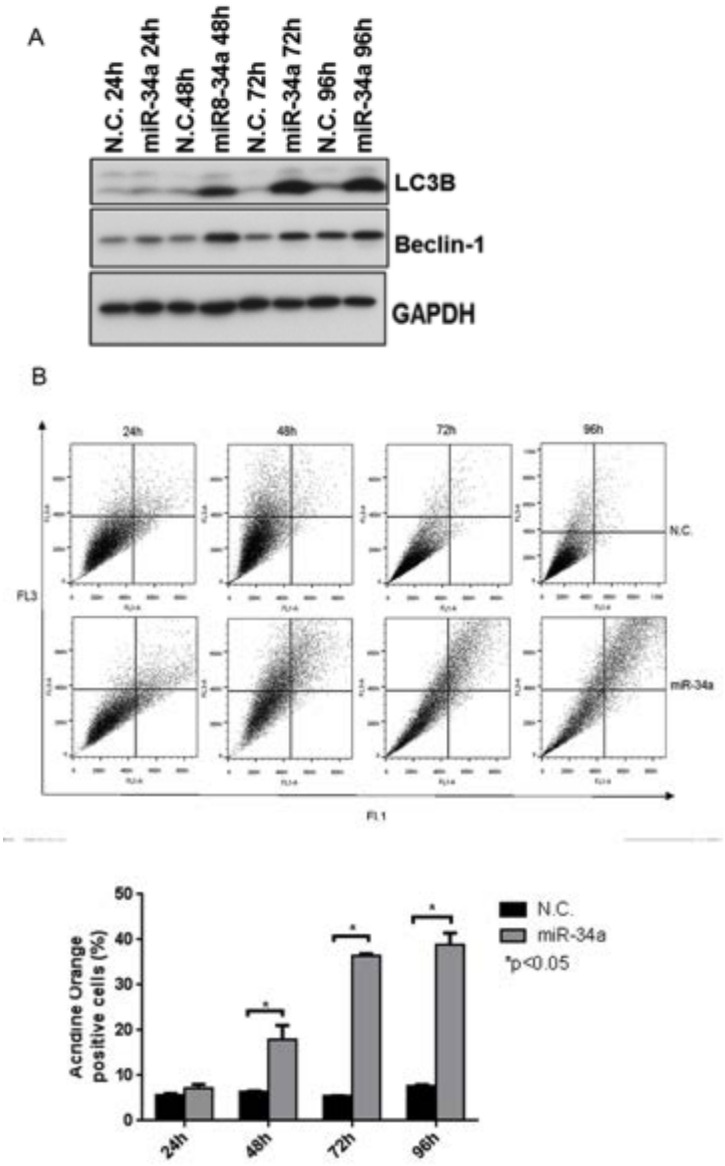

Figure 35 - miR-34a overexpression induces autophagy in PC3 cells

Western blots for LC3B, Beclin-1 and GAPDH for N.C. and miR-34a transfected cells for different time points are shown (A). Acridine orange staining for N.C. or miR-34a transfected cells for different time points was analyzed by Gallios FACS and quantified (B). *denotes $p<0.05$ as measured by student's t test.

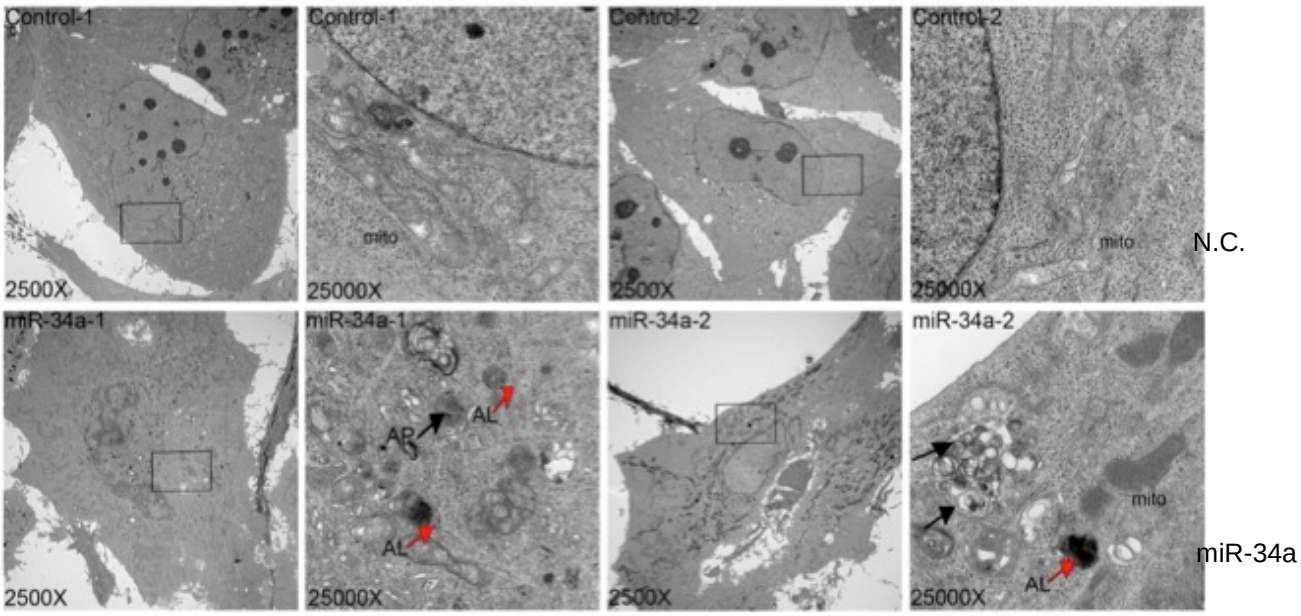

Figure 36 - TEM in miR-34a overexpressing PC3 cells

TEM images at 2500X and 25000X magnification were captured for N.C. and miR-34a transfected PC3 cells at 72h. Black arrows indicate autophagosome (AP)-like structures and red arrows indicate autolysosome (AL)-like structures.

Overexpression of miR-34a induces autophagy in multiple cell lines

I next examined whether miR-34a induced autophagy in other PCa cell lines. The overexpression of miR-34a increased Beclin-1 expression in PC3MM2 cells and LC3II expression in both PC3MM2 and C42B4 cells **(Fig. 37A)**. These increases are similar to those observed in PC3 cells. An increase in acridine orange-positive cells is observed in both PC3MM2 and C42B4 cells **(Fig. 37B)** with miR-34a overexpression at 72 hours post-transfection. To study whether miR-34a-mediated autophagy occurs in other cell types, I transfected HepG2 (a hepatocellular carcinoma cell line), A549 (a lung cancer cell line), MDA MB 231 (a breast cancer cell line) and SKOV3 (an ovarian cancer cell line) with N.C. or miR-34a and measured Beclin-1 and LC3II expression. Overexpression of miR-34a in these cell lines increased LC3BII and often Beclin-1 levels at the 72-hour time point, similar to what is observed in prostate cell lines **(Fig. 38A)**. Overexpression of miR-34a induced cell morphology changes in A549 and HepG2 that are similar to the changes observed in PC3 cells with increase in cell size and flattened appearance **(Fig. 38B)**. These results suggest that miR-34a induces autophagy in PCa and other cancer cell lines examined in this study.

A B

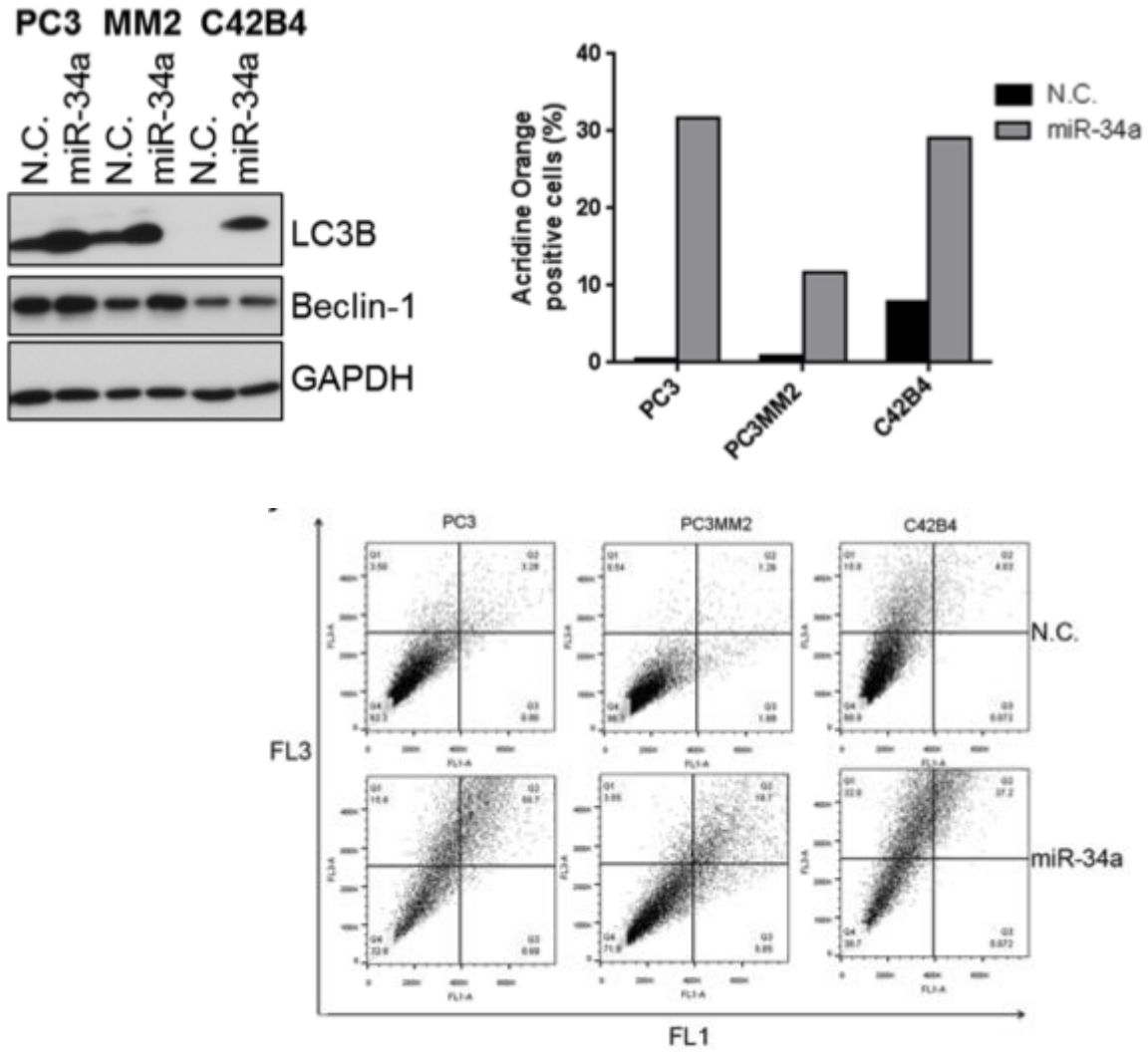

Figure 37 - miR-34a induces autophagy in prostate cancer cell lines

Western blots for Beclin-1, LC3B and GAPDH after 72h transfection with N.C. or miR-34a is shown (A). Acridine orange staining quantification (above) and graphs (below) are shown at 72h after N.C. or miR-34a transfection (B) in PCa cell lines (PC3, PC3MM2, and C42B4).

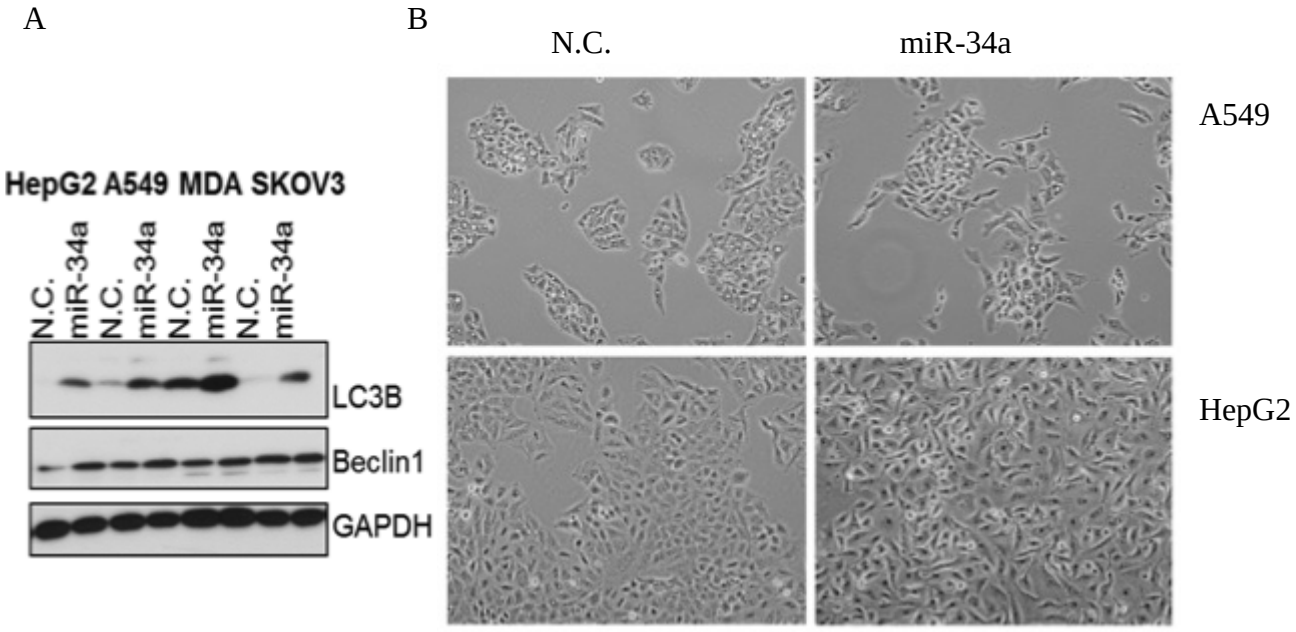

Figure 38 - miR-34a induces autophagy in other cancer cell lines

Western blots for Beclin-1, LC3B and GAPDH after 72h transfection with N.C. or miR-34a are shown for cancer cell lines (HepG2, A549, MDA MB231 and SKOV3) (A). Bright field images at 10x magnification are shown for A549 and HepG2 at 72h post-transfection with N.C. or miR-34a (B)

Discussion

The data presented in this chapter suggest that overexpression of miR-34a induces autophagy with increase in LC3II and Beclin-1 expression and increase in acidic vesicular organelles (AVOs) as well as increase in autophagic structures (APs and ALs). Overexpression of miR-34a induces autophagy in all cancer cell types examined in this chapter, suggesting the effects of miR-34a overexpression are not prostate-specific. These results are contrary to findings of Liu et al. that suggest that miR-34a inhibits autophagy in retinoblastoma cell line by inhibiting HMGB1 under serum starvation and chemotherapy conditions [91]. They did not test whether miR-34a inhibits HMGB1 and autophagy in other cell types. Expression of HMGB1 at mRNA levels was not affected by miR-34a overexpression in PC3 cell line (data not shown), suggesting that HMGB1 was not mediating miR-34a induced autophagy in this system. Downregulation of MET or Axl, miR-34a targets previously reported to induce autophagy along with apoptosis [105, 106] could be mediating miR-34a-induced autophagy observed in this chapter. Also, the levels of miR-34a expression, along with different cellular stress conditions could be responsible for autophagy inhibition or initiation, since loss of miR-34a-HMGB1 pathway was reported to inhibit autophagy and increase ROS production under chemotherapy [91]. In this dissertation, miR-34a expression is increased several folds and autophagy occurs under complete growth medium conditions which could explain the difference in the result with previously published report. The molecular intermediates required for miR-34a-mediated autophagy remains to be identified. In the next chapter, I focused on determining whether miR-34a induces canonical autophagy by studying the involvement of essential autophagy genes.

Chapter 7

Overexpression of miR-34a Induces a Non-Canonical Form of Autophagy

Autophagy is now a general term for defined events that often occur in response to cellular stress involved in mediating degradation of damaged cellular components. However, an increasing amount of evidence demonstrates that there is not a single pathway that leads to "classical" autophagy, rather many forms of autophagy have been reported to affect cell growth and proliferation, for example, including an Atg5/Atg7-independent "alternative" macroautophagy and Beclin-1-independent autophagy [93, 95, 125]. The proteomic analysis of autophagic network in human cells identified a complex network of over 700 interactions and more than 400 interacting proteins in this pathway suggesting requirement of different intermediates for the diverse forms of autophagy observed in mammalian systems [126]. To determine the molecular pathways critical to miR-34a-induced autophagy, in this chapter I examined the involvement of key intermediates in the canonical autophagic pathway- Beclin-1 which is involved in autophagosome formation; ATG5 and ATG7 which are involved in autophagosome elongation and completion and ATG4 involved in LC3 processing and recycling [96, 122]. I used lentiviral shRNA constructs to knockdown Beclin-1; siRNA sequences to knockdown ATG5, ATG7 and ATG4, and doxycline inducible shATG7 PC3 cells to determine their effects of miR-34a induced autophagy and cell proliferation.

miR-34a-induced autophagy does not rely on Beclin-1 expression

Since, miR-34a increased Beclin-1 protein expression (chapter 6); I determined whether miR-34a-induced autophagy is mediated through Beclin-1. A lentiviral shRNA was used to knockdown Beclin-1 in PC3 cells and cells were then FACS sorted for GFP to get PC3 shBeclin-1 cells. PC3 and shBeclin-1 cells were then transfected with N.C. or miR-34a for 72 hours. Knockdown of Beclin-1 did not change cell morphology, whereas

overexpression of miR-34a in shBeclin-1 cells induced similar morphological changes as observed in PC3 cells with miR-34a overexpression **(Fig. 39)**. As shown in **Fig. 40**, protein **(Fig. 40A)** and mRNA **(Fig. 41B)** expression of Beclin-1 was decreased following lentiviral infection, while ATG7 mRNA expression was unaffected **(Fig. 41A).** These results suggest specific knockdown of Beclin-1 was achieved. I next examined the effects of Beclin-1 knockdown on miR-34a-induced autophagy by determining if conversion of LC3 to LC3II occurred. My results demonstrate that miR-34a overexpression increases LC3II expression **(Fig. 40A** lane 1 vs. 2**)** with or without Beclin-1 knockdown **(Fig. 40A**, lane 3 vs. 4**)**, suggesting that miR-34a induces autophagy independent of Beclin-1.

To determine if miR-34a still downregulates critical targets in Beclin-1 knockdown cells, I examined the expression of its known targets, MET and Axl. As expected, overexpression of miR-34a was still effective in inhibiting these targets as shown by decrease in MET protein and mRNA expression **(Fig. 40 and 41B)** and decrease in Axl expression **(Fig. 41C)** in shBeclin-1 cells. I also examined the effects of miR-34a on proliferation in Beclin-1 knockdown cells and consistent with my previous data, miR-34a overexpression decreased cell proliferation compared to N.C. **(Fig. 42**, column 1 vs. 2**)**. Beclin-1 knockdown also decreased cell proliferation compared to N.C. **(Fig. 42**, column 1 vs. 3**)**; however, miR-34a overexpression further decreased proliferation in shBeclin-1 cells **(Fig. 42** column 3 vs. 4**)**. Analysis of acridine orange positive (AO+) cells demonstrated an increase in AO+ cells with miR-34a overexpression, irrespective of Beclin-1 knockdown **(Fig. 43A)**. Additionally, cell cycle analysis demonstrated a 5-fold increase in the sub G1 fraction of cells following miR-34a overexpression in both control and shBeclin-1 cells **(Fig. 44B)**.

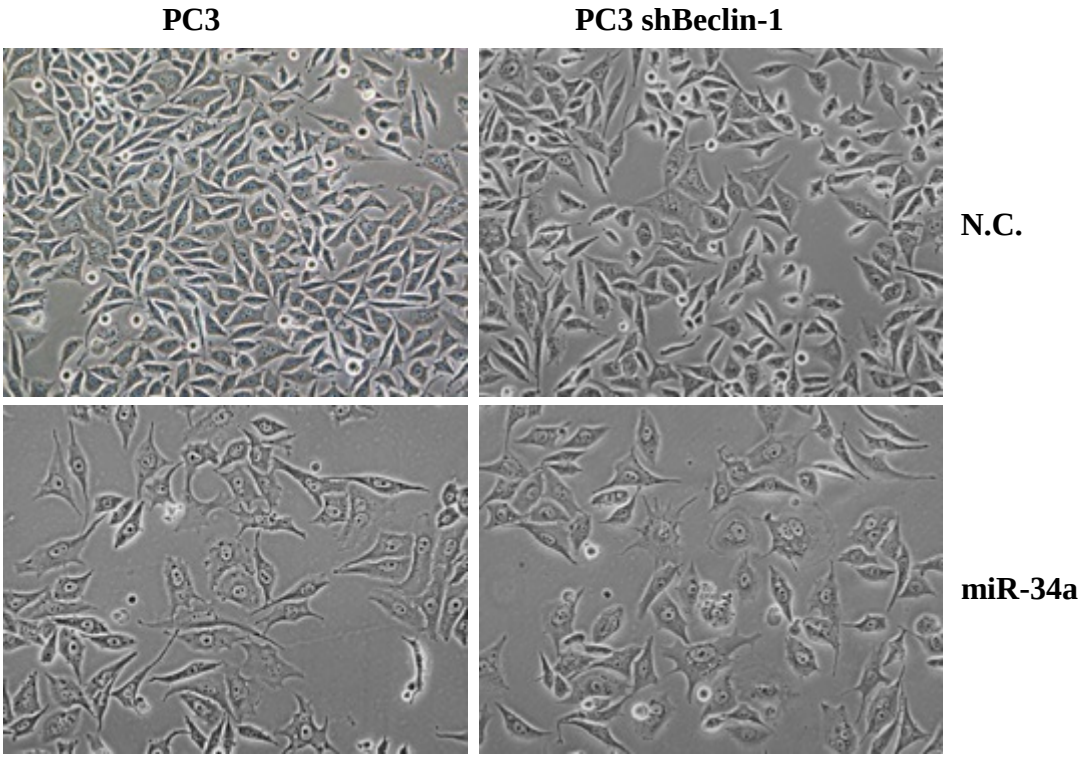

Figure 39 - Morphology of miR-34a overexpressing PC3 cells with Beclin-1 knockdown

PC3 and PC3 cells with shBeclin-1 were transfected with N.C. or miR-34a for 72h and bright field microscopy was used to capture images at 10x magnification using Nikon camera.

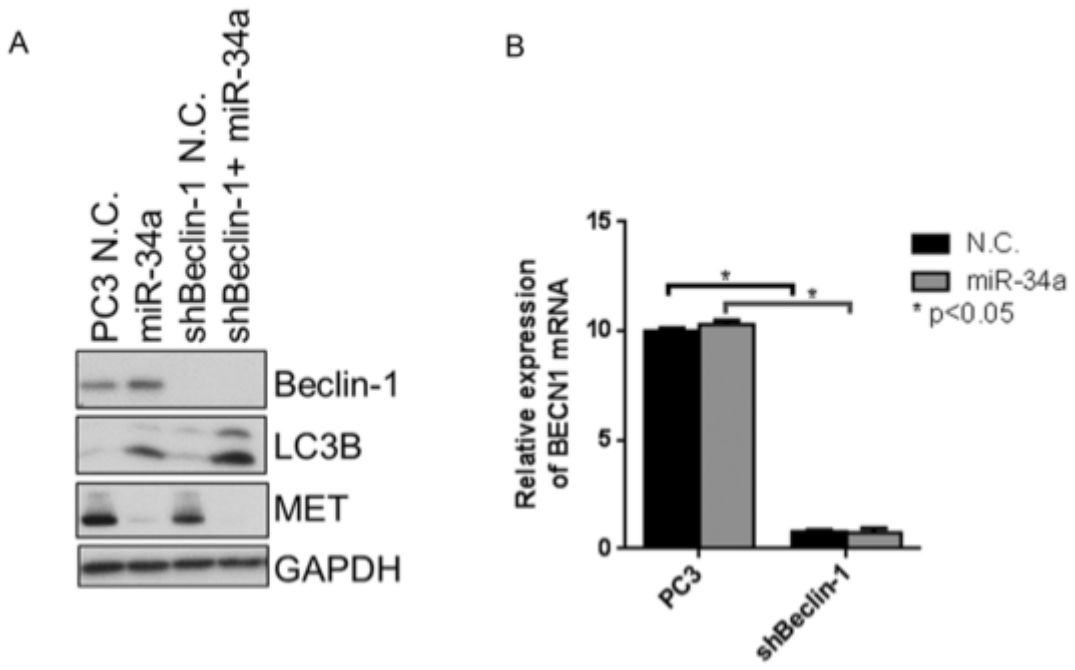

Figure 40 - Beclin-1 knockdown in PC3 cells

Western blot for Beclin-1, LC3B, MET and GAPDH are shown for PC3 and PC3 shBeclin-1 cells with N.C. or miR-34a transfection (A). mRNA expression was measured using SYBR Green qPCR and plotted for Beclin-1 (B). * denotes $p<0.05$ as measured by t test.

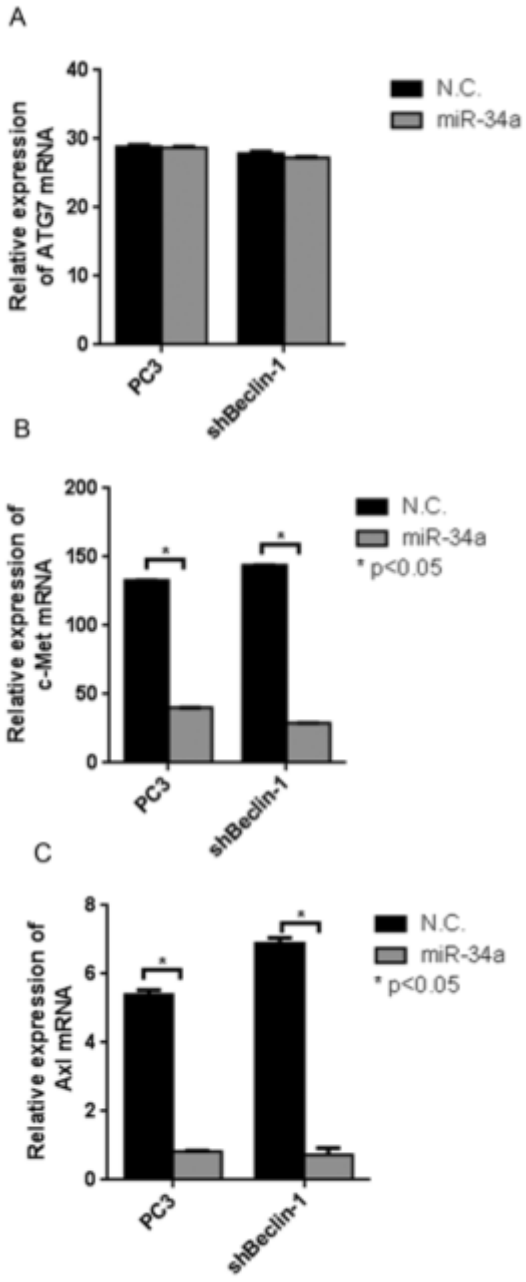

Figure 41 – mRNA expression analysis with Beclin-1 knockdown in PC3 cells

mRNA expression for ATG7, c-Met and Axl (A-C) was measured using SYBR Green qPCR in PC3 and shBeclin-1 cells transfected with N.C. or miR-34a. * denotes $p<0.05$ as measured by student's t test.

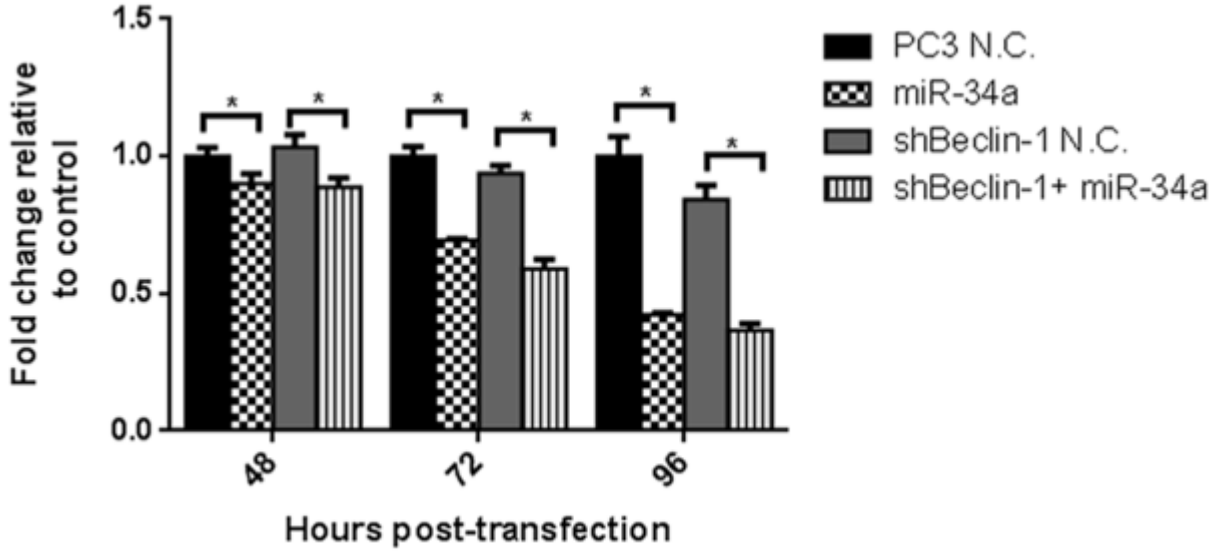

Figure 42 - Effects of miR-34a overexpression on proliferation in shBeclin-1 cells

Hoechst proliferation assay at different time points for PC3 and PC3 shBeclin-1 with N.C. or miR-34a transfection is graphed. * denotes $p<0.05$ as measured by t test.

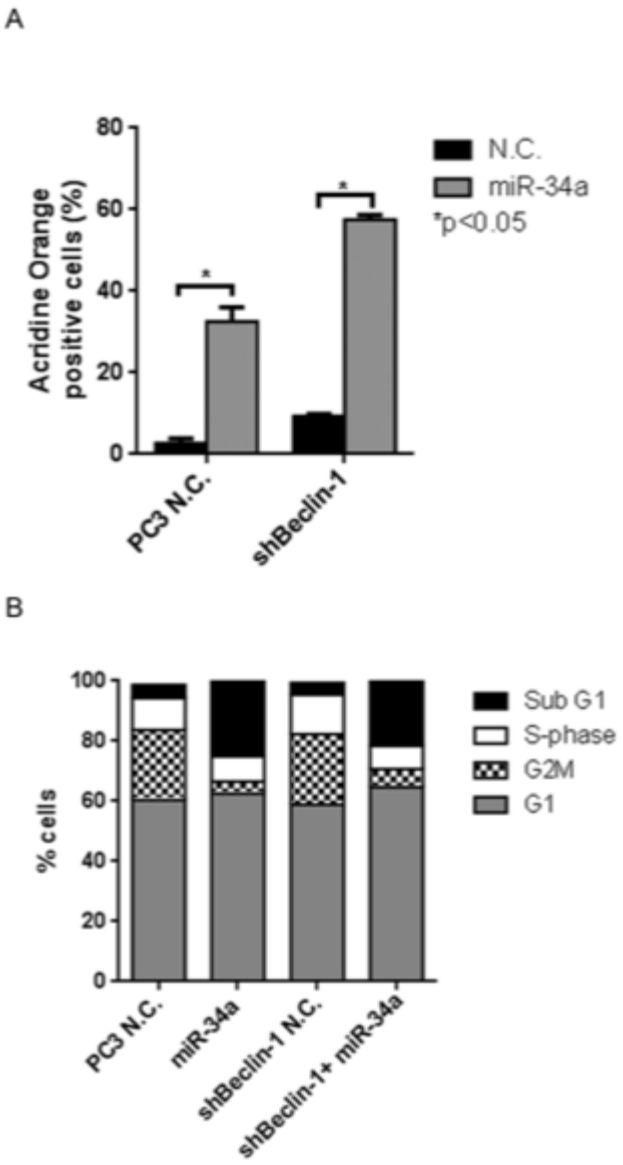

Figure 43 - Acridine Orange and cell cycle analysis in PC3 cells with Beclin-1 knockdown and miR-34a overexpression

Acridine orange positive cells were quantified by Gallios FACS and plotted (A) at 72 hours post N.C. or miR-34a transfection. Propidium iodide was used for cell cycle analysis at 72 hours post N.C. or miR-34a transfection and different phases are plotted (B). * denotes $p<0.05$ as measured by student's t test.

These data suggest that miR-34a-induced effects on autophagy, cell proliferation, and apoptosis are mediated in a Beclin-1-independent manner.

miR-34a induces ATG5/7-independent autophagy

I next determined whether ATG5 and ATG7, canonically involved in autophagosome elongation and completion [122] were required for the form of autophagy observed upon miR-34a overexpression. I used two sequences of siRNA to robustly knockdown ATG5 and ATG7 expression in PC3 cells and then transfected them with N.C. or miR-34a. Success of knockdown was determined by immunoblotting and qPCR. ATG5 and ATG7 were reduced more than 90% at the protein **(Fig. 44A and Fig. 45A)** and mRNA **(Fig. 44B and Fig. 45B)** levels by corresponding siRNAs. The mRNA expression of ATG7 in siATG5 **(Fig. 44C)** and ATG5 in siATG7 **(Fig. 45C)** cells is unaffected, suggesting specificity of knockdown of the targeted gene. Knockdown of ATG5 and ATG7 did not change cell morphology whereas overexpression of miR-34a in siATG5 and siATG7 cells induced similar morphological changes as observed in PC3 cells with miR-34a overexpression **(Fig. 46 and Fig. 47)**. As expected, siATG5 and siATG7 decreased LC3II levels compared to N.C. **(Fig. 44A and 45A**, lane 1 vs. lane 3 and lane 1 vs. 5**)** confirming that knocking down these gene products inhibits basal autophagy. I then examined the effects of miR-34a overexpression on autophagy when either ATG5 or ATG7 is reduced by siRNA knockdown. As observed previously with PC3 cells, miR-34a overexpression increased conversion of LC3 to LC3II as indicated by increase in LC3II band compared to N.C. **(Fig. 44A and 45A** lane 1 vs. 2**)**.

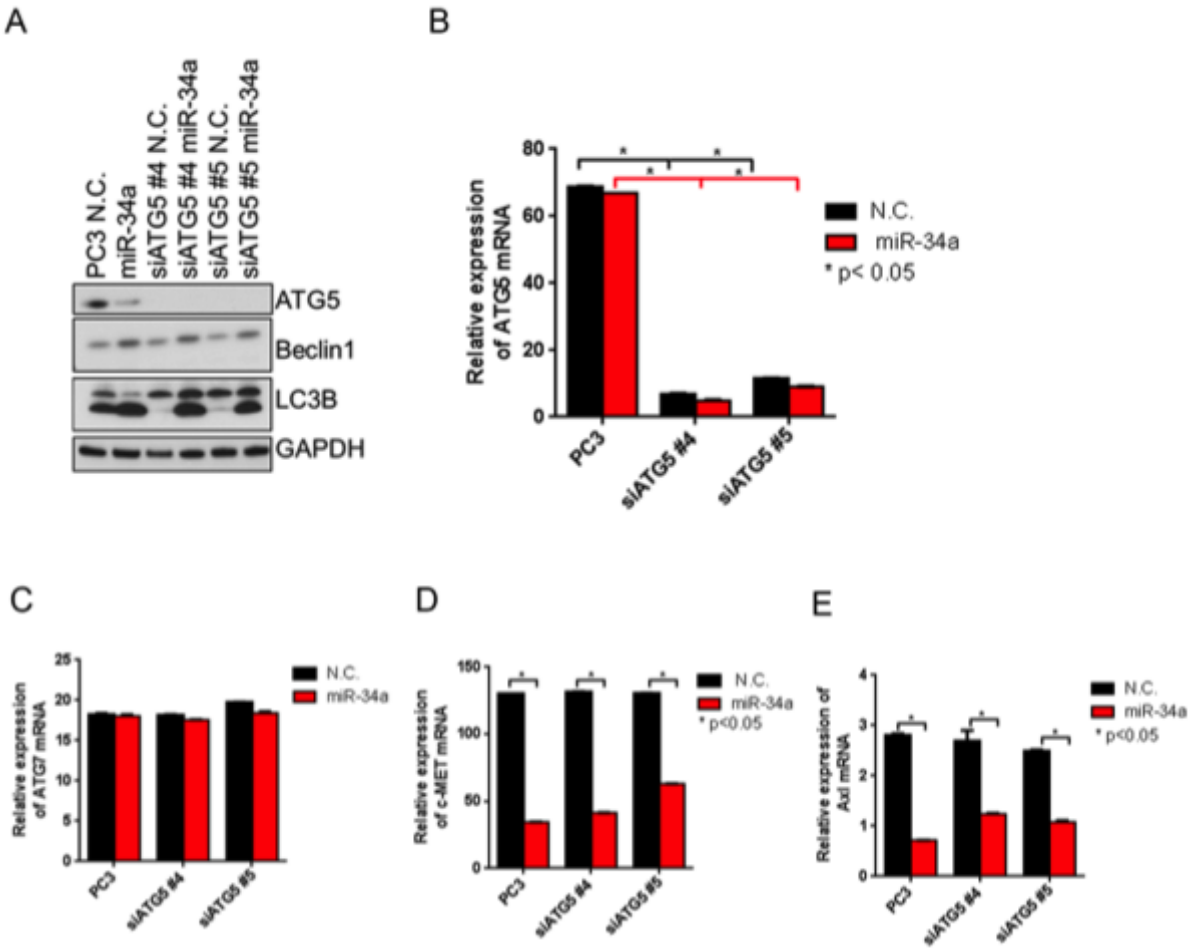

Figure 44 - Effects of ATG5 knockdown in PC3 cells

Western blots for N.C., miR-34a and two siATG5 sequences with N.C. or miR-34a transfection for ATG5, LC3B and GAPDH are shown (A). mRNA expression for ATG5, ATG7, c-Met and Axl for N.C., miR-34a and two siATG5 sequences with N.C. or miR-34a transfection after 72h was measured by SYBR Green qPCR and plotted. * denotes $p<0.05$ as measured by t test.

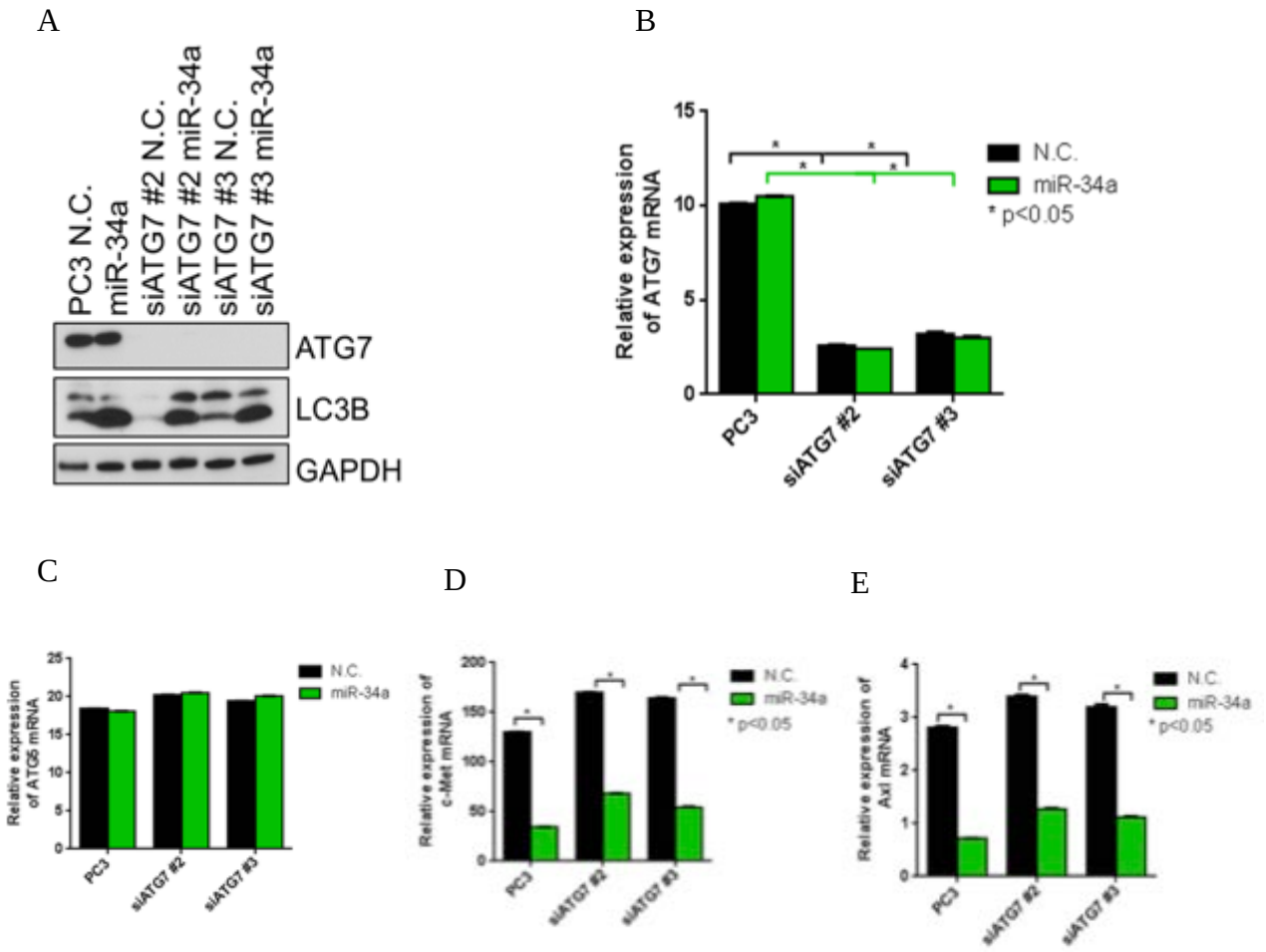

Figure 45 - Effects of ATG7 knockdown in PC3 cells

Western blots for N.C., miR-34a and two siATG7 sequences with N.C. or miR-34a transfection for ATG7, LC3B and GAPDH are shown (A). mRNA expression for ATG7, ATG5, c-Met and Axl for N.C., miR-34a and two siATG7 sequences with N.C. or miR-34a transfection after 72h was measured by SYBR Green qPCR and plotted. * denotes $p<0.05$ as measured by t test.

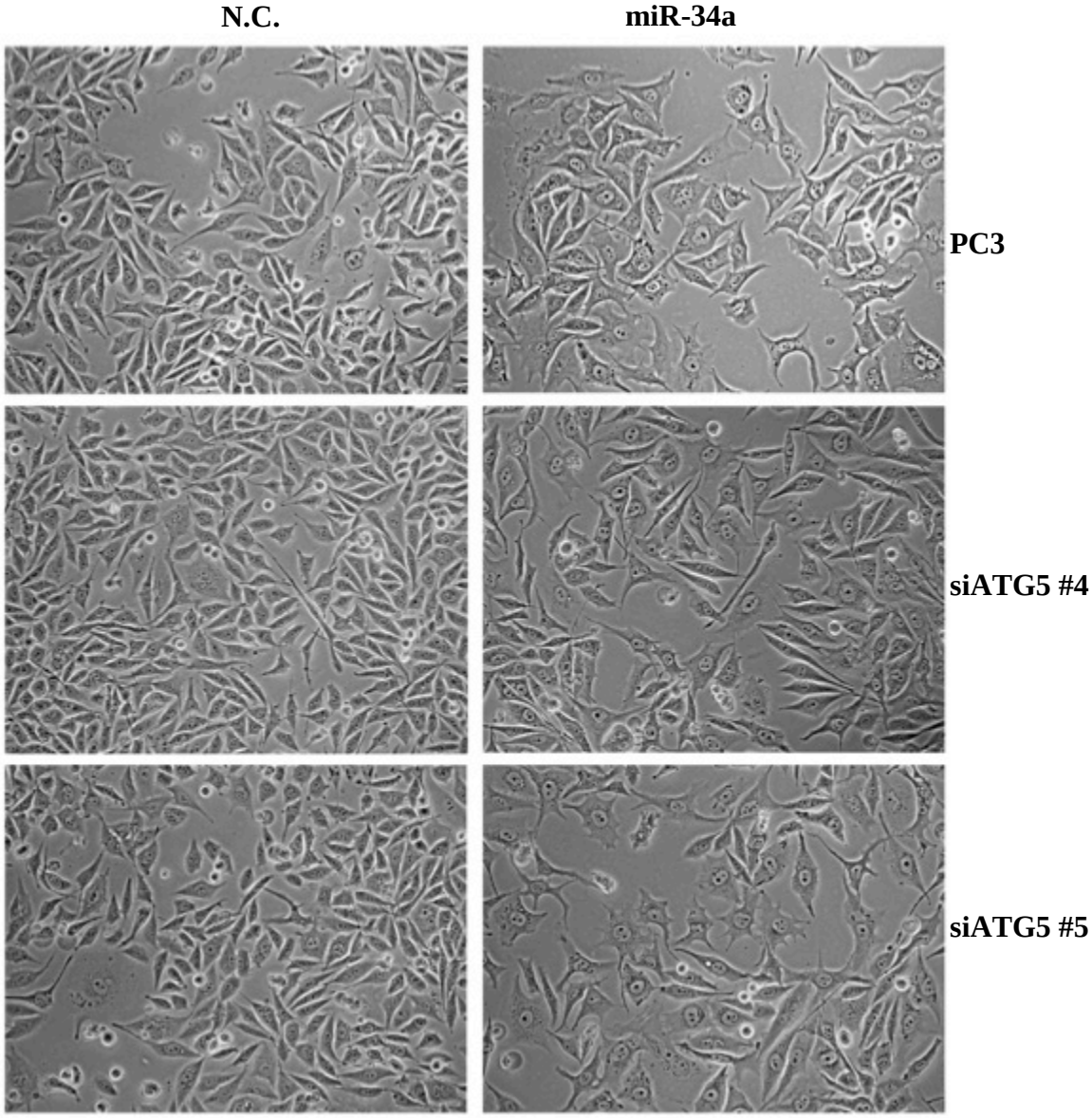

Figure 46 - Morphology of miR-34a overexpressing PC3 cells with ATG5 knockdown

PC3 and PC3 cells with siRNA sequences of ATG5 were transfected with N.C. or miR-34a for 72h and bright field microscopy was used to capture images at 10x magnification using Nikon camera.

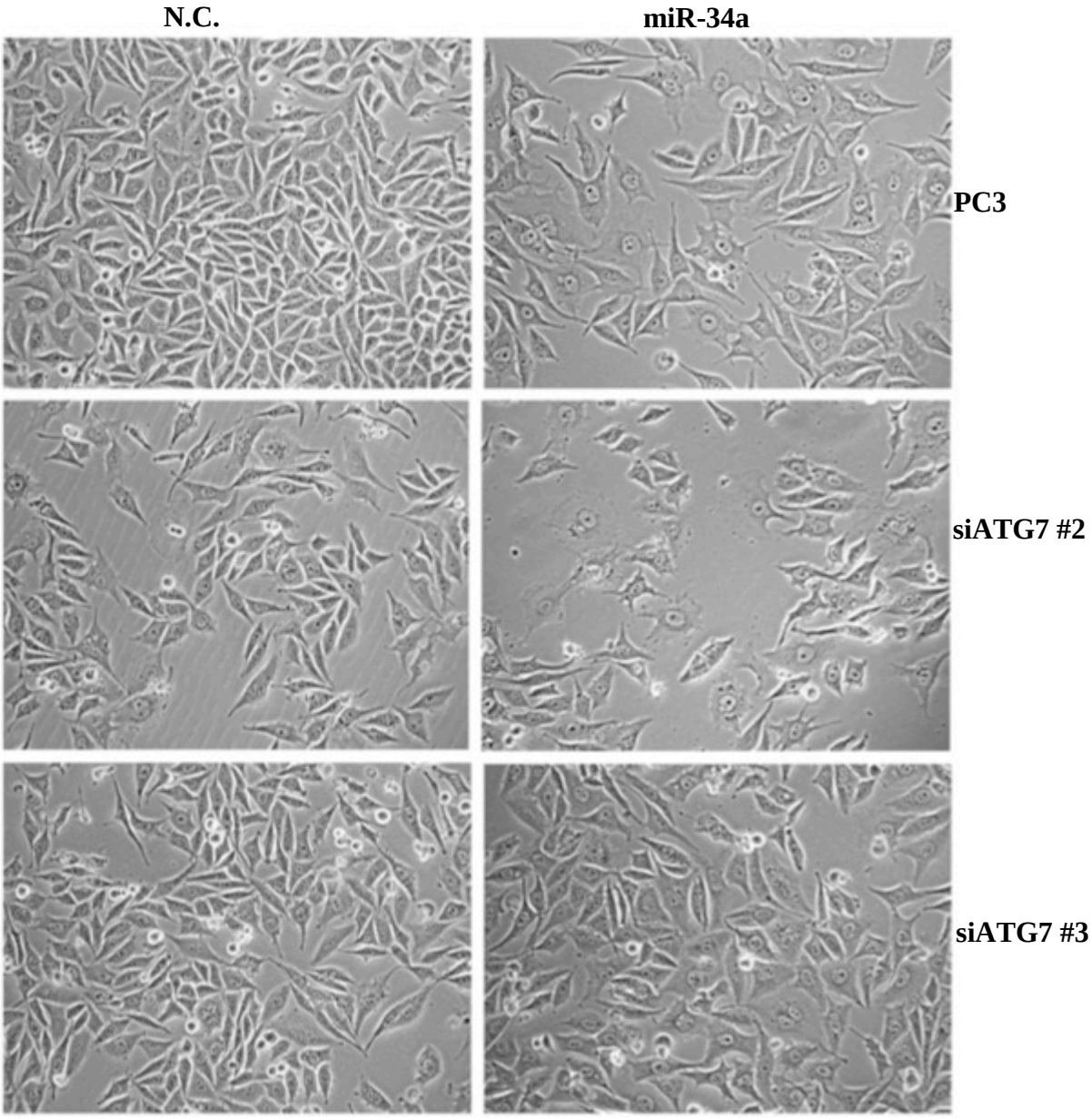

Figure 47 - Morphology of miR-34a overexpressing PC3 cells with ATG7 knockdown

PC3 and PC3 cells with siRNA sequences of ATG7 were transfected with N.C. or miR-34a for 72h and bright field microscopy was used to capture images at 10x magnification using Nikon camera.

Surprisingly, in the cells in which either ATG5 or ATG7 is reduced, miR-34a overexpression still increased LC3II levels compared to N.C. **(Fig. 44A and 46A**, lane 3 vs. 4 and lane 5 vs. 6**)**. This result suggests that miR-34a-induced autophagy is independent of ATG5 and ATG7. Interestingly, miR-34a overexpression itself was sufficient to decrease ATG5 protein (**Fig. 44A** lane 1 vs. 2**)**, further suggesting that ATG5 is not involved miR-34a-mediated autophagy. Both *c-met* **(Fig. 44D and 46D)** and *Axl* **(Fig. 44E and 45E)** mRNA levels were decreased with miR-34a overexpression in siATG5 and siATG7 cells, demonstrating miR-34a still downregulates these targets that are involved in mediating autophagy [105, 106]

To determine the effects of miR-34a on proliferation in cells with reduced ATG5 and ATG7, a Hoechst proliferation assay was performed. Overexpression of miR-34a decreases proliferation compared to N.C. **(Fig. 48A and 48B** column 1 vs. 2**)**, consistent with my previous data. Reduced ATG5 and ATG7 expression decreased basal autophagy and cell proliferation compared to N.C. **(Fig. 48A and 48B** column 3 and 4 vs. column 1**)** consistent with previous reports [107]. However, miR-34a overexpression further decreased proliferation in cells with reduced ATG5 **(Fig. 48A** column 3 vs. 4 and 5 vs. 6**)** and ATG7 **(Fig. 48B** column 3 vs. 4 and 5 vs. 6**)**. This result suggests that ATG5 and ATG7 affect canonical autophagy and cell proliferation, but not miR-34a-induced autophagy and its effect on cell proliferation.

A

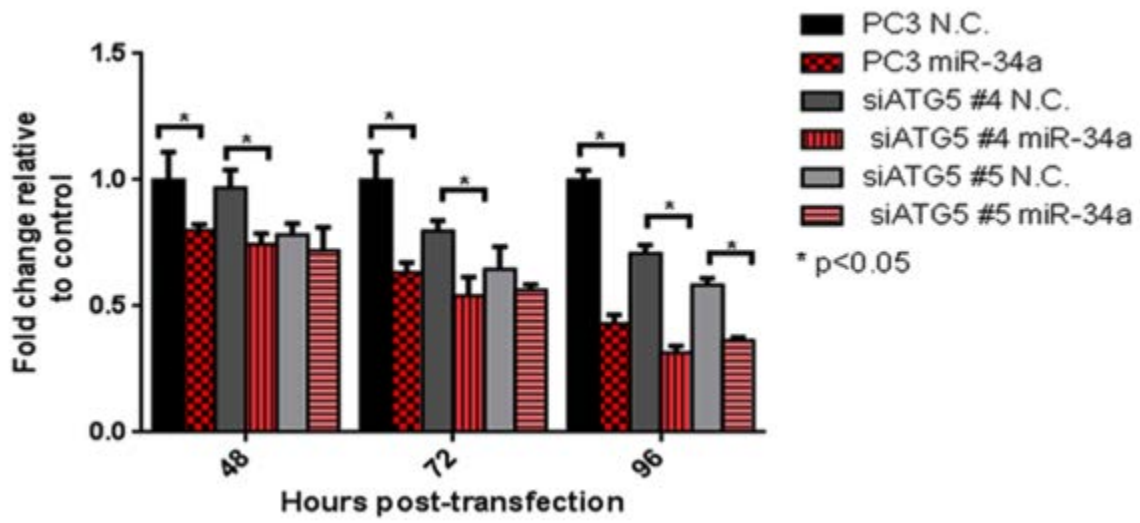

B

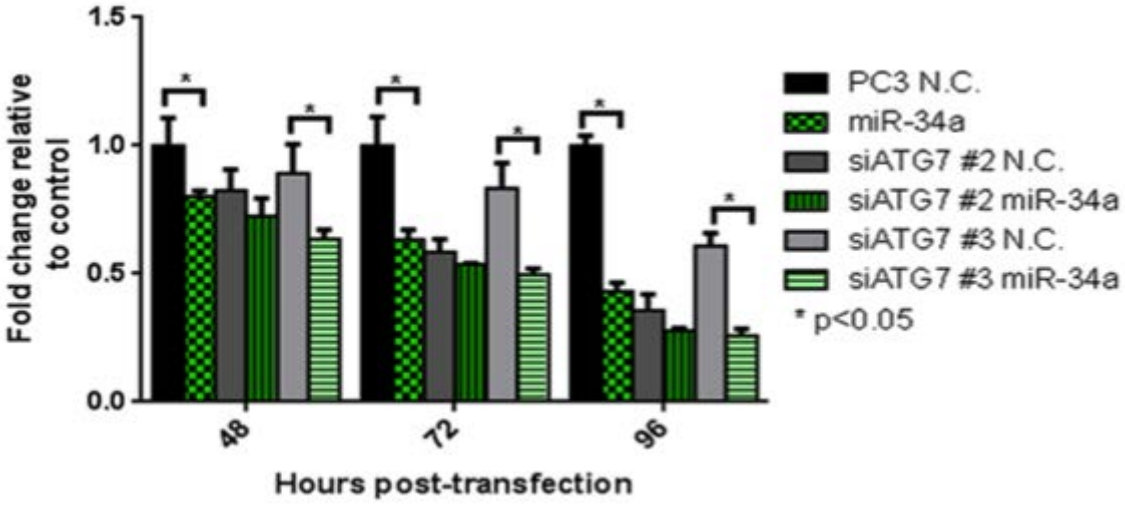

Figure 48 - Cell Proliferation in siATG5 and siATG7 cells with miR-34a overexpression

Hoechst proliferation assay at different time points for N.C., miR-34a and two siATG5 (A) and two siATG7 (B) sequences with N.C. or miR-34a transfection is graphed. * denotes $p<0.05$ as measured by student's t test.

To minimize potential effects due to transient transfection, I also examined PC3 cells with doxycycline-inducible shATG7 to assess the effects of miR-34a overexpression when ATG7 is stably reduced. Upon addition of doxycycline, ATG7 protein **(Fig. 49A)** and mRNA **(Fig. 49B)** are decreased without affecting ATG5 mRNA levels **(Fig. 51A)**, confirming the inducible knockdown of ATG7. Overexpression of miR-34a in the absence or presence of doxycycline (in which shATG7 was induced) led to similar morphologic alterations observed by miR-34a transfection alone; changes similar to that observed in PC3 and siATG7 cells with mR-34a overexpression **(Fig. 50)**. As a control, miR-34a overexpression still decreased mRNA levels of c-Met **(Fig. 51B)** and Axl **(Fig. 51C)** in both non-induced and shATG7 conditions. To examine the effects of shATG7 on miR-34a-induced autophagy, I determined LC3II protein expression. Consistent with my results in PC3 transiently transfected with siATG7, an increase in LC3II expression was observed with miR-34a overexpression in both non-induced **(Fig. 49A)** and Dox-induced shATG7 **(Fig. 49A** lane 3 vs. 4**)** cells. This result supports the previous data that miR-34a effects on LC3II are independent of decreased ATG7 expression. Further, a decrease in cell proliferation was observed in non-induced cells with miR-34a overexpression **(Fig. 52** column 1 vs. 2**)**. Similar to results obtained with siATG7, shATG7 decreased proliferation compared to N.C. at 96 hours **(Fig. 52** column 1 vs. 3**)** and miR-34a overexpression further decreases proliferation in cells with reduced ATG7 at 96 hours (**Fig. 52** column 3 vs. 4**)**. Taken together, these data suggest that miR-34a overexpression induces autophagy that is independent of decreased ATG5 and ATG7 expression.

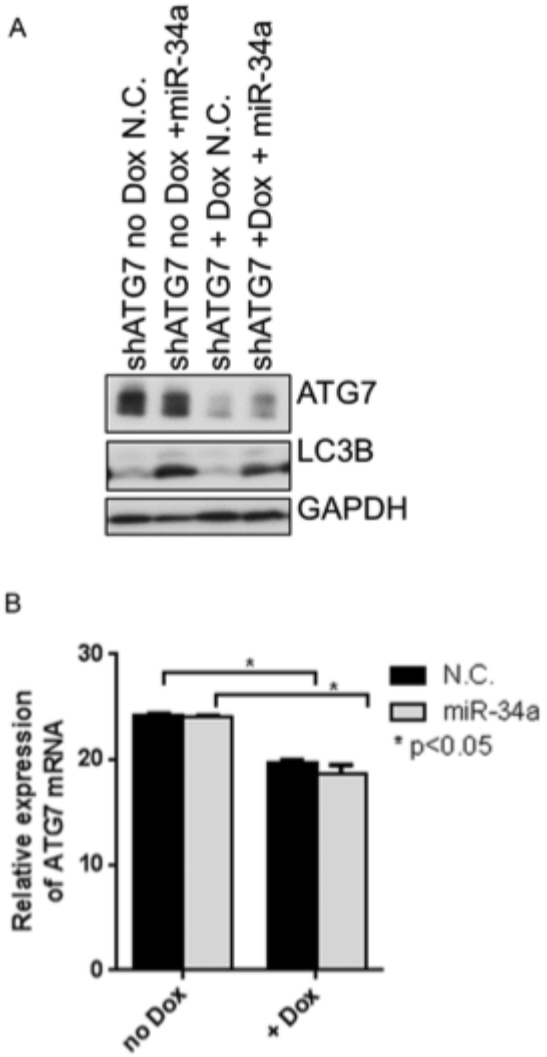

Figure 49 - Effects of miR-34a overexpression in doxycycline inducible shATG7 PC3 cells

Western blots for ATG7, LC3B and GAPDH (A) and mRNA expression for ATG7 (B) in non-induced and Dox-induced shATG7 cells transfected with N.C. or miR-34a is plotted * denotes $p<0.05$ as measured by student's t test.

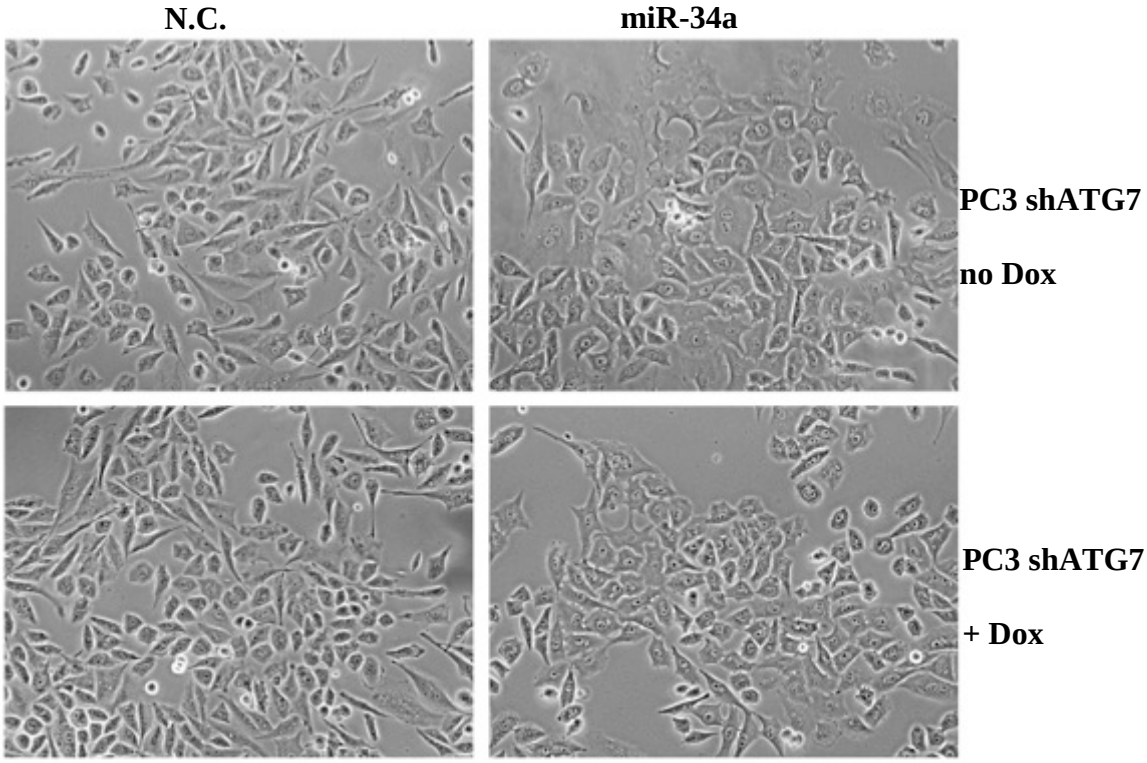

Figure 50 - Morphology of miR-34a overexpressing in doxycycline inducible shATG7 PC3 cells

Non-induced and doxycycline-induced shATG7 PC3 cells with were transfected with N.C. or miR-34a for 72h and bright field microscopy was used to capture images at 10x magnification using Nikon camera.

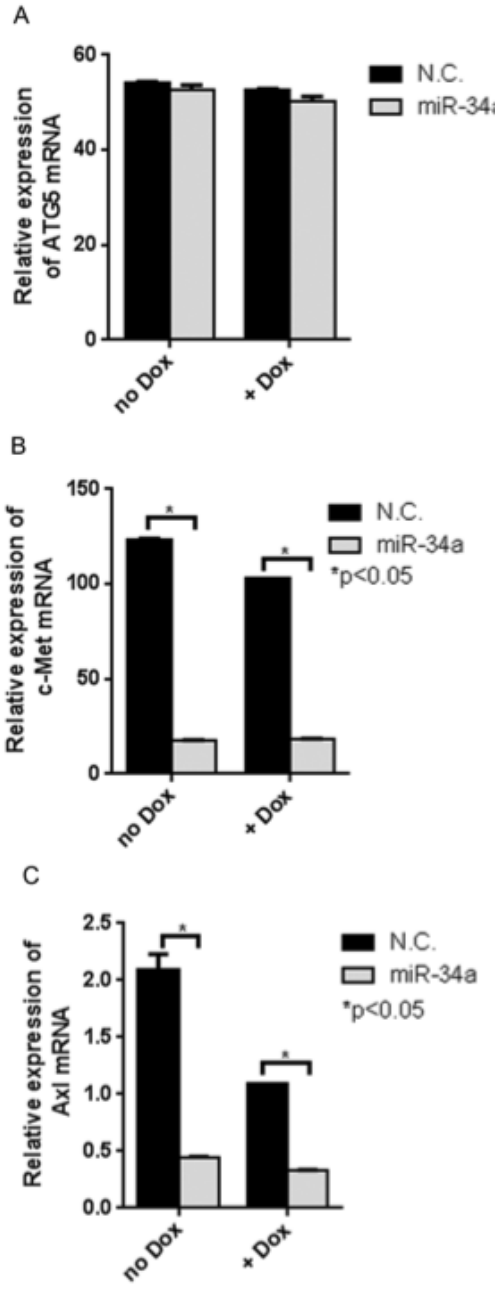

Figure 51 – mRNA expression analysis with miR-34a overexpression in doxycycline inducible shATG7 PC3 cells

mRNA expression for ATG5, c-Met and Axl was measured in non-induced and Dox-induced shATG7 cells transfected with N.C. or miR-34a * denotes $p<0.05$ as measured by student's t test.

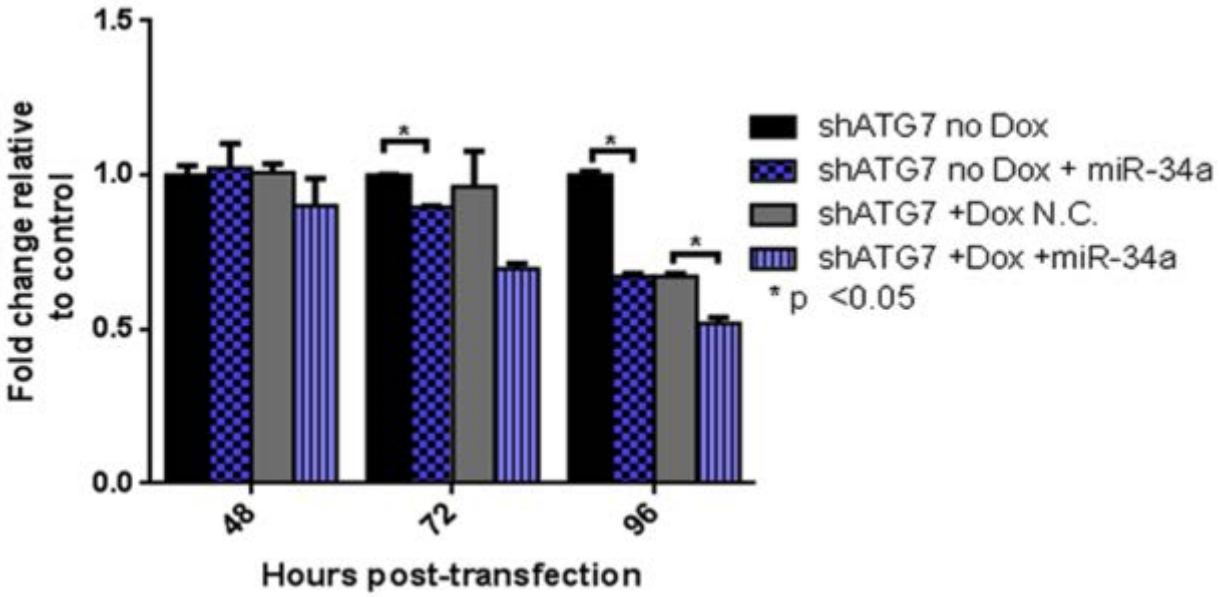

Figure 52 - Cell Proliferation in doxycycline inducible shATG7 PC3 cells

Hoechst proliferation assay at different time points for PC3 shATG7 no Dox and +Dox with N.C. or miR-34a transfection is graphed. * denotes p value <0.05 as measured by student's t test.

ATG4 knockdown effects autophagy independent of miR-34a overexpression

Since, knockdown of ATG7 and ATG5, the intermediates involved in the downstream processing of LC3II did not affect the form of autophagy induced by miR-34a overexpression; I examined whether ATG4, a cysteine protease involved upstream in the conversion of pro-LC3 to LC3I is required for miR-34a induced autophagy. ATG4 has four isoforms, ATG4A, ATG4B, ATG4C and ATG4D with overlapping and distinct functions. I used siRNA sequences to knock down all four isoforms of ATG4 in PC3 cells and then transfected the cells with either control (N.C.) or miR-34a mimics for 72 hours. The overexpression of miR-34a in PC3 cells led to altered cellular morphology that was similar to that observed with previous knockdowns or by overexpression of miR-34a alone; however, knockdown of ATG4 alone induced morphological changes with cells appearing larger and flattened **(Fig. 53)** compared to control cells. Overexpression of miR-34a in siATG4 cells further altered the morphology of the cells with increases in cell size and in the perinuclear region **(Fig. 53)**. Next, I prepared protein lysates and performed immunoblotting for different ATG4 isoforms. All isoforms of ATG4 (A-D) were reduced with siRNA sequences confirming that the knockdown was efficient in decreasing ATG4 expression **(Fig. 54A)**. LC3II expression was increased with miR-34a overexpression compared to N.C. cells. However, knockdown of ATG4 alone increased LC3II expression, while the overexpression of miR-34a in siATG4 cells further increased LC3II expression **(Fig. 54A)**. This result suggests that knockdown of ATG4 itself has effects on increasing LC3II levels, independent of autophagy induced by miR-34a. Cell cycle analysis demonstrated increases in the sub G1 fraction of cells and decrease in S-phase following miR-34a overexpression in both control and siATG4 cells **(Fig. 54B)**.

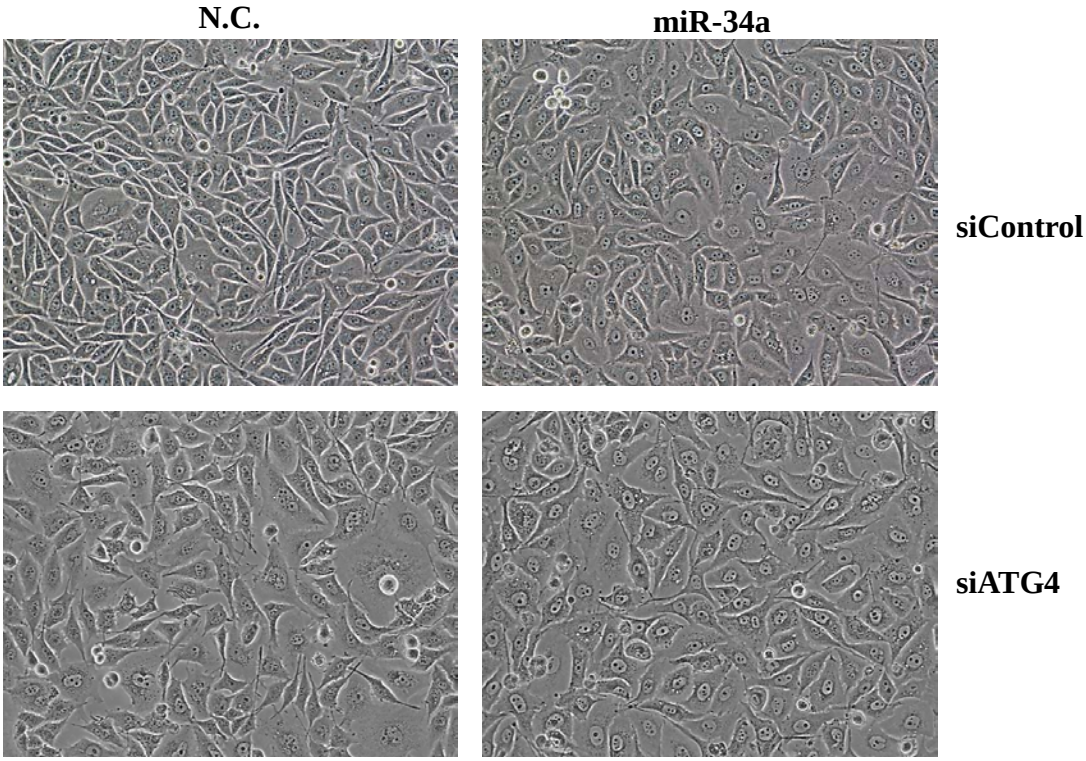

Figure 53 - Morphology of PC3 cells with ATG4 knockdown and miR-34a overexpression

PC3 cells were transfected with control siRNA or ATG4 siRNAs and then after 24 hours, transfected again with N.C. or miR-34a mimics and bright field images were taken with Nikon digital camera.

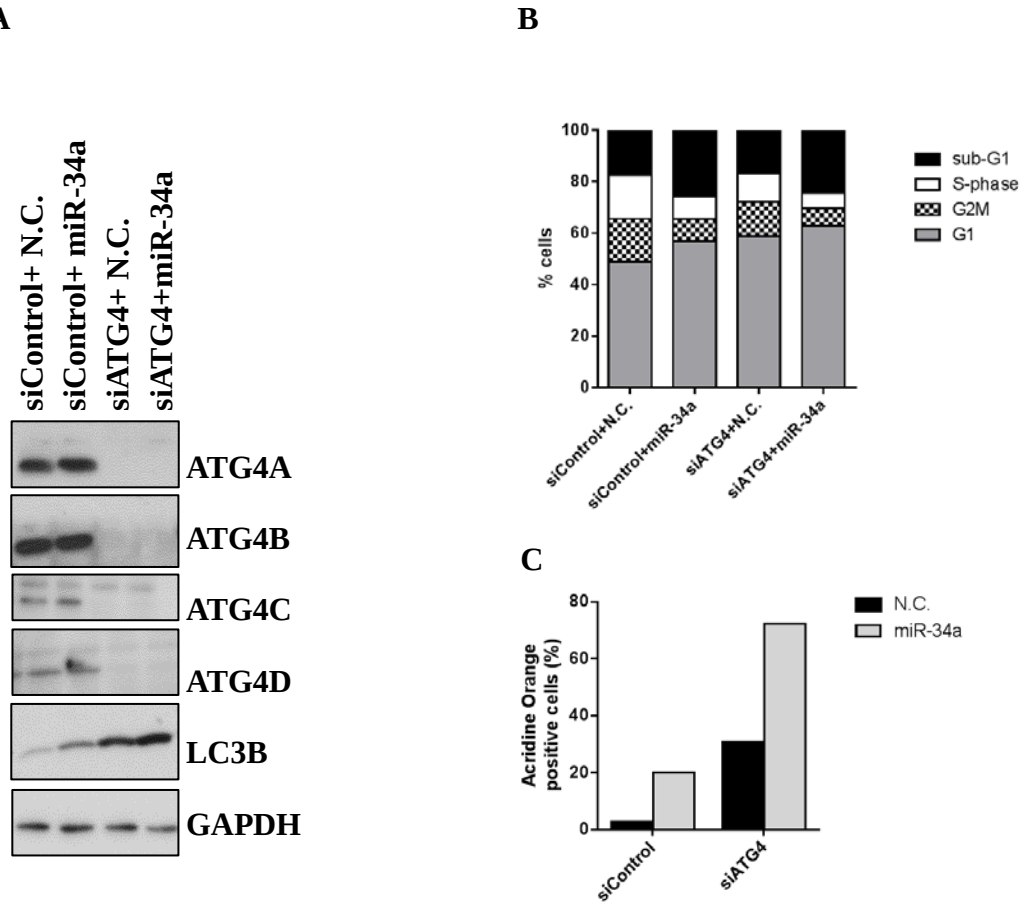

Figure 54 - Effects of ATG4 knockdown in PC3 cells

PC3 cells were transfected with control siRNA or ATG4 siRNAs and then after 24 hours, transfected again with N.C. or miR-34a mimics. After 72 hours of miRNA transfection, cells were harvested for protein for immunoblotting with ATG4 antibodies (ATG4A, 4B, 4C and 4D) and LC3B (A); for cell cycle analysis with PI (B) and for acridine orange FACS analysis (C).

Analysis of acridine orange positive (AO+) cells demonstrated an increase in AO+ cells with miR-34a overexpression **(Fig. 54C)**, while ATG4 knockdown itself increased AO+ cells and miR-34a overexpression further increased AO+ cells with ATG4 knockdown **(Fig. 54C)**. Confocal imaging with AO to visualize the acidic vesicular organelles further corroborated the FACS results with increased accumulation of acridine orange in cytoplasm with miR-34a overexpression compared to control **(Fig. 55, top panel)**. ATG4 knockdown also increased cytoplasmic acridine orange staining similar to FACS results and overexpression of miR-34a further increased AO stained acidic vesicular organelles in ATG4 knockdown cells **(Fig. 55, bottom panel).** These results suggest that ATG4 knockdown has effects on impaired autophagy with increased accumulation of LC3II and acridine orange positive cells independent of miR-34a and overexpression of miR-34a can induce autophagy even with ATG4 knockdown.

Discussion

Results from chapters 6 and 7 provide definitive evidence that overexpression of miR-34a induces autophagy, with both molecular markers (e.g., increase in lipidation of LC3 to form LC3II, increase in acidic vesicular organelles) and morphologic criteria (presence of autophagosomes and autolysosomes by TEM) occurring **(Figures 35-38, 40, 44-45 and 49)**. However, as discussed in the Introduction, recent studies demonstrate that molecular pathways leading to autophagy are diverse, suggesting there may not be a single “canonical” pathway. In this chapter, I demonstrate that the form of autophagy induced with miR-34a overexpression does not rely on the expression of Beclin-1, ATG5 or ATG7, whose gene products “classically” play essential roles in mediating autophagy following nutrient

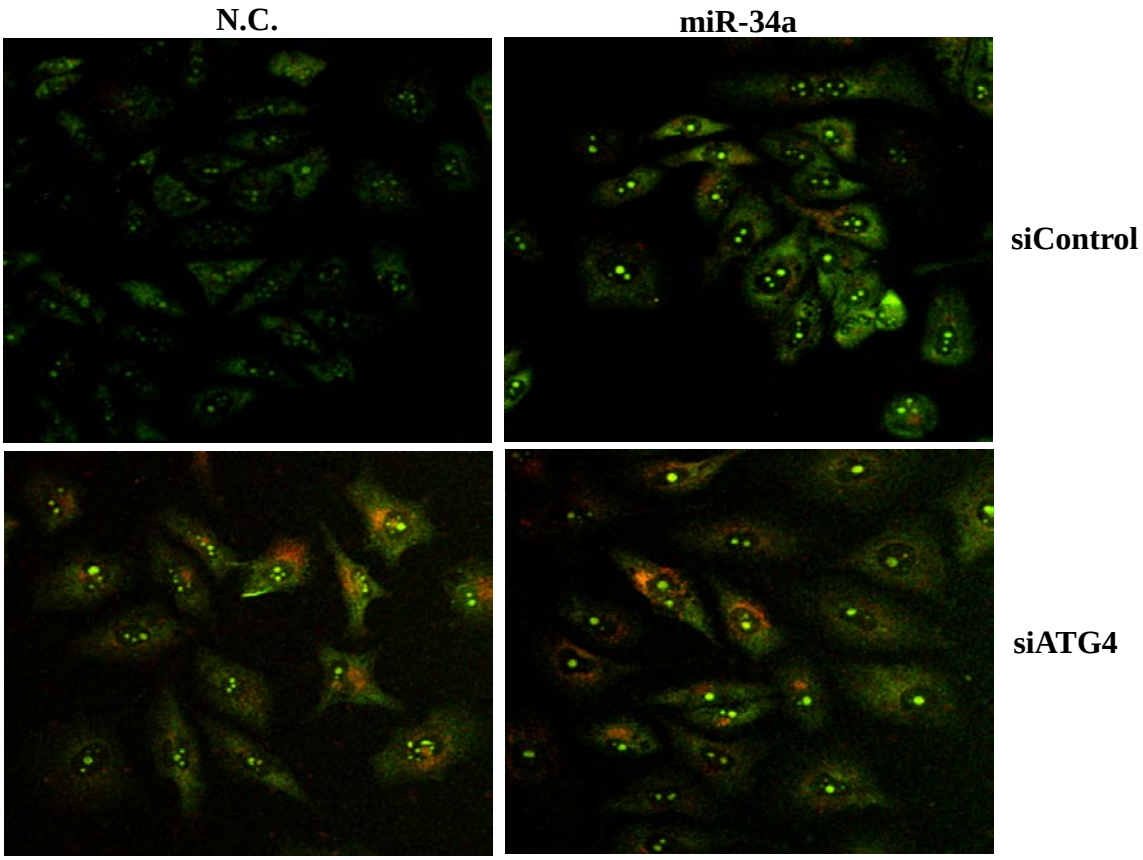

Figure 55 - Acridine Orange staining in PC3 cells with ATG4 knockdown and miR-34a overexpression

PC3 cells were transfected with control siRNA or ATG4 siRNAs and then after 24 hours, transfected again with N.C. or miR-34a mimics. After 72 hours of miRNA transfection, acridine orange was added for an hour and cells were fixed with 4% paraformaldehyde and sucrose solution. Fixed cells were then imaged with confocal microscope at 20X magnification.

starvation, metabolic stress or by chemotherapeutic agents [92, 124] though possible effects of incomplete knockdown cannot be excluded. ATG4 knockdown has effects on autophagy independent of miR-34a overexpression.

My results with ATG5 and ATG7 agree with those of Nishida et al., who first reported an Atg5/Atg7-independent "alternative" macroautophagy in which autophagosomes and autolysosomes were still observed in mouse cells with *Atg5* or *Atg7* knockout [95]. However, lipidation of LC3 to form LC3II did not occur in this alternative autophagy observed in their $Atg5^{-/-}$ or $Atg7^{-/-}$ MEF cells [95]. Thus, autophagy I observe has some of the characteristics of being ATG5/ATG7 independent; however robust increase in LC3II expression in both siRNA and shRNA mediated knockdown of ATG5 and ATG7 respectively, suggest that additional molecular intermediates may play a role in promoting this "non-canonical" autophagy.

Since, miR-34a overexpression increased Beclin-1 protein expression, I expected Beclin-1 knockdown to inhibit miR-34a-induced autophagy. Surprisingly, miR-34a still increased LC3II expression in shBeclin-1 cells similar to what was observed in control PC3 cells overexpressing miR-34a. ATG4 is involved in LC3 processing and recycling. A recent study in CML demonstrated that ATG4B is a direct target of miR-34a and is overexpressed in CML [144]. Knockdown of ATG4B led to increase in LC3II and p62 indicative of impaired autophagy [144]. I did not observe decrease of ATG4B protein levels with miR-34a overexpression suggesting that it might not be a target of miR-34a in this system. My results with the knockdown of all four isoforms of ATG4 increased LC3II with increased accumulation of acidic vesicular organelles as determined by acridine orange staining suggesting that ATG4 knockdown could have separate effects on autophagy that are different

from miR-34a-mediated-autophagy. These results suggest that the form of autophagy induced with miR-34a requires different intermediates than those involved during the canonical autophagy.

Either Axl or MET inhibition is known to induce autophagy in diverse tumor cell lines [105, 106]. These studies however, did not demonstrate whether canonical or non-canonical form of autophagy was induced upon Axl or MET inhibition. My results demonstrate that overexpression of miR-34a still inhibited MET and Axl expression even in Beclin-1 or ATG5/ATG7 knockdown cells suggesting that downregulation of these targets could be involved in miR-34a-mediated autophagy. Inhibition of autophagy genes studied in this chapter decreased cell proliferation; however overexpression of miR-34a causes further decrease in proliferation in Beclin-1 or ATG5/ATG7 knockdown cells. These results implicate a role of miR-34a-mediated autophagy in decreasing cell proliferation either alone or in combination with apoptosis that needs to be further examined.

Chapter 8

Expression of miR-34a in Human Prostate Cancer Samples

In this dissertation, I have determined that miR-34a is downregulated in metastatic prostate cancer cell lines and its delivery in *in vivo* models is effective in decreasing tumor growth. Overexpression of miR-34a can induce non-canonical form of autophagy in cell line models. The relationship between miR-34a expression and autophagy in prostate cancer clinical samples is not known. Also, data supporting inverse correlation of miR-34a expression with disease aggressiveness suggests a trend toward decreased miR-34a expression with increasing Gleason score [89]. Previous studies using publically available datasets or qPCR for miR-34a expression have reported decreased miR-34a in prostate cancer with further decreases in expression with PCa progression [89, 127]. However, methods used in these studies show large variations in miR-34a expression providing no visualization of expression in different cell types. In this chapter, I determined miR-34a expression in human prostate cancer samples by *in situ* hybridization that allowed for direct visualization of miR-34a expression in normal prostate cells vs. prostate cancer tissue. Tissue microarrays (TMAs) from different stages and grades of PCa provide a large cohort of clinical specimens that can be stained with miR-34a and quantified to determine whether there is inverse correlation in miR-34a expression with progressive PCa.

Expression of miR-34a is decreased in human prostate cancer specimens

To examine miR-34a expression in human prostate gland and cancer tissue, I received human PCa samples from the Department of GU Medical oncology. H&E and *in situ* hybridization (ISH) was performed on these samples that allowed visualization of heterogeneity and tissue-specific identification of miR-34a expression. Similar areas from H&E and ISH slides were imaged. High expression of miR-34a is observed in the normal

prostate gland, with expression almost exclusively in the basal cell layer **(Fig. 56A and 56E**, inset, **56B and 56F**, inset**)** while the luminal cells do not stain for miR-34a in the normal gland **(Fig. 56A and 56E**, inset, **56B and 56F**, inset**)**. In the tissue in which normal prostate gland and adjoining prostate cancer are present **(Fig. 56C and 56D)**, miR-34a expression is lost in the cancerous tissue **(Fig. 56G and 56H)**. This result suggests that there is a decreased miR-34a expression in human PCa samples.

Results from a small sample set suggest that miR-34a expression is decreased in prostate cancer compared to normal gland. More samples would be required to do miR-34a staining and quantification of expression to determine whether miR-34a expression decreases with disease progression. *In situ* hybridization demonstrates that miR-34a has differential expression in basal vs. luminal cells of the prostate gland. As discussed in Introduction (Chapter 1), it has been demonstrated that PCa can arise from both luminal and basal cells in *Pten*-null mouse model and there is evidence of basal to luminal cell differentiation [12]. It remains to be determined whether loss of miR-34a occurs in prostate cancer arising from basal cells and whether re-expression of miR-34a in luminal cells will inhibit cancer development. Loss of miR-34a could be one of the mechanisms of aberrant activation c-Myc that can promote cancer initiation. It will be the focus of future studies to determine the expression of miR-34a targets in different prostate cell types and in cancer tissue. This study highlights the further need to understand the regulation of miR-34a expression in prostate gland for better understanding of its role in cancer initiation and development.

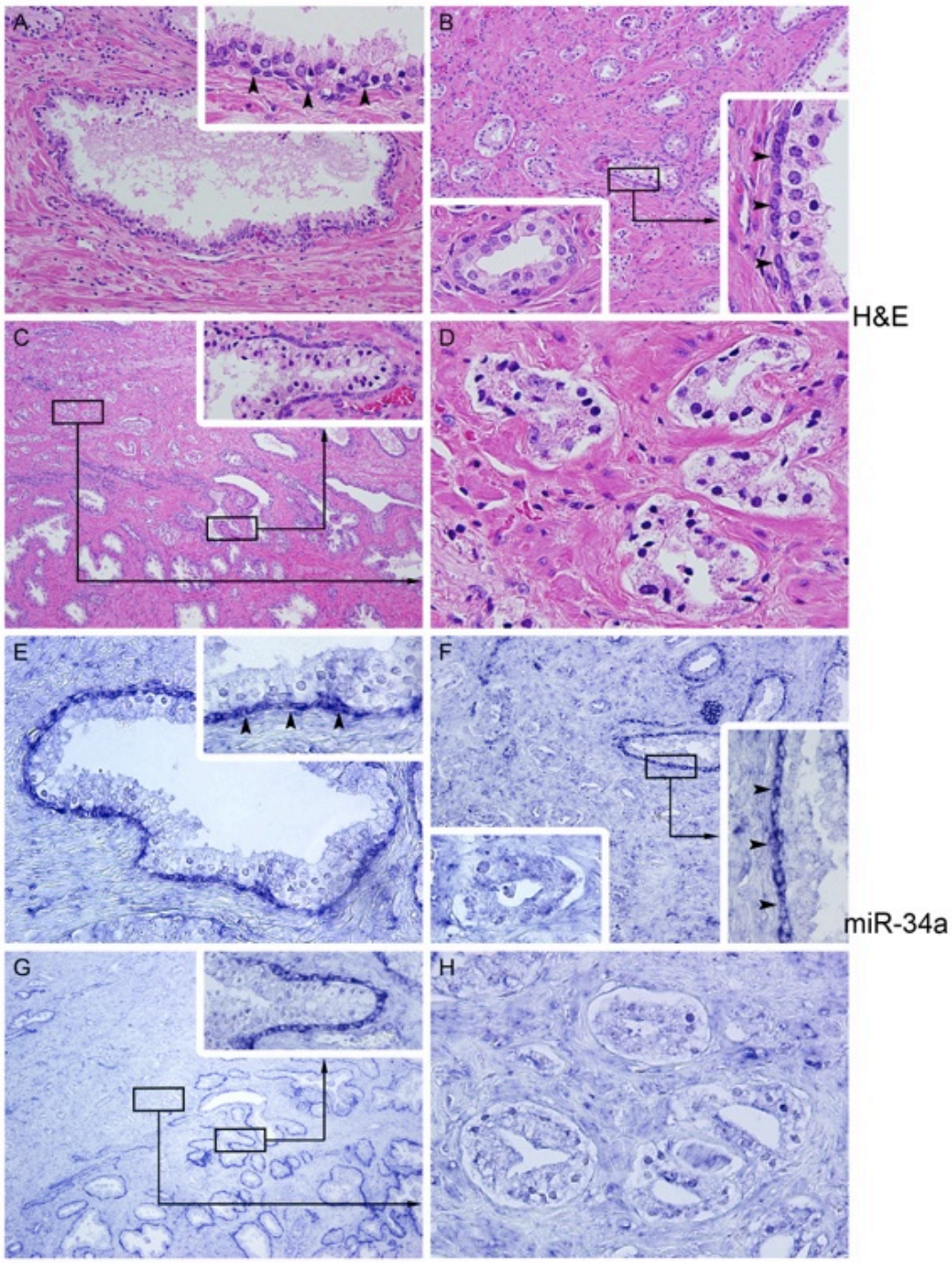

Figure 56 - miR-34a is downregulated in PCa

The expression of miR-34a was measured by *in situ* hybridization. Similar areas for H&E (A-D) and miR-34a ISH (E-H) were captured and are shown above.

Chapter 9

Discussion

When organ-confined, prostate cancer is curable. However, when prostate cancer metastasizes, most frequently to the bone, it is almost always lethal. Despite newly approved FDA therapies that prolong survival, increased lifespan for men with metastatic PCa is relatively minimal. The failure of therapies could be attributed to development of *de novo* resistance mediated by interactions with the microenvironment or acquired resistance mediated by alterations in the tumor cell that promote tumor growth. It is thus essential to develop novel strategies for treatment of advanced disease, which will require a better understanding of PCa progression and tumor growth in the bone.

In this dissertation, I have focused on understanding several aspects of prostate cancer biology related to regulation of specific tyrosine kinases that play a role in PCa progression and targeting multiple gene products associated with metastatic disease. The thesis raised issues with respect to targeting individual molecules, demonstrated the promise of using miRNA-mediated strategies to target multiple molecules and revealed the complicated inter-related biologic consequences of this targeting, apoptosis and autophagy.

Activation of IGF-1/1R pathway induces ligand-independent delayed MET activation

In cancer, several growth factor receptors and receptor tyrosine kinases are aberrantly expressed contributing to tumor development and progression [128, 129]. One mechanism of receptor activation is mediated through binding of its ligand and activation of downstream signaling pathway [130]. However, recent studies have identified ligand-independent receptor cross talk mechanisms in cancer. There are numerous mechanisms by which this occurs, including amplification of non-targeted receptor with overlapping functions, activation of a non-targeted receptor, or reactivation of a targeted receptor [41, 43, 131]. A

well-studied example is crosstalk between EGFR and MET. EGFR activation has been demonstrated to lead to delayed MET activation in non-small cell lung cancer cell lines [43], MET is amplified after erlotinib or gefinitib treatment in lung tumors [42, 132]. Thus, to understand which therapies might be effective in combination and/or how to best use targeted therapies, cross talk mechanisms need to be better understood. A theoretical publication [133] suggested specific classes of receptors that perform overlapping functions and are likely to be activated upon inhibition of a targeted kinase. Biologically, my goal was to determine if kinases known to be activated and have targeted inhibitors in clinical trial would lead to cross talk that might explain the lack of success of some of these trials. In prostate cancer and in PCa bone metastasis, IGF-1R and MET receptors are overexpressed and predict poor prognosis [36, 40, 112, 113, 134, 135]. Multiple inhibitors to both of these signaling axes are in clinical trials [113, 136]. These trails have generally led to failure, both through development of resistance and re-activation of targets. Thus, to determine whether re-activation of targeted kinase occurs through cross talk with other receptors, I studied IGF-1R mediated MET activation in Chapter 3 of this dissertation. I demonstrated that in cell lines that express both IGF-1R and MET receptor tyrosine kinases, activation of IGF-1R by IGF-1 induces delayed phosphorylation of MET which is independent of its ligand, HGF. This implies that in cancers where both receptors are present on cancer cells, presence of IGF-1 in the tumor microenvironment can lead to MET phosphorylation.

It was next important to determine if the phosphorylation led to activated MET functions and further, to examine if IGF-1R biologic functions were mediated through MET. Activation of IGF-1/1R and MET pathway was biologically functional as determined by phosphorylation of catalytic tyrosine sites on MET indicative of full MET activation and also

demonstrated by activation of downstream Akt, Src and MAPK signaling pathways. Activation and expression of IGF-1R was essential for IGF-1 to phosphorylate MET as in the absence of IGF-1R this delayed MET activation was abolished. This result is similar to findings of Dulak et al. on cross talk between EGFR and MET, where they demonstrate that activation of EGFR by EGF leads to MET activation [43]. However, unlike their result, MET expression did not increase upon IGF-1 stimulation.

Dasatinib (a multi-targeted pan Src family kinase inhibitor)-mediated inhibition of Src phosphorylation diminished both IGF-mediated (Chapter 3) and EGF-mediated-MET [43] activation, demonstrating that activated Src serves as the central regulator of atleast several receptor cross talk mechanisms. In line with this observation, constitutive activation of Src was sufficient to induce MET phosphorylation even in the absence of IGF-1. However, in this study it was not determined whether Src directly mediates MET activation. I speculate that activation of Src enhances the activity of a transcription factor that then induces transcription of unknown protein/s that interact with MET and trigger its phosphorylation either directly or indirectly through other adaptor or MET-binding partner/s. The results from treatment of cells with pan-transcription inhibitor actinomycin D that abolished IGF-1 induced MET phosphorylation further corroborates the role of transcriptional component/s in mediating IGF-1/1R induced MET activation. Dulak, et al. also implicate transcriptional involvement of unknown factor/s in mediating growth factor cross talk with EGF and MET [43]. It will be the focus of future studies to determine if common transcription factors are involved in cross talk among receptors, and then identify MET binding proteins in the complex that could be involved in mediating IGF-1/1R to MET activation, as IGF-1R does not directly lead to MET phosphorylation. These results are

summarized in the model of IGF-1/1R induced MET phosphorylation that requires Src activation and unknown transcriptional mediators and further leads to activation of downstream signaling pathways including migration **(Fig. 57)**.

Though several mechanisms for ligand independent MET activation including upregulation of plexins, G-coupled receptors, integrin binding, have been reported, I investigated whether integrins are involved in inducing delayed MET phosphorylation, as β1integrins interact with MET, and are themselves known to be important in PCa bone metastasis [137] and have been implicated in MET activation [41]. For these experiments, I determined whether cross talk between IGF-1R and MET still occurred in integrin β1 knockdown cells (PC3 cells). However, knockdown of integrin β1did not inhibit IGF-1-induced MET phosphorylation suggesting integrin β1 was not involved. It remains to be investigated whether other integrins for example, integrin β3 implicated in prostate cancer progression [138] could be a mediator in IGF-1/1R-induced MET activation. I did not study bi-directional IGF-1/1R activation upon HGF stimulation and this will be another area for exploration to further understand receptor cross talk mechanism.

In summary, this study adds to previous works suggesting combinatorial targeting of multiple tyrosine kinases as a better therapeutic approach in cancers where more than one kinase is activated. MET activation through ligand-independent mechanisms in different cancers indicates that MET activation might serve as a converging node required by other kinases to mediate their biological effects. This is highlighted in my study where MET knockdown abolishes IGF-1-induced migration.

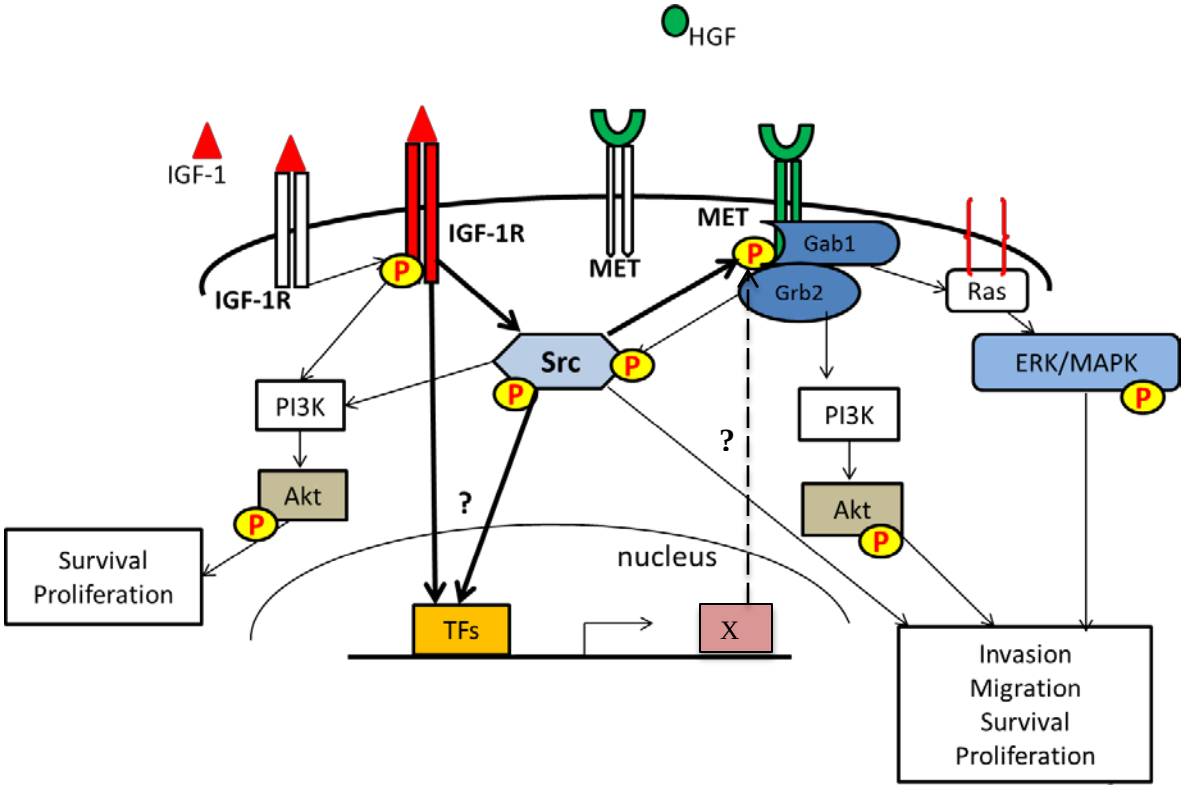

Figure 57 - Model of Ligand Independent MET activation by IGF-1/1R pathway

This figure illustrates that activation of IGF-1R by IGF-1 increases MET phosphorylation but not its expression and does not require MET ligand, HGF but requires Src activation and transcription (bold arrows) through an unidentified factor X.

Taken together, these findings implicate that cross talk mechanism between receptor tyrosine kinases might be responsible for failure of small molecule ATP inhibitors against targeted-kinases. There could be common transcription-mediated pathways involving unidentified transcription factors and proteins/kinases that activate more than one RTK and understanding these pathways as well as identifying the common transcription factor might be one approach to targeting multiple kinases. These findings further implicate that targeting multiple aberrantly expressed kinases through strategies that not only inhibit their activation but also their expression might be more important in cancer therapeutics.

miR-34a is decreased in metastatic PCa cell lines and its delivery decreases prostate tumor growth

The above study had several implications, as described, but led to questions such as, elimination of cross talk through downregulation of an activated receptor; and are in line with the seeming necessity for inhibiting multiple targets for better therapeutic efficacy. Thus, delivery of tumor suppressive miRNAs, which downregulate the expression of multiple targets is now an emerging approach with therapeutic promise. In Chapters 4 and 5 of this dissertation, I focused on miR-34a, a miRNA downregulated in many cancers and considered a tumor suppressive miRNA since it targets many oncogenic proteins. Specifically, this miRNA was chosen in prostate cancers as it downregulates MET, thus extending my previous work, miR-34a also downregulates Axl, an emerging target for advanced-stage PCa and c-Myc, an important oncogene de-repressed at earlier stages of PCa, and has additional targets not assessed in this thesis, such as, Bcl-2, Notch1, cyclin D1, CDK4, CDK6, etc. which may augment apoptosis and cell cycle arrest [75, 139]. Increased expression of MET,

Axl and Myc has been reported in primary and advanced PCa [25, 38, 40, 46-48, 51, 117] as discussed in Introduction (Chapter 1) section. In the last few years, targeting MET activation is an attractive area of research in pre-clinical and clinical studies. However, MET inhibitors have limited success and are associated with severe toxic effects in clinical trials [4]. Recently, the dual VEGFR2 and MET small molecule inhibitor, Cabozatinib failed to demonstrate statistical significance in prolonging overall survival (OS) in Phase III clinical trial of men with mCRPC. Axl inhibitors have just entered phase 1 clinical trial [140] and have not been tested for use with advanced PCa. c-Myc being a transcription factor is not considered as a "druggable" target and targeting Myc-dependent synthetic lethal interactions is being further explored [54]. This presents a need for a therapeutic strategy that will inhibit multiple targets promoting growth and progression in prostate cancer. Importantly, miR-34a inhibited all three targets *in vitro* and *in vivo* in PCa as shown in Chapter 4 and 5 results, making it a useful candidate for potentially inhibiting tumor growth in bones. These data is in agreement with previous reports examining these targets in breast, non-small cell lung, colorectal, and prostate cancer [45, 53, 82-85, 87], although none of these targets have been examined simultaneously before my studies. Thus, miR-34a was a potential candidate for replacement therapy that would inhibit prostate tumor growth in the bone.

The first issue to be addressed was the relationship between miR-34a expression and aggressiveness and metastatic potential of well-characterized tumor cell lines. My *in vitro* data demonstrated that miR-34a expression decreases with aggressiveness and metastatic potential of PCa cell lines. I further demonstrated that miR-34a effects properties associated with metastasis including decrease in migration, invasion, proliferation; cell cycle changes and increase in apoptosis, demonstrating direct anti-tumor effects. Although other groups

have shown that miR-34a induces senescence [141], I did not observe senescence upon miR-34a overexpression by using SA-β-galactosidase assay (data not shown).

During the course of my studies, the attractiveness of this approach became obviously popular, as many studies in miR-34a in prostate and other cancers have appeared since my work was initiated. But several unanswered questions still remained, including whether delivery of miR-34a would affect growth of bone metastasis, which as noted many times in this thesis is the major killer from prostate cancer. To address the effects of miR-34a delivery on tumor growth in the bone I used an intra-femoral mouse model for my therapeutic experiment and demonstrated that miR-34a delivery through chitosan nanoparticles decreased tumor growth. Due to lack of current animal models for PCa that lead to spontaneous bone metastasis, I used direct injection of tumor cells in the femur to best represent PCa bone metastasis. This is the first study to demonstrate a therapeutic benefit of miR-34a in the treatment of established prostate tumors in the bone. Although Liu et al. used miR-34a delivery for orthotopic PC3 tumors in mice [84], my study provides evidence to support miR-34a delivery in advanced PCa as well. Krzeszinski et al. recently showed that delivery of miR-34a decreases bone metastases of breast cancer and melanoma cell line in intra-cardiac mouse model by inhibiting osteoclast activity [74]. They used genetic and pharmacologic model to demonstrate that decreased bone metastasis was due to altered expression of miR-34a in the bone microenvironment, providing convincing evidence that, for these models, that primary effectiveness was due to a single protein in osteoclasts, Tgif2, and emphasizes the importance of targeting the tumor microenvironment [74]. However, therapies in osteoblastic PCa bone metastasis that target primarily microenvironment, as determined in part, by their failure to reduce PSA and tumor remaining in bone scans, such as

cabozatinib and Rad 223 [4, 60] suggest that targeting microenvironment in PCa bone metastases is insufficient to have prolonged efficacy and overall survival. Thus, the goal from the beginning of my studies was to attempt to target tumor cells. My findings along with those of Krzeszinski, et al suggest that miR-34a can be useful in targeting both the tumor as well as the microenvironment, and may account for growth inhibition in bone that exceeded the tumor reduction in sub-cutaneous studies. A potential role of Tgif2 inhibition in prostate cancer bone metastasis models would be an interesting subject of future work.

In previous studies, delivery of downregulated miRNAs has been shown to inhibit tumor growth in different *in vivo* models without any severe toxic effects [68, 75, 85, 86, 88]. Likewise, in my study, I observed that delivery of miR-34a led to inhibition of tumor growth without any toxic effects in the mice. Since, no current therapies are effective in treating PCa metastatic to bone without severe toxicities; this study presents an alternative treatment strategy to circumvent this problem. A more detailed understanding of the biology resulting from this strategy will be required if miR-34a delivery is to become therapeutically relevant.

This dissertation did not address the mechanism of miR-34a downregulation in PCa, which can be explored in future research. Previous studies have reported that miR-34a is regulated by p53-dependent and p53-independent mechanisms [79, 80, 139]. p53 is mutated in PC3 and PC3MM2 cells, indicating that loss of p53 might be involved in miR-34a downregulation in these cell lines [84]. However, since p53 mutations are not as common in PCa (>20%) and generally occur at later stages [6, 142], other mechanisms including hypermethylation of miR-34a promoter are very likely be responsible for downregulation of its expression, given the frequency of miR-34a decreases I observed in human specimens.

My results from *in vivo* studies demonstrate stronger induction of apoptosis by miR-34a delivery compared to miR-34a overexpression *in vitro*, which increased apoptosis by 20-30%. Downregulation of miR-34a targets, MET and Axl, studied in this dissertation have led to increase in apoptosis and autophagy leading to decrease in cell viability [105, 106]. This led me to speculate whether autophagy along with apoptosis could be involved in miR-34a overexpression mediated decrease in cancer cell growth.

Overexpression of miR-34a induces non-canonical form of autophagy

A major part of my thesis focused on autophagy, for several reasons. As discussed above, knockdown of either MET or Axl in different systems has been shown to induce autophagy. Further, overexpression of miR-34a induced morphological characteristics, including increases in cell size and with transmission electron microscopy, autophagosomes and autolysosomes were detected upon miR-34a overexpression. As autophagy has received considerable attention both for its role in cellular survival and potentially promoting tumorigenesis, as well as its role in cellular death and tumor suppression, understanding whether autophagy occurred and by what mechanism became important to my work. Prolonged treatment with targeted molecular therapy induces autophagy leading to cell death [97] and treatment with chemotherapeutic agent, Rottlerin induces autophagy associated with cell death in different cancer cell lines [99, 120], further emphasizing the complex biological effects of autophagy in cancer models. Since, my studies involved prolonged miR-34a treatment, with miR-34a delivered every three days in *in vivo* studies and the overexpression *in vitro* was over a time course of four days, it was important to assess whether autophagy was induced in my system.

The goal of my work with miR-34a-induced autophagy was to determine whether autophagy inhibited or augmented miR-34a therapeutic effects. To do this it was important to first inhibit autophagy and then use miR-34a overexpression to determine its effects on cell proliferation and autophagy marker, LC3II expression. I used bafilomycin A1 that inhibits late stage autophagy by preventing fusion between autophagosomes and lysosomes. However, bafilomycin is a toxic chemical with other cellular targets that led to more than 90% cell death in PC3 cells (data not shown). To overcome the toxicities of chemical inhibitors, I used knockdown of genes involved in the autophagy pathway to inhibit autophagy and then overexpress miR-34a. Knockdown of Beclin-1, ATG5, ATG7 and ATG4 was not very toxic to the cells and effective in inhibiting basal autophagy. However miR-34a overexpression still induced autophagy even with the knockdown of these genes with increase in LC3II and decrease in cell proliferation. Thus, implicating that miR-34a did not require these genes for mediating its molecular and biological effects.

Nishida et al. reported an ATG5/ATG7-independent macroautophagy that did not increase LC3II expression [95]. Contrary to this finding, my results with miR-34a overexpression demonstrate increase in LC3II even in ATG5 and ATG7 knockdown cells. Scarlatti, et al. reported that resveratrol (Res) induces Beclin-1-independent non-canonical autophagy in breast cancer cells with increase in LC3II upon Res treatment in Beclin-1 knockdown cells [125]. Similar to this finding, my results in Chapter 7 demonstrate increase in LC3II in shBeclin-1 cells with miR-34a overexpression. These data suggest existence of compensatory mechanism through other E1 and E3-like enzymes that are involved in mediating LC3 conversion upon autophagy induction by miR-34a. Different intermediates could be recruited to induce autophagy as Liu et al. demonstrated that miR-34a inhibits

autophagy under starvation or chemotherapy that enhances cell death by inhibiting HGMB1 expression in retinoblastoma cells [91]. This led me to speculate that under conditions of serum starvation, miR-34a could inhibit protective autophagy that promotes cell survival whereas in complete growth medium conditions, miR-34a overexpression induces a form of autophagy that promotes cell death.

Taken together, these findings further implicate that diverse forms of autophagy are induced with different cellular stresses through several intermediates that might lead to different biological effects. Identification of key molecular intermediates involved in the form of autophagy induced by miR-34a overexpression will be important in delineating the mechanism and biological effects of miR-34a-mediated autophagy. ATG4 is a cysteine protease that mediates conversion of LC3 to LC3I that is further processed to LC3II, a lipidated of LC3, and is also required in deplidation to LC3I [143]. Knockdown of ATG4 homologue, ATG4B in chronic myeloid leukemia (CML) leads to impaired autophagy with increase in LC3II and decrease in cell viability and cell proliferation [144]. It was further demonstrated that miR-34a directly targets and inhibits ATG4B though the effects of miR-34a on autophagy were not examined [144]. These results suggest that downregulation of ATG4B could lead to impaired autophagy. To determine whether ATG4B was targeted by miR-34a in my system and could be involved in miR-34a mediated autophagy, I performed knockdown of ATG4B and then overexpressed miR-34a to assess the effects on autophagy. The other homologues of ATG4 including ATG4A, ATG4C and ATG4D with overlapping functions [143] could negate the effects of miR-34a inhibition of ATG4B and thus, I used siRNAs to knockdown all four isoforms of ATG4 which led to increased LC3II and acridine orange positive cells indicative of autophagy. In my studies, ATG4B or the other isoforms do

not appear to be a direct target of miR-34a. Future studies could focus on knockdown of individual homologues to examine the involvement of ATG4 isoforms in miR-34a-mediated autophagy or their effects on autophagy independent of miR-34a.

Downregulation of miR-34a targets, Axl and MET can induce autophagy through unidentified mechanisms [105, 106]. In this study, I tried to determine at least in part, the mechanism of autophagy induced through downregulation of these receptor tyrosine kinases by miR-34a. Future work will focus on determining whether downregulation of MET and Axl alone or in combination is sufficient to induce the form of autophagy as observed with miR-34a overexpression. As summarized in **Figure 58**, miR-34a could be mediating its effects indirectly through inhibition of RTKs, Axl and MET. Other autophagy intermediates including Beclin-1, ATG5 and ATG7 are not involved in miR-34a-mediated autophagy while ATG4 knockdown itself affects autophagy independent of miR-34a overexpression **(Fig. 58)**. There could be other direct targets of miR-34a involved in autophagy induction and it will be the focus of future studies to identify direct or indirect modulators of miR-34a-induced autophagy.

This study highlights that miR-34a could have different effects on autophagy in different cellular and tumor contexts under different conditions and it will be important to determine whether autophagy is induced or inhibited in patients on MRX34 clinical trial, to understand the therapeutic effects of miR-34a delivery.

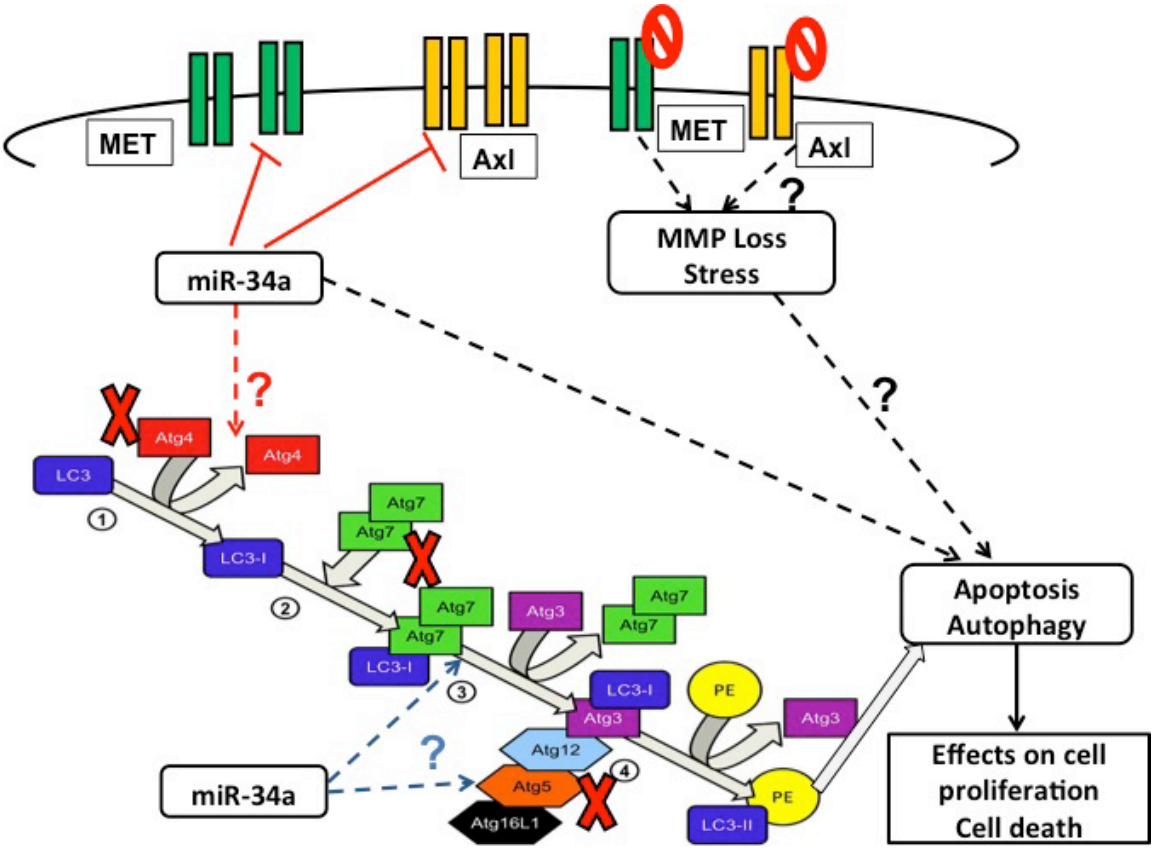

Figure 56 - Model of miR-34a-induced autophagy

This figure illustrates that miR-34a overexpression induces apoptosis and a form of autophagy that is independent of Beclin-1, ATG5 and ATG7, which are involved in conversion of LC3I to LC3II (Blue dotted arrow). Autophagy induced with miR-34a overexpression could be through inhibition of RTKs, Axl and MET that can then lead to apoptosis, autophagy (Black dotted arrows) and decreased cell proliferation. Alternatively, other direct targets of miR-34a could lead to autophagy induction. Downregulation of ATG4 (red dotted arrow) led to increase in LC3II independent of miR-34a.

Modified with permission from "Randall-Demello S, Chieppa M and Eri R (2013). Intestinal epithelium and autophagy: partners in gut homeostasis. Frontiers in Immunology. Doi 10.3389/fimmu.2013.00301."

Summary and Future Directions

In conclusion, in this dissertation I have demonstrated ligand-independent delayed MET activation through IGF-1/1R pathway that requires IGF-1R, activated Src and transcription. Future studies will focus on identifying the transcriptional intermediate that mediates MET phosphorylation by identifying binding proteins in MET complex.

Clinical and *in vitro* data implicates an inverse relationship between miR-34a expression and prostate cancer progression with decreased in miR-34a expression in metastatic prostate cancer cell lines. I further demonstrated that decreased miR-34a expression leads to upregulation of targets that promote PCa progression, and *in vivo* miR-34a replacement therapy could be a useful treatment for advanced PCa. Overexpression of miR-34a induced a form of non-canonical autophagy independent of ATG5, ATG7 and Beclin-1 expression. Further studies will focus on examining involvement of other direct targets of miR-34a including growth factor receptors in mediating the form of autophagy induced by miR-34a.

I demonstrated that miR-34a delivery could be a therapeutic strategy for PCa bone metastasis. It would require more studies with other xenograft models to determine the efficacy of miR-34a treatment for clinical applications. Also, it will be important to study whether prolonged treatment with miR-34a results in residual tumor resistant to miR-34a therapy. It is possible that resistance to miR-34a therapy can arise upon longer treatment duration and that will be an area of further exploration. Combination miRNA therapies focusing on delivering two or more miRNAs downregulated in cancers can be developed to test whether it will be more effective than single miRNA delivery. I studied expression of IGF-1 and IGF-1R targeting miR-145 in prostate cancer cell lines (data not shown) as an

extension to my current research. The expression of miR-45 is downregulated in prostate cancer cell lines and its overexpression decreased IGF-1 secretion as well as phosphorylation of IGF-1R (data not shown). Future studies can determine whether miR-145 modulates IGF-1/1R signaling and whether dual miRNA delivery of miR-145 and miR-34a to target IGF-1/1R pathway along with MET, Axl and c-Myc signaling axes in prostate xenograft models will be more effective than single miRNA-delivery.

Inhibition of growth factor receptors could lead to different forms of autophagy as demonstrated by downregulation of Axl and MET and antagonism of prolactin receptor [97, 105, 106] than autophagy mediated by targeting direct intermediates with different biological consequences. This work attempted to understand the form of autophagy induced by miR-34a and whether it was mediated indirectly through downregulation of some of these receptors or directly through modulating essential autophagy genes. It can be further examined whether single or combined knockdown of Axl and MET is sufficient to induce the form of autophagy mediated by miR-34a overexpression. Further, inhibition of apoptosis and cell proliferation in the presence and absence of miR-34a will help in defining the biological effects of this non-canonical autophagy. Finally, determining the expression of autophagy markers and whether miR-34a influences autophagy in patients would be useful in understanding the therapeutic applicability of miR-34a delivery strategy for cancer treatment.

Bibliography

1. Siegel, R., J. Ma, Z. Zou, and A. Jemal, *Cancer statistics, 2014.* CA Cancer J Clin, 2014. **64**(1): p. 9-29.
2. Society, A.C., *Cancer Facts & Figures 2014.* American Cancer Society, Atlanta, Georgia, USA, 2014.
3. Bubendorf, L., A. Schopfer, U. Wagner, G. Sauter, H. Moch, N. Willi, T.C. Gasser, and M.J. Mihatsch, *Metastatic patterns of prostate cancer: an autopsy study of 1,589 patients.* Hum Pathol, 2000. **31**(5): p. 578-83.
4. Lee, R.J. and M.R. Smith, *Targeting MET and vascular endothelial growth factor receptor signaling in castration-resistant prostate cancer.* Cancer J, 2013. **19**(1): p. 90-8.
5. Logothetis, C.J., G.E. Gallick, S.N. Maity, J. Kim, A. Aparicio, E. Efstathiou, and S.H. Lin, *Molecular classification of prostate cancer progression: foundation for marker-driven treatment of prostate cancer.* Cancer Discov, 2013. **3**(8): p. 849-61.
6. Abate-Shen, C. and M.M. Shen, *Molecular genetics of prostate cancer.* Genes Dev, 2000. **14**(19): p. 2410-34.
7. Xin, L., *Cells of origin for cancer: an updated view from prostate cancer.* Oncogene, 2013. **32**(32): p. 3655-63.
8. Grossmann, M.E., H. Huang, and D.J. Tindall, *Androgen receptor signaling in androgen-refractory prostate cancer.* J Natl Cancer Inst, 2001. **93**(22): p. 1687-97.
9. Sun, Y., J. Niu, and J. Huang, *Neuroendocrine differentiation in prostate cancer.* Am J Transl Res, 2009. **1**(2): p. 148-62.

10. Okada, H., A. Tsubura, A. Okamura, H. Senzaki, Y. Naka, Y. Komatz, and S. Morii, *Keratin profiles in normal/hyperplastic prostates and prostate carcinoma.* Virchows Arch A Pathol Anat Histopathol, 1992. **421**(2): p. 157-61.

11. Verhagen, A.P., F.C. Ramaekers, T.W. Aalders, H.E. Schaafsma, F.M. Debruyne, and J.A. Schalken, *Colocalization of basal and luminal cell-type cytokeratins in human prostate cancer.* Cancer Res, 1992. **52**(22): p. 6182-7.

12. Choi, N., B. Zhang, L. Zhang, M. Ittmann, and L. Xin, *Adult murine prostate basal and luminal cells are self-sustained lineages that can both serve as targets for prostate cancer initiation.* Cancer Cell, 2012. **21**(2): p. 253-65.

13. McNeal, J.E., *Origin and development of carcinoma in the prostate.* Cancer, 1969. **23**(1): p. 24-34.

14. McNeal, J.E., E.A. Redwine, F.S. Freiha, and T.A. Stamey, *Zonal distribution of prostatic adenocarcinoma. Correlation with histologic pattern and direction of spread.* Am J Surg Pathol, 1988. **12**(12): p. 897-906.

15. Gleason, D.F., *Histologic grading of prostate cancer: a perspective.* Hum Pathol, 1992. **23**(3): p. 273-9.

16. Rosenthal, S.A. and H.M. Sandler, *Treatment strategies for high-risk locally advanced prostate cancer.* Nature Reviews Urology, 2010. **7**(1): p. 31-38.

17. Dong, J.T., *Chromosomal deletions and tumor suppressor genes in prostate cancer.* Cancer Metastasis Rev, 2001. **20**(3-4): p. 173-93.

18. Alcaraz, A., S. Takahashi, J.A. Brown, J.F. Herath, E.J. Bergstralh, J.J. Larson-Keller, M.M. Lieber, and R.B. Jenkins, *Aneuploidy and aneusomy of chromosome 7*

detected by fluorescence in situ hybridization are markers of poor prognosis in prostate cancer. Cancer Res, 1994. **54**(15): p. 3998-4002.

19. Quinn, D.I., S.M. Henshall, and R.L. Sutherland, *Molecular markers of prostate cancer outcome.* Eur J Cancer, 2005. **41**(6): p. 858-87.

20. Van Den Berg, C., X.Y. Guan, D. Von Hoff, R. Jenkins, Bittner, C. Griffin, O. Kallioniemi, Visakorpi, McGill, J. Herath, and et al., *DNA sequence amplification in human prostate cancer identified by chromosome microdissection: potential prognostic implications.* Clin Cancer Res, 1995. **1**(1): p. 11-8.

21. Taylor, B.S., N. Schultz, H. Hieronymus, A. Gopalan, Y. Xiao, B.S. Carver, V.K. Arora, P. Kaushik, E. Cerami, B. Reva, Y. Antipin, N. Mitsiades, T. Landers, I. Dolgalev, J.E. Major, M. Wilson, N.D. Socci, A.E. Lash, A. Heguy, J.A. Eastham, H.I. Scher, V.E. Reuter, P.T. Scardino, C. Sander, C.L. Sawyers, and W.L. Gerald, *Integrative genomic profiling of human prostate cancer.* Cancer Cell, 2010. **18**(1): p. 11-22.

22. Gurel, B., T.Z. Ali, E.A. Montgomery, S. Begum, J. Hicks, M. Goggins, C.G. Eberhart, D.P. Clark, C.J. Bieberich, J.I. Epstein, and A.M. De Marzo, *NKX3.1 as a marker of prostatic origin in metastatic tumors.* Am J Surg Pathol, 2010. **34**(8): p. 1097-105.

23. Macleod, K.F., *The RB tumor suppressor: a gatekeeper to hormone independence in prostate cancer?* J Clin Invest, 2010. **120**(12): p. 4179-82.

24. Wang, Y., Y.X. Zhang, C.Z. Kong, Z. Zhang, and Y.Y. Zhu, *Loss of P53 facilitates invasion and metastasis of prostate cancer cells.* Mol Cell Biochem, 2013. **384**(1-2): p. 121-7.

25. Koh, C.M., C.J. Bieberich, C.V. Dang, W.G. Nelson, S. Yegnasubramanian, and A.M. De Marzo, *MYC and Prostate Cancer.* Genes Cancer, 2010. **1**(6): p. 617-28.

26. Ellwood-Yen, K., T.G. Graeber, J. Wongvipat, M.L. Iruela-Arispe, J. Zhang, R. Matusik, G.V. Thomas, and C.L. Sawyers, *Myc-driven murine prostate cancer shares molecular features with human prostate tumors.* Cancer Cell, 2003. **4**(3): p. 223-38.

27. Mehra, R., S.A. Tomlins, R. Shen, O. Nadeem, L. Wang, J.T. Wei, K.J. Pienta, D. Ghosh, M.A. Rubin, A.M. Chinnaiyan, and R.B. Shah, *Comprehensive assessment of TMPRSS2 and ETS family gene aberrations in clinically localized prostate cancer.* Mod Pathol, 2007. **20**(5): p. 538-44.

28. Tomlins, S.A., B. Laxman, S.M. Dhanasekaran, B.E. Helgeson, X. Cao, D.S. Morris, A. Menon, X. Jing, Q. Cao, B. Han, J. Yu, L. Wang, J.E. Montie, M.A. Rubin, K.J. Pienta, D. Roulston, R.B. Shah, S. Varambally, R. Mehra, and A.M. Chinnaiyan, *Distinct classes of chromosomal rearrangements create oncogenic ETS gene fusions in prostate cancer.* Nature, 2007. **448**(7153): p. 595-9.

29. Demichelis, F. and M.A. Rubin, *TMPRSS2-ETS fusion prostate cancer: biological and clinical implications.* J Clin Pathol, 2007. **60**(11): p. 1185-6.

30. Cairns, P., M. Esteller, J.G. Herman, M. Schoenberg, C. Jeronimo, M. Sanchez-Cespedes, N.H. Chow, M. Grasso, L. Wu, W.B. Westra, and D. Sidransky, *Molecular detection of prostate cancer in urine by GSTP1 hypermethylation.* Clin Cancer Res, 2001. **7**(9): p. 2727-30.

31. Chiam, K., C. Ricciardelli, and T. Bianco-Miotto, *Epigenetic biomarkers in prostate cancer: Current and future uses.* Cancer Lett, 2014. **342**(2): p. 248-56.

32. Jeronimo, C. and R. Henrique, *Epigenetic biomarkers in urological tumors: A systematic review.* Cancer Lett, 2014. **342**(2): p. 264-74.

33. Bianco-Miotto, T., K. Chiam, G. Buchanan, S. Jindal, T.K. Day, M. Thomas, M.A. Pickering, M.A. O'Loughlin, N.K. Ryan, W.A. Raymond, L.G. Horvath, J.G. Kench, P.D. Stricker, V.R. Marshall, R.L. Sutherland, S.M. Henshall, W.L. Gerald, H.I. Scher, G.P. Risbridger, J.A. Clements, L.M. Butler, W.D. Tilley, D.J. Horsfall, C. Ricciardelli, and B. Australian Prostate Cancer, *Global levels of specific histone modifications and an epigenetic gene signature predict prostate cancer progression and development.* Cancer Epidemiol Biomarkers Prev, 2010. **19**(10): p. 2611-22.

34. Trusolino, L., A. Bertotti, and P.M. Comoglio, *MET signalling: principles and functions in development, organ regeneration and cancer.* Nat Rev Mol Cell Biol, 2010. **11**(12): p. 834-48.

35. Varkaris, A., P.G. Corn, S. Gaur, F. Dayyani, C.J. Logothetis, and G.E. Gallick, *The role of HGF/c-Met signaling in prostate cancer progression and c-Met inhibitors in clinical trials.* Expert Opin Investig Drugs, 2011. **20**(12): p. 1677-84.

36. Ryan, C.J., M. Rosenthal, S. Ng, J. Alumkal, J. Picus, G. Gravis, K. Fizazi, F. Forget, J.P. Machiels, S. Srinivas, M. Zhu, R. Tang, K.S. Oliner, Y. Jiang, E. Loh, S. Dubey, and W.R. Gerritsen, *Targeted MET inhibition in castration-resistant prostate cancer: a randomized phase II study and biomarker analysis with rilotumumab plus mitoxantrone and prednisone.* Clin Cancer Res, 2013. **19**(1): p. 215-24.

37. van Leenders, G., B. van Balken, T. Aalders, C. Hulsbergen-van de Kaa, D. Ruiter, and J. Schalken, *Intermediate cells in normal and malignant prostate epithelium*

express c-MET: implications for prostate cancer invasion. Prostate, 2002. **51**(2): p. 98-107.

38. Humphrey, P.A., X. Zhu, R. Zarnegar, P.E. Swanson, T.L. Ratliff, R.T. Vollmer, and M.L. Day, *Hepatocyte growth factor and its receptor (c-MET) in prostatic carcinoma.* Am J Pathol, 1995. **147**(2): p. 386-96.

39. Verras, M., J. Lee, H. Xue, T.H. Li, Y. Wang, and Z. Sun, *The androgen receptor negatively regulates the expression of c-Met: implications for a novel mechanism of prostate cancer progression.* Cancer Res, 2007. **67**(3): p. 967-75.

40. Knudsen, B.S., G.A. Gmyrek, J. Inra, D.S. Scherr, E.D. Vaughan, D.M. Nanus, M.W. Kattan, W.L. Gerald, and G.F. Vande Woude, *High expression of the Met receptor in prostate cancer metastasis to bone.* Urology, 2002. **60**(6): p. 1113-7.

41. Lai, A.Z., J.V. Abella, and M. Park, *Crosstalk in Met receptor oncogenesis.* Trends Cell Biol, 2009. **19**(10): p. 542-51.

42. Engelman, J.A., K. Zejnullahu, T. Mitsudomi, Y. Song, C. Hyland, J.O. Park, N. Lindeman, C.M. Gale, X. Zhao, J. Christensen, T. Kosaka, A.J. Holmes, A.M. Rogers, F. Cappuzzo, T. Mok, C. Lee, B.E. Johnson, L.C. Cantley, and P.A. Janne, *MET amplification leads to gefitinib resistance in lung cancer by activating ERBB3 signaling.* Science, 2007. **316**(5827): p. 1039-43.

43. Dulak, A.M., C.T. Gubish, L.P. Stabile, C. Henry, and J.M. Siegfried, *HGF-independent potentiation of EGFR action by c-Met.* Oncogene, 2011. **30**(33): p. 3625-35.

44. Breindel, J.L., J.W. Haskins, E.P. Cowell, M. Zhao, D.X. Nguyen, and D.F. Stern, *EGF receptor activates MET through MAPK to enhance non-small cell lung carcinoma invasion and brain metastasis.* Cancer Res, 2013. **73**(16): p. 5053-65.

45. Mudduluru, G., P. Ceppi, R. Kumarswamy, G.V. Scagliotti, M. Papotti, and H. Allgayer, *Regulation of Axl receptor tyrosine kinase expression by miR-34a and miR-199a/b in solid cancer.* Oncogene, 2011. **30**(25): p. 2888-99.

46. Mishra, A., J. Wang, Y. Shiozawa, S. McGee, J. Kim, Y. Jung, J. Joseph, J.E. Berry, A. Havens, K.J. Pienta, and R.S. Taichman, *Hypoxia stabilizes GAS6/Axl signaling in metastatic prostate cancer.* Mol Cancer Res, 2012. **10**(6): p. 703-12.

47. Paccez, J.D., M. Vogelsang, M.I. Parker, and L.F. Zerbini, *The receptor tyrosine kinase Axl in cancer: biological functions and therapeutic implications.* Int J Cancer, 2014. **134**(5): p. 1024-33.

48. Shiozawa, Y., E.A. Pedersen, L.R. Patel, A.M. Ziegler, A.M. Havens, Y. Jung, J. Wang, S. Zalucha, R.D. Loberg, K.J. Pienta, and R.S. Taichman, *GAS6/AXL axis regulates prostate cancer invasion, proliferation, and survival in the bone marrow niche.* Neoplasia, 2010. **12**(2): p. 116-27.

49. Paccez, J.D., G.J. Vasques, R.G. Correa, J.F. Vasconcellos, K. Duncan, X. Gu, M. Bhasin, T.A. Libermann, and L.F. Zerbini, *The receptor tyrosine kinase Axl is an essential regulator of prostate cancer proliferation and tumor growth and represents a new therapeutic target.* Oncogene, 2013. **32**(6): p. 689-98.

50. Dang, C.V., *MYC on the path to cancer.* Cell, 2012. **149**(1): p. 22-35.

51. Hawksworth, D., L. Ravindranath, Y. Chen, B. Furusato, I.A. Sesterhenn, D.G. McLeod, S. Srivastava, and G. Petrovics, *Overexpression of C-MYC oncogene in*

prostate cancer predicts biochemical recurrence. Prostate Cancer Prostatic Dis, 2010. **13**(4): p. 311-5.

52. Gao, L., J. Schwartzman, A. Gibbs, R. Lisac, R. Kleinschmidt, B. Wilmot, D. Bottomly, I. Coleman, P. Nelson, S. McWeeney, and J. Alumkal, *Androgen receptor promotes ligand-independent prostate cancer progression through c-Myc upregulation.* PLoS One, 2013. **8**(5): p. e63563.

53. Yamamura, S., S. Saini, S. Majid, H. Hirata, K. Ueno, G. Deng, and R. Dahiya, *MicroRNA-34a modulates c-Myc transcriptional complexes to suppress malignancy in human prostate cancer cells.* PLoS One, 2012. **7**(1): p. e29722.

54. Horiuchi, D., B. Anderton, and A. Goga, *Taking on challenging targets: making MYC druggable.* Am Soc Clin Oncol Educ Book, 2014: p. e497-502.

55. Civenni, G., A. Malek, D. Albino, R. Garcia-Escudero, S. Napoli, S. Di Marco, S. Pinton, M. Sarti, G.M. Carbone, and C.V. Catapano, *RNAi-mediated silencing of Myc transcription inhibits stem-like cell maintenance and tumorigenicity in prostate cancer.* Cancer Res, 2013. **73**(22): p. 6816-27.

56. Jin, J.K., F. Dayyani, and G.E. Gallick, *Steps in prostate cancer progression that lead to bone metastasis.* Int J Cancer, 2011. **128**(11): p. 2545-61.

57. Casimiro, S., T.A. Guise, and J. Chirgwin, *The critical role of the bone microenvironment in cancer metastases.* Mol Cell Endocrinol, 2009. **310**(1-2): p. 71-81.

58. Fili, S., M. Karalaki, and B. Schaller, *Mechanism of bone metastasis: the role of osteoprotegerin and of the host-tissue microenvironment-related survival factors.* Cancer Lett, 2009. **283**(1): p. 10-9.

59. Cookson, M.S., B.J. Roth, P. Dahm, C. Engstrom, S.J. Freedland, M. Hussain, D.W. Lin, W.T. Lowrance, M.H. Murad, W.K. Oh, D.F. Penson, and A.S. Kibel, *Castration-resistant prostate cancer: AUA Guideline.* J Urol, 2013. **190**(2): p. 429-38.

60. Thoreson, G.R., B.A. Gayed, P.H. Chung, and G.V. Raj, *Emerging therapies in castration resistant prostate cancer.* Can J Urol, 2014. **21**(2 Supp 1): p. 98-105.

61. Jansson, M.D. and A.H. Lund, *MicroRNA and cancer.* Mol Oncol, 2012. **6**(6): p. 590-610.

62. Kim, V.N., *MicroRNA biogenesis: coordinated cropping and dicing.* Nat Rev Mol Cell Biol, 2005. **6**(5): p. 376-85.

63. Bader, A.G., D. Brown, and M. Winkler, *The promise of microRNA replacement therapy.* Cancer Res, 2010. **70**(18): p. 7027-30.

64. Iorio, M.V. and C.M. Croce, *MicroRNA dysregulation in cancer: diagnostics, monitoring and therapeutics. A comprehensive review.* EMBO Mol Med, 2012. **4**(3): p. 143-59.

65. Calin, G.A., C.D. Dumitru, M. Shimizu, R. Bichi, S. Zupo, E. Noch, H. Aldler, S. Rattan, M. Keating, K. Rai, L. Rassenti, T. Kipps, M. Negrini, F. Bullrich, and C.M. Croce, *Frequent deletions and down-regulation of micro- RNA genes miR15 and miR16 at 13q14 in chronic lymphocytic leukemia.* Proc Natl Acad Sci U S A, 2002. **99**(24): p. 15524-9.

66. Croce, C.M., *Causes and consequences of microRNA dysregulation in cancer.* Nat Rev Genet, 2009. **10**(10): p. 704-14.

67. Ibrahim, A.F., U. Weirauch, M. Thomas, A. Grunweller, R.K. Hartmann, and A. Aigner, *MicroRNA replacement therapy for miR-145 and miR-33a is efficacious in a model of colon carcinoma.* Cancer Res, 2011. **71**(15): p. 5214-24.

68. Takeshita, F., L. Patrawala, M. Osaki, R.U. Takahashi, Y. Yamamoto, N. Kosaka, M. Kawamata, K. Kelnar, A.G. Bader, D. Brown, and T. Ochiya, *Systemic delivery of synthetic microRNA-16 inhibits the growth of metastatic prostate tumors via downregulation of multiple cell-cycle genes.* Mol Ther, 2010. **18**(1): p. 181-7.

69. Bowman, K. and K.W. Leong, *Chitosan nanoparticles for oral drug and gene delivery.* Int J Nanomedicine, 2006. **1**(2): p. 117-28.

70. Han, H.D., L.S. Mangala, J.W. Lee, M.M. Shahzad, H.S. Kim, D. Shen, E.J. Nam, E.M. Mora, R.L. Stone, C. Lu, S.J. Lee, J.W. Roh, A.M. Nick, G. Lopez-Berestein, and A.K. Sood, *Targeted gene silencing using RGD-labeled chitosan nanoparticles.* Clin Cancer Res, 2010. **16**(15): p. 3910-22.

71. Rampino, A., M. Borgogna, P. Blasi, B. Bellich, and A. Cesaro, *Chitosan nanoparticles: preparation, size evolution and stability.* Int J Pharm, 2013. **455**(1-2): p. 219-28.

72. Sharma, K., S. Somavarapu, A. Colombani, N. Govind, and K.M. Taylor, *Crosslinked chitosan nanoparticle formulations for delivery from pressurized metered dose inhalers.* Eur J Pharm Biopharm, 2012. **81**(1): p. 74-81.

73. Pecot, C.V., R. Rupaimoole, D. Yang, R. Akbani, C. Ivan, C. Lu, S. Wu, H.D. Han, M.Y. Shah, C. Rodriguez-Aguayo, J. Bottsford-Miller, Y. Liu, S.B. Kim, A. Unruh, V. Gonzalez-Villasana, L. Huang, B. Zand, M. Moreno-Smith, L.S. Mangala, M.

Taylor, et al., *Tumour angiogenesis regulation by the miR-200 family.* Nat Commun, 2013. **4**: p. 2427.

74. Krzeszinski, J.Y., W. Wei, H. Huynh, Z. Jin, X. Wang, T.C. Chang, X.J. Xie, L. He, L.S. Mangala, G. Lopez-Berestein, A.K. Sood, J.T. Mendell, and Y. Wan, *miR-34a blocks osteoporosis and bone metastasis by inhibiting osteoclastogenesis and Tgif2.* Nature, 2014.

75. Bader, A.G., *miR-34 - a microRNA replacement therapy is headed to the clinic.* Front Genet, 2012. **3**: p. 120.

76. Calin, G.A., C. Sevignani, C.D. Dumitru, T. Hyslop, E. Noch, S. Yendamuri, M. Shimizu, S. Rattan, F. Bullrich, M. Negrini, and C.M. Croce, *Human microRNA genes are frequently located at fragile sites and genomic regions involved in cancers.* Proc Natl Acad Sci U S A, 2004. **101**(9): p. 2999-3004.

77. Chang, T.C., E.A. Wentzel, O.A. Kent, K. Ramachandran, M. Mullendore, K.H. Lee, G. Feldmann, M. Yamakuchi, M. Ferlito, C.J. Lowenstein, D.E. Arking, M.A. Beer, A. Maitra, and J.T. Mendell, *Transactivation of miR-34a by p53 broadly influences gene expression and promotes apoptosis.* Mol Cell, 2007. **26**(5): p. 745-52.

78. Corney, D.C., A. Flesken-Nikitin, A.K. Godwin, W. Wang, and A.Y. Nikitin, *MicroRNA-34b and MicroRNA-34c are targets of p53 and cooperate in control of cell proliferation and adhesion-independent growth.* Cancer Res, 2007. **67**(18): p. 8433-8.

79. Christoffersen, N.R., R. Shalgi, L.B. Frankel, E. Leucci, M. Lees, M. Klausen, Y. Pilpel, F.C. Nielsen, M. Oren, and A.H. Lund, *p53-independent upregulation of miR-*

34a during oncogene-induced senescence represses MYC. Cell Death Differ, 2010. **17**(2): p. 236-45.

80. Navarro, F., D. Gutman, E. Meire, M. Caceres, I. Rigoutsos, Z. Bentwich, and J. Lieberman, *miR-34a contributes to megakaryocytic differentiation of K562 cells independently of p53.* Blood, 2009. **114**(10): p. 2181-92.

81. Siemens, H., J. Neumann, R. Jackstadt, U. Mansmann, D. Horst, T. Kirchner, and H. Hermeking, *Detection of miR-34a promoter methylation in combination with elevated expression of c-Met and beta-catenin predicts distant metastasis of colon cancer.* Clin Cancer Res, 2013. **19**(3): p. 710-20.

82. Dang, Y., D. Luo, M. Rong, and G. Chen, *Underexpression of miR-34a in hepatocellular carcinoma and its contribution towards enhancement of proliferating inhibitory effects of agents targeting c-MET.* PLoS One, 2013. **8**(4): p. e61054.

83. Mackiewicz, M., K. Huppi, J.J. Pitt, T.H. Dorsey, S. Ambs, and N.J. Caplen, *Identification of the receptor tyrosine kinase AXL in breast cancer as a target for the human miR-34a microRNA.* Breast Cancer Res Treat, 2011. **130**(2): p. 663-79.

84. Liu, C., K. Kelnar, B. Liu, X. Chen, T. Calhoun-Davis, H. Li, L. Patrawala, H. Yan, C. Jeter, S. Honorio, J.F. Wiggins, A.G. Bader, R. Fagin, D. Brown, and D.G. Tang, *The microRNA miR-34a inhibits prostate cancer stem cells and metastasis by directly repressing CD44.* Nat Med, 2011. **17**(2): p. 211-5.

85. Wiggins, J.F., L. Ruffino, K. Kelnar, M. Omotola, L. Patrawala, D. Brown, and A.G. Bader, *Development of a lung cancer therapeutic based on the tumor suppressor microRNA-34.* Cancer Res, 2010. **70**(14): p. 5923-30.

86. Trang, P., J.F. Wiggins, C.L. Daige, C. Cho, M. Omotola, D. Brown, J.B. Weidhaas, A.G. Bader, and F.J. Slack, *Systemic delivery of tumor suppressor microRNA mimics using a neutral lipid emulsion inhibits lung tumors in mice.* Mol Ther, 2011. **19**(6): p. 1116-22.

87. Kasinski, A.L. and F.J. Slack, *miRNA-34 prevents cancer initiation and progression in a therapeutically resistant K-ras and p53-induced mouse model of lung adenocarcinoma.* Cancer Res, 2012. **72**(21): p. 5576-87.

88. Di Martino, M.T., E. Leone, N. Amodio, U. Foresta, M. Lionetti, M.R. Pitari, M.E. Cantafio, A. Gulla, F. Conforti, E. Morelli, V. Tomaino, M. Rossi, M. Negrini, M. Ferrarini, M. Caraglia, M.A. Shammas, N.C. Munshi, K.C. Anderson, A. Neri, P. Tagliaferri, and P. Tassone, *Synthetic miR-34a mimics as a novel therapeutic agent for multiple myeloma: in vitro and in vivo evidence.* Clin Cancer Res, 2012. **18**(22): p. 6260-70.

89. Kong, D., E. Heath, W. Chen, M. Cher, I. Powell, L. Heilbrun, Y. Li, S. Ali, S. Sethi, O. Hassan, C. Hwang, N. Gupta, D. Chitale, W.A. Sakr, M. Menon, and F.H. Sarkar, *Epigenetic silencing of miR-34a in human prostate cancer cells and tumor tissue specimens can be reversed by BR-DIM treatment.* Am J Transl Res, 2012. **4**(1): p. 14-23.

90. Kashat, M., L. Azzouz, S.H. Sarkar, D. Kong, Y. Li, and F.H. Sarkar, *Inactivation of AR and Notch-1 signaling by miR-34a attenuates prostate cancer aggressiveness.* Am J Transl Res, 2012. **4**(4): p. 432-42.

91. Liu, K., J. Huang, M. Xie, Y. Yu, S. Zhu, R. Kang, L. Cao, D. Tang, and X. Duan, *MIR34A regulates autophagy and apoptosis by targeting HMGB1 in the retinoblastoma cell.* Autophagy, 2014. **10**(3): p. 442-52.

92. Mathew, R., V. Karantza-Wadsworth, and E. White, *Role of autophagy in cancer.* Nature Reviews Cancer, 2007. **7**(12): p. 961-7.

93. Chang, T.K., B.V. Shravage, S.D. Hayes, C.M. Powers, R.T. Simin, J. Wade Harper, and E.H. Baehrecke, *Uba1 functions in Atg7- and Atg3-independent autophagy.* Nat Cell Biol, 2013. **15**(9): p. 1067-78.

94. Kang, R., H.J. Zeh, M.T. Lotze, and D. Tang, *The Beclin 1 network regulates autophagy and apoptosis.* Cell Death Differ, 2011. **18**(4): p. 571-80.

95. Nishida, Y., S. Arakawa, K. Fujitani, H. Yamaguchi, T. Mizuta, T. Kanaseki, M. Komatsu, K. Otsu, Y. Tsujimoto, and S. Shimizu, *Discovery of Atg5/Atg7-independent alternative macroautophagy.* Nature, 2009. **461**(7264): p. 654-8.

96. White, E. and R.S. DiPaola, *The double-edged sword of autophagy modulation in cancer.* Clin Cancer Res, 2009. **15**(17): p. 5308-16.

97. Wen, Y., B. Zand, B. Ozpolat, M.J. Szczepanski, C. Lu, E. Yuca, A.R. Carroll, N. Alpay, C. Bartholomeusz, I. Tekedereli, Y. Kang, R. Rupaimoole, C.V. Pecot, H.J. Dalton, A. Hernandez, A. Lokshin, S.K. Lutgendorf, J. Liu, W.N. Hittelman, W.Y. Chen, G. Lopez-Berestein, M. Szajnik, N.T. Ueno, R.L. Coleman, and A.K. Sood, *Antagonism of tumoral prolactin receptor promotes autophagy-related cell death.* Cell Rep, 2014. **7**(2): p. 488-500.

98. Zhai, B., F. Hu, X. Jiang, J. Xu, D. Zhao, B. Liu, S. Pan, X. Dong, G. Tan, Z. Wei, H. Qiao, H. Jiang, and X. Sun, *Inhibition of Akt reverses the acquired resistance to*

sorafenib by switching protective autophagy to autophagic cell death in hepatocellular carcinoma. Mol Cancer Ther, 2014. **13**(6): p. 1589-98.

99. Kumar, D., S. Shankar, and R.K. Srivastava, *Rottlerin-induced autophagy leads to the apoptosis in breast cancer stem cells: molecular mechanisms.* Mol Cancer, 2013. **12**(1): p. 171.

100. Roca, H., Z. Varsos, and K.J. Pienta, *CCL2 protects prostate cancer PC3 cells from autophagic death via phosphatidylinositol 3-kinase/AKT-dependent survivin up-regulation.* J Biol Chem, 2008. **283**(36): p. 25057-73.

101. Frankel, L.B. and A.H. Lund, *MicroRNA regulation of autophagy.* Carcinogenesis, 2012. **33**(11): p. 2018-25.

102. Zhai, H., A. Fesler, and J. Ju, *MicroRNA: a third dimension in autophagy.* Cell Cycle, 2013. **12**(2): p. 246-50.

103. Xu, Y., Y. An, Y. Wang, C. Zhang, H. Zhang, C. Huang, H. Jiang, X. Wang, and X. Li, *miR-101 inhibits autophagy and enhances cisplatin-induced apoptosis in hepatocellular carcinoma cells.* Oncol Rep, 2013. **29**(5): p. 2019-24.

104. Tazawa, H., S. Yano, R. Yoshida, Y. Yamasaki, T. Sasaki, Y. Hashimoto, S. Kuroda, M. Ouchi, T. Onishi, F. Uno, S. Kagawa, Y. Urata, and T. Fujiwara, *Genetically engineered oncolytic adenovirus induces autophagic cell death through an E2F1-microRNA-7-epidermal growth factor receptor axis.* Int J Cancer, 2012. **131**(12): p. 2939-50.

105. Keating, A.K., G.K. Kim, A.E. Jones, A.M. Donson, K. Ware, J.M. Mulcahy, D.B. Salzberg, N.K. Foreman, X. Liang, A. Thorburn, and D.K. Graham, *Inhibition of Mer*

and Axl receptor tyrosine kinases in astrocytoma cells leads to increased apoptosis and improved chemosensitivity. Mol Cancer Ther, 2010. **9**(5): p. 1298-307.

106. Liu, Y., J.H. Liu, K. Chai, S. Tashiro, S. Onodera, and T. Ikejima, *Inhibition of c-Met promoted apoptosis, autophagy and loss of the mitochondrial transmembrane potential in oridonin-induced A549 lung cancer cells.* J Pharm Pharmacol, 2013. **65**(11): p. 1622-42.

107. Shi, Y., J.J. Han, J.B. Tennakoon, F.F. Mehta, F.A. Merchant, A.R. Burns, M.K. Howe, D.P. McDonnell, and D.E. Frigo, *Androgens promote prostate cancer cell growth through induction of autophagy.* Mol Endocrinol, 2013. **27**(2): p. 280-95.

108. Park, S.I., J. Zhang, K.A. Phillips, J.C. Araujo, A.M. Najjar, A.Y. Volgin, J.G. Gelovani, S.J. Kim, Z. Wang, and G.E. Gallick, *Targeting SRC family kinases inhibits growth and lymph node metastases of prostate cancer in an orthotopic nude mouse model.* Cancer Res, 2008. **68**(9): p. 3323-33.

109. Bladt, F., D. Riethmacher, S. Isenmann, A. Aguzzi, and C. Birchmeier, *Essential role for the c-met receptor in the migration of myogenic precursor cells into the limb bud.* Nature, 1995. **376**(6543): p. 768-71.

110. Su, A.I., J.B. Welsh, L.M. Sapinoso, S.G. Kern, P. Dimitrov, H. Lapp, P.G. Schultz, S.M. Powell, C.A. Moskaluk, H.F. Frierson, Jr., and G.M. Hampton, *Molecular classification of human carcinomas by use of gene expression signatures.* Cancer Res, 2001. **61**(20): p. 7388-93.

111. Kimura, T., T. Kuwata, S. Ashimine, M. Yamazaki, C. Yamauchi, K. Nagai, A. Ikehara, Y. Feng, D.S. Dimitrov, S. Saito, and A. Ochiai, *Targeting of bone-derived insulin-like growth factor-II by a human neutralizing antibody suppresses the growth*

of prostate cancer cells in a human bone environment. Clin Cancer Res, 2010. **16**(1): p. 121-9.

112. Hellawell, G.O., G.D. Turner, D.R. Davies, R. Poulsom, S.F. Brewster, and V.M. Macaulay, *Expression of the type 1 insulin-like growth factor receptor is up-regulated in primary prostate cancer and commonly persists in metastatic disease.* Cancer Res, 2002. **62**(10): p. 2942-50.

113. Dayyani, F., N.U. Parikh, A.S. Varkaris, J.H. Song, S. Moorthy, T. Chatterji, S.N. Maity, A.R. Wolfe, J.M. Carboni, M.M. Gottardis, C.J. Logothetis, and G.E. Gallick, *Combined Inhibition of IGF-1R/IR and Src family kinases enhances antitumor effects in prostate cancer by decreasing activated survival pathways.* PLoS One, 2012. **7**(12): p. e51189.

114. Montagnani Marelli, M., R.M. Moretti, P. Procacci, M. Motta, and P. Limonta, *Insulin-like growth factor-I promotes migration in human androgen-independent prostate cancer cells via the alphavbeta3 integrin and PI3-K/Akt signaling.* Int J Oncol, 2006. **28**(3): p. 723-30.

115. Arias-Salgado, E.G., S. Lizano, S. Sarkar, J.S. Brugge, M.H. Ginsberg, and S.J. Shattil, *Src kinase activation by direct interaction with the integrin beta cytoplasmic domain.* Proc Natl Acad Sci U S A, 2003. **100**(23): p. 13298-302.

116. Mitra, A.K., K. Sawada, P. Tiwari, K. Mui, K. Gwin, and E. Lengyel, *Ligand-independent activation of c-Met by fibronectin and alpha(5)beta(1)-integrin regulates ovarian cancer invasion and metastasis.* Oncogene, 2011. **30**(13): p. 1566-76.

117. Sainaghi, P.P., L. Castello, L. Bergamasco, M. Galletti, P. Bellosta, and G.C. Avanzi, *Gas6 induces proliferation in prostate carcinoma cell lines expressing the Axl receptor.* J Cell Physiol, 2005. **204**(1): p. 36-44.

118. Hayes, J., P.P. Peruzzi, and S. Lawler, *MicroRNAs in cancer: biomarkers, functions and therapy.* Trends Mol Med, 2014. **20**(8): p. 460-9.

119. Deng, X., M. Cao, J. Zhang, K. Hu, Z. Yin, Z. Zhou, X. Xiao, Y. Yang, W. Sheng, Y. Wu, and Y. Zeng, *Hyaluronic acid-chitosan nanoparticles for co-delivery of MiR-34a and doxorubicin in therapy against triple negative breast cancer.* Biomaterials, 2014. **35**(14): p. 4333-44.

120. Kumar, D., S. Shankar, and R.K. Srivastava, *Rottlerin induces autophagy and apoptosis in prostate cancer stem cells via PI3K/Akt/mTOR signaling pathway.* Cancer Lett, 2014. **343**(2): p. 179-89.

121. Rikiishi, H., *Novel Insights into the Interplay between Apoptosis and Autophagy.* Int J Cell Biol, 2012. **2012**: p. 317645.

122. Kroemer, G. and B. Levine, *Autophagic cell death: the story of a misnomer.* Nat Rev Mol Cell Biol, 2008. **9**(12): p. 1004-10.

123. Amaravadi, R.K., J. Lippincott-Schwartz, X.M. Yin, W.A. Weiss, N. Takebe, W. Timmer, R.S. DiPaola, M.T. Lotze, and E. White, *Principles and current strategies for targeting autophagy for cancer treatment.* Clin Cancer Res, 2011. **17**(4): p. 654-66.

124. Klionsky, D.J., F.C. Abdalla, H. Abeliovich, R.T. Abraham, A. Acevedo-Arozena, K. Adeli, L. Agholme, M. Agnello, P. Agostinis, J.A. Aguirre-Ghiso, H.J. Ahn, O. Ait-Mohamed, S. Ait-Si-Ali, T. Akematsu, S. Akira, H.M. Al-Younes, M.A. Al-Zeer,

M.L. Albert, R.L. Albin, J. Alegre-Abarrategui, et al., *Guidelines for the use and interpretation of assays for monitoring autophagy.* Autophagy, 2012. **8**(4): p. 445-544.

125. Scarlatti, F., R. Maffei, I. Beau, P. Codogno, and R. Ghidoni, *Role of non-canonical Beclin 1-independent autophagy in cell death induced by resveratrol in human breast cancer cells.* Cell Death Differ, 2008. **15**(8): p. 1318-29.

126. Behrends, C., M.E. Sowa, S.P. Gygi, and J.W. Harper, *Network organization of the human autophagy system.* Nature, 2010. **466**(7302): p. 68-76.

127. Corcoran, C., S. Rani, and L. O'Driscoll, *miR-34a is an intracellular and exosomal predictive biomarker for response to docetaxel with clinical relevance to prostate cancer progression.* Prostate, 2014. **74**(13): p. 1320-34.

128. Blume-Jensen, P. and T. Hunter, *Oncogenic kinase signalling.* Nature, 2001. **411**(6835): p. 355-65.

129. Gschwind, A., O.M. Fischer, and A. Ullrich, *The discovery of receptor tyrosine kinases: targets for cancer therapy.* Nature Reviews Cancer, 2004. **4**(5): p. 361-70.

130. Fischer, O.M., A. Gschwind, and A.A. Ullrich, *Cell surface growth factor receptor molecules as targets for cancer therapy.* Discov Med, 2004. **4**(22): p. 166-71.

131. Lemmon, M.A. and J. Schlessinger, *Cell signaling by receptor tyrosine kinases.* Cell, 2010. **141**(7): p. 1117-34.

132. Bean, J., C. Brennan, J.Y. Shih, G. Riely, A. Viale, L. Wang, D. Chitale, N. Motoi, J. Szoke, S. Broderick, M. Balak, W.C. Chang, C.J. Yu, A. Gazdar, H. Pass, V. Rusch, W. Gerald, S.F. Huang, P.C. Yang, V. Miller, M. Ladanyi, C.H. Yang, and W. Pao, *MET amplification occurs with or without T790M mutations in EGFR mutant lung*

tumors with acquired resistance to gefitinib or erlotinib. Proc Natl Acad Sci U S A, 2007. **104**(52): p. 20932-7.

133. Wagner, J.P., A. Wolf-Yadlin, M. Sevecka, J.K. Grenier, D.E. Root, D.A. Lauffenburger, and G. MacBeath, *Receptor tyrosine kinases fall into distinct classes based on their inferred signaling networks.* Sci Signal, 2013. **6**(284): p. ra58.

134. Birchmeier, C., W. Birchmeier, E. Gherardi, and G.F. Vande Woude, *Met, metastasis, motility and more.* Nat Rev Mol Cell Biol, 2003. **4**(12): p. 915-25.

135. Chan, J.M., M.J. Stampfer, J. Ma, P. Gann, J.M. Gaziano, M. Pollak, and E. Giovannucci, *Insulin-like growth factor-I (IGF-I) and IGF binding protein-3 as predictors of advanced-stage prostate cancer.* J Natl Cancer Inst, 2002. **94**(14): p. 1099-106.

136. Dayyani, F., G.E. Gallick, C.J. Logothetis, and P.G. Corn, *Novel therapies for metastatic castrate-resistant prostate cancer.* J Natl Cancer Inst, 2011. **103**(22): p. 1665-75.

137. Lee, Y.C., J.K. Jin, C.J. Cheng, C.F. Huang, J.H. Song, M. Huang, W.S. Brown, S. Zhang, L.Y. Yu-Lee, E.T. Yeh, B.W. McIntyre, C.J. Logothetis, G.E. Gallick, and S.H. Lin, *Targeting constitutively activated beta1 integrins inhibits prostate cancer metastasis.* Mol Cancer Res, 2013. **11**(4): p. 405-17.

138. Goel, H.L., J. Li, S. Kogan, and L.R. Languino, *Integrins in prostate cancer progression.* Endocr Relat Cancer, 2008. **15**(3): p. 657-64.

139. Chen, F. and S.J. Hu, *Effect of microRNA-34a in cell cycle, differentiation, and apoptosis: a review.* J Biochem Mol Toxicol, 2012. **26**(2): p. 79-86.

140. Sheridan, C., *First Axl inhibitor enters clinical trials.* Nat Biotechnol, 2013. **31**(9): p. 775-6.

141. Tazawa, H., N. Tsuchiya, M. Izumiya, and H. Nakagama, *Tumor-suppressive miR-34a induces senescence-like growth arrest through modulation of the E2F pathway in human colon cancer cells.* Proc Natl Acad Sci U S A, 2007. **104**(39): p. 15472-7.

142. Agell, L., S. Hernandez, S. de Muga, J.A. Lorente, N. Juanpere, R. Esgueva, S. Serrano, A. Gelabert, and J. Lloreta, *KLF6 and TP53 mutations are a rare event in prostate cancer: distinguishing between Taq polymerase artifacts and true mutations.* Modern Pathology, 2008. **21**(12): p. 1470-78.

143. Chen, Y., X.R. Liu, Y.Q. Yin, C.J. Lee, F.T. Wang, H.Q. Liu, X.T. Wu, and J. Liu, *Unravelling the multifaceted roles of Atg proteins to improve cancer therapy.* Cell Prolif, 2014. **47**(2): p. 105-12.

144. Rothe, K., H. Lin, K.B. Lin, A. Leung, H.M. Wang, M. Malekesmaeili, R.R. Brinkman, D.L. Forrest, S.M. Gorski, and X. Jiang, *The core autophagy protein ATG4B is a potential biomarker and therapeutic target in CML stem/progenitor cells.* Blood, 2014. **123**(23): p. 3622-34.

Vita

Sanchaika Gaur was born in Bijnor, Uttar Pradesh, India, the daughter of Manjula and Som Pratap Gaur. After completing her high school education at Delhi Public School R.K. Puram, New Delhi, India in 2005, she entered The University at Buffalo, SUNY Buffalo in Buffalo, NY. She received the degree of Bachelor of Science *summa cum laude* majoring in Biotechnology from SUNY Buffalo in May 2009. She worked at Kinex Pharmaceuticals for from January—July 2009 as a Biology/Biochemistry Technician. In August 2009, she entered The University of Texas Graduate School of Biomedical Sciences at Houston, Texas. She is a recipient of the CPRIT Innovation in Cancer Prevention Research (ICPR) pre-doctoral fellowship by the School of Public Health at UTHealth.